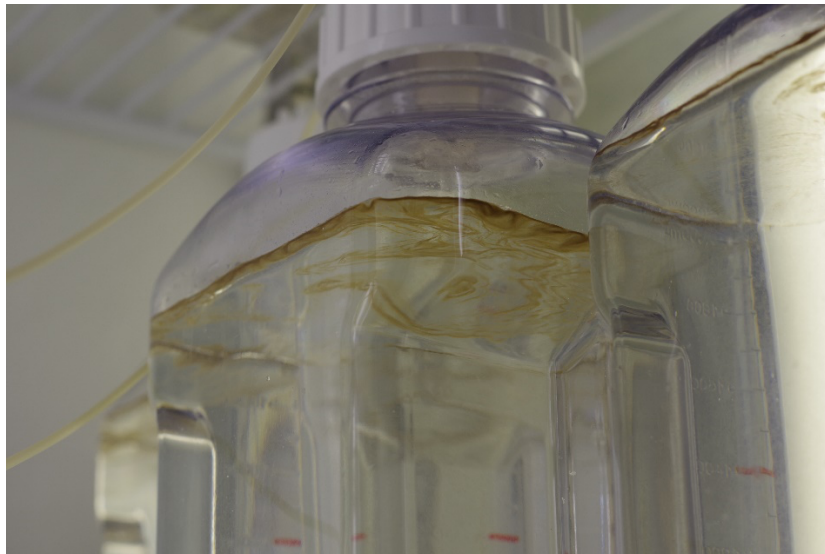


Physiological and elemental changes of *Trichodesmium* in response to growth limitation by phosphorus, iron and zinc



Dissertation

vorgelegt von

Xuechao Wang

zur Erlangung des akademischen Grades eines Doktors der

Naturwissenschaften

– **Dr. rer. nat** –

an der Mathematisch-Naturwissenschaftlichen Fakultät

der Christian-Albrechts-Universität zu Kiel

Kiel, Juni 2022

Erster Gutachter und Betreuer: Prof. Dr. Eric Achterberg

Zweiter Gutachter: Prof. C. Mark Moore

Tag der Disputation: 08. Juni 2022

Zum Druck genehmigt

Abstract

Trichodesmium spp. is a colonial, diazotrophic (N₂ fixing) cyanobacterium found in the oligotrophic (sub-)tropical ocean. It contributes an estimated 50% of the total N₂ fixed in the ocean. In regions where *Trichodesmium* is abundant, concentrations of dissolved inorganic phosphorus (DIP) can be depleted, potentially to growth-limiting levels. To cope with low DIP concentrations, *Trichodesmium* are able to utilize part of the more abundant dissolved organic P pool (DOP; e.g., phosphoesters and phosphonate). To obtain P from the DOP pool, *Trichodesmium* requires the utilization of enzymes such as alkaline phosphatase (AP), which hydrolyses phosphoesters, and C-P lyase, which is responsible for the catabolism of phosphonate. Both AP and C-P lyase are metalloenzymes, specifically, (i) the AP enzyme PhoA requires zinc (Zn) and magnesium (Mg), PhoD/X requires calcium (Ca) and iron (Fe); and (ii) C-P lyases contain Zn and Fe. As the concentrations of these metals in the open ocean can often be extremely low and their physicochemical speciation further constrains their bioavailability, the potentially enhanced trace element requirements for P acquisition enzymes under stronger P limitation has the potential to exert control on the growth of *Trichodesmium* and thereby impact global nitrogen and carbon cycles. In this thesis, I applied a continuous culture technique under trace-metal-controlled conditions to vary the supply of DIP, DOP, Fe and Zn to test the impact of the relative availability of P sources, Fe, and Zn availability on the growth and physiological changes in *Trichodesmium*. First, to explore effects of different P sources on the growth of *Trichodesmium*, *Trichodesmium* was grown with either DIP or DOP (methylphosphonic acid, MPA). This study (Chapter 2) revealed 3.5-fold elevated Zn requirements of *Trichodesmium* when MPA was used as the sole source of P in comparison to

growth on DIP, which I hypothesize was due to enhanced Zn requirements for P scavenging enzymes. This observation suggested an important level of interaction between the cycles of P and Zn in the ocean. Next, *Trichodesmium* were grown from a gradient of Fe depleted to repleted conditions, with P again supplied as either DIP or DOP (MPA). To track the physiological response of *Trichodesmium* to Fe limitation, changes in the concentration of the particulate targeted metabolites were also examined. This study (Chapter 3) found a shift from P limitation, or P-Fe co-limitation, into stronger Fe limitation in the Fe depleted DIP treatment and a shift from strong P limitation through to Fe-P co-limitation in the Fe depleted DOP treatment. Reduced Fe supply resulted in increased intracellular Zn:C, Mn:C, Cu:C and Mo:C ratios and a decreased Fe:C ratio in the Fe depleted DIP treatment. Conversely, reduced Fe supply resulted in an increased intracellular Zn:C ratio and decreased Fe:C, P:C and N:C ratios in the Fe depleted DOP treatment. No significant changes were observed in the carbon-normalized abundance of targeted metabolites produced by *Trichodesmium*, whether in the Fe depleted, Fe recovery condition or transition phase from Fe depleted to Fe recovery condition. These findings provided for the first time the elemental stoichiometry of *Trichodesmium* grown under Fe limitation and Fe-P co-limitation conditions and revealed the response of *Trichodesmium* to nutrient limitation from the perspective of metabolite changes. The final study (Chapter 4) explored the response of *Trichodesmium* to Zn limitation. This study revealed ~10-fold elevated nickel (Ni) requirement of *Trichodesmium* under Zn limitation, regardless of whether the supplied source of P was DIP or DOP. This finding provided for the first time (i) a novel perspective on the relatively high Ni demand for *Trichodesmium*, and (ii) the elemental stoichiometry of *Trichodesmium* grown under Zn depleted conditions. Together, the research presented in this thesis demonstrates that *Trichodesmium* can significantly change its elemental

stoichiometry in response to different elemental limitation conditions. Ultimately, these data will provide a useful resource for ocean biogeochemical models that may in the future resolve P, Fe and Zn.

Kurzfassung

Trichodesmium spp. ist ein koloniales, diazotrophes (N₂-bindendes) Cyanobakterium, das in den oligotrophen (sub-)tropischen Ozeanen vorkommt. Es trägt zu ~50 % zum gesamten im Ozean gebundenen N₂ bei. In Regionen, in denen *Trichodesmium* reichlich vorkommt, können die Konzentrationen von gelöstem anorganischem Phosphor (DIP) bis zu einem wachstumslimitierenden Niveau abnehmen. Um mit niedrigen DIP-Konzentrationen zurechtzukommen, kann *Trichodesmium* einen Teil des reichlich vorhandenen gelösten organischen P-Pools (DOP; z. B. Phosphoester und Phosphonat) nutzen. Um P aus dem DOP-Pool zu gewinnen, benötigt *Trichodesmium* Enzyme wie die alkalische Phosphatase (AP), die Phosphoester hydrolysiert, und die C-P Lyase, die für den Abbau von Phosphonat verantwortlich ist. Sowohl AP als auch C-P Lyase sind Metalloenzyme, und zwar (i) das AP-Enzym PhoA benötigt Zink (Zn) und Magnesium (Mg), PhoD/X benötigt Calcium (Ca) und Eisen (Fe); und (ii) C-P-Lyasen enthalten Zn und Fe. Da die Konzentrationen dieser Metalle im offenen Ozean oft extrem niedrig sind und ihre physikalisch-chemische Speziation ihre Bioverfügbarkeit weiter einschränkt, hat der potenziell erhöhte Bedarf an Spurenelementen für Enzyme zur P-Akquisition bei stärkerer P-Limitierung das Potenzial, das Wachstum von *Trichodesmium* zu kontrollieren und dadurch den globalen Stickstoff- und Kohlenstoffkreislauf zu beeinflussen. In dieser Arbeit habe ich eine kontinuierliche Kulturtechnik unter spurenmittelkontrollierten Bedingungen angewandt, um die Versorgung mit DIP, DOP, Fe und Zn zu variieren und die Auswirkungen der relativen Verfügbarkeit von P-Quellen, Fe und Zn auf das Wachstum und die physiologischen Veränderungen von *Trichodesmium* zu testen. Um die Auswirkungen verschiedener P-Quellen auf das Wachstum von *Trichodesmium* zu

untersuchen, wurde *Trichodesmium* zunächst entweder mit DIP oder DOP (Methylphosphonsäure, MPA) kultiviert. Diese Studie (Kapitel 2) ergab einen 3,5-fach erhöhten Zn-Bedarf von *Trichodesmium*, wenn MPA als einzige P-Quelle verwendet wurde, im Vergleich zum Wachstum mit DIP, was ich auf einen erhöhten Zn-Bedarf für P-fangende Enzyme zurückführe. Diese Beobachtung deutet auf eine wichtige Wechselwirkung zwischen den P- und Zn-Zyklen im Meer hin. Als Nächstes wurde *Trichodesmium* in einem Gradienten von Fe-armen bis zu erhöhten Bedingungen gezüchtet, wobei P wiederum entweder als DIP oder DOP (MPA) zugeführt wurde. Um die physiologische Reaktion von *Trichodesmium* auf die Fe-Limitierung zu verfolgen, wurden auch Veränderungen in der Konzentration von gezielten partikulären Metaboliten untersucht. In dieser Studie (Kapitel 3) wurde eine Verschiebung von einer P-Limitierung oder P-Fe Co-Limitierung zu einer stärkeren Fe-Limitierung unter Fe-armen Bedingungen mit Zugabe von DIP und eine Verschiebung von einer starken P-Limitierung zu einer Fe-P Co-Limitierung unter Fe-armen Bedingungen mit Zugabe von DOP festgestellt. Eine verringerte Fe-Versorgung führte zu erhöhten Zn:C-, Mn:C-, Cu:C- und Mo:C-Verhältnissen und zu einem verringerten Fe:C-Verhältnis in der Fe-armen DIP-Behandlung. Umgekehrt führte eine verringerte Fe-Zufuhr zu einem erhöhten Zn:C-Verhältnis und einem verringerten Fe:C-, P:C- und N:C-Verhältnis in der Fe-armen DOP-Behandlung. Es wurden keine signifikanten Veränderungen in der kohlenstoffnormierten Häufigkeit in gezielten von *Trichodesmium* produzierten Metaboliten beobachtet, weder im Fe-armen noch im Fe-reichen Zustand noch in der Übergangsphase vom Fe-armen zum Fe-reichen Zustand. Diese Ergebnisse lieferten zum ersten Mal die Elementstöchiometrie von *Trichodesmium*, das unter Bedingungen der Fe-Limitierung und der Fe-P-Ko-Limitierung gewachsen ist, und zeigten die Reaktion von *Trichodesmium* auf die Nährstofflimitierung aus der Perspektive der Metabolitenveränderungen.

In der letzten Studie (Kapitel 4) wurde die Reaktion von *Trichodesmium* auf eine Zn-Limitierung untersucht. Diese Studie ergab, dass *Trichodesmium* unter Zn-Limitierung einen ~10-fach erhöhten Bedarf an Nickel (Ni) hat, unabhängig davon, ob die zugeführte P-Quelle DIP oder DOP war. Dieses Ergebnis lieferte (i) eine neue Perspektive auf den relativ hohen Ni-Bedarf von *Trichodesmium* und (ii) zum ersten Mal die Elementstöchiometrie von *Trichodesmium*, das unter Zn-armen Bedingungen wächst. Zusammengefasst zeigen die in dieser Arbeit vorgestellten Untersuchungen, dass *Trichodesmium* seine Elementstöchiometrie als Reaktion auf unterschiedliche Bedingungen der Elementverarmung erheblich verändern kann. Letztendlich werden diese Daten eine nützliche Ressource für biogeochemische Ozeanmodelle darstellen, die in Zukunft P, Fe und Zn auflösen können.

Acknowledgements

Firstly I would like to thank my supervisor Prof. Dr. Eric Achterberg for giving me the opportunity to carry out my doctoral research and for the continued guidance, support, assistance and advice.

I would like to thank my co-supervisor Dr. Thomas Browning for his patient guidance and constant encouragement over the course of the research and dissertation writing over the past four years. Thanks for your continued communication with me allowing me to gain an excellent scientific training. Your guidance and knowledge sharing has pushed me to keep learning and thinking, which brought my work to a higher level.

I would like to thank my co-supervisor Dr. Martha Gledhill for her guidance throughout the research. Her training of my laboratory skills was key to the completion of my experiments and her sharing of experience and constructive comments have continued to expand my research ideas.

I would like to thank Birgit Reiner, Andre Mutzberg, Tim Steffens, Dominik Jasinski and Kerstin Nachtigall for all the administrative and technical support. Thanks to Dr. Insa Rapp for the help with German-language issues. Thanks to Ali Alhashem, Jaw Chuen Yong, Münevver Nehir, Dr. Mario Esposito, Dr. Maria Martinez, Dr. Pablo Lodeiro, Dr. Fengjie Liu, Dr. Xunchi Zhu, Dr. Linbin Zhou, Dr. Zuozhu Wen, Dr. Aaron Beck, Dr. Felix Geißler, Dr. Jan-Lucas Menzel, Dr. Ruifang Xie, Siao Jean Khoo, Dr. Stephan Krisch, Te Liu, Zhongwei Yuan and all members of the AG. Achterberg at GEOMAR for the excellent collaboration and I really enjoyed the time with all of you.

I thank my country, China, I thank China Scholarship Council for providing financial support. I thank my parents for their patience, understanding and contribution, I haven't been home for more than three years due to the epidemic of COVID-19 and I miss you very much.

Acknowledgements

I would like to deeply thank my girlfriend Dr. Tingting Wang, many thanks for your 11 years of companionship. Thanks for your patience, which allowed me to calm down in my impatience. Thanks for your positive thoughts, which brought me out of my self-doubt in time. Thanks for your understanding and contribution, which allowed me to focus more on my research. Will you spend the rest of your life with me?

Thank you all for your contribution to this PhD project!

Contents

<i>Abstract</i>	v
<i>Kurzfassung</i>	ix
<i>Acknowledgements</i>	xiii
<i>Chapter 1. Introduction</i>	1
1.1 Marine Primary Production and Phytoplankton	1
1.2 Requirements for phytoplankton growth	2
1.3 Nutrient limitation in the ocean	8
1.4 Abundance of diazotrophs in the ocean and their growth environment	12
1.5 Cellular strategies to cope with nutrient stress.....	16
1.5.1 Phosphorus Physiology in Phytoplankton	16
1.5.2 Iron Physiology in Phytoplankton.....	19
1.6 Metabolites and what measuring them might tell us about phytoplankton in the ocean	
20	
1.7 The exponentially fed batch culture	21
1.8 Thesis objectives	22
<i>Chapter 2. Phosphorus limitation enhances diazotroph zinc quotas</i>	25
2.1 Introduction	27
2.2 Materials and methods	28
2.3 Results and Discussion	33
<i>Chapter 3. Phosphorus sources affect the elemental stoichiometry of Trichodesmium under Fe limitation</i>	41
3.1 Introduction	43
3.2 Materials and methods	45

3.3	Results and Discussion	51
3.3.1	<i>Trichodesmium</i> responses to Fe availability	51
3.4	Conclusions	62
<i>Chapter 4. Zinc limitation enhances nickel quotas of Trichodesmium</i>		65
4.1	Introduction	67
4.2	Materials and methods	69
4.3	Results and Discussion	72
4.3.1	Absence of EDTA in the culture media	72
4.3.2	<i>Trichodesmium</i> responses to Zn depletion	74
4.3.3	Elemental quotas of <i>Trichodesmium</i> response to Zn depletion.....	76
4.4	Conclusions	82
<i>Chapter 5. Conclusions and future directions</i>		83
5.1	Overall conclusions	85
5.2	Future directions	88
<i>References.....</i>		101

Chapter 1. Introduction

1.1 Marine Primary Production and Phytoplankton

Net primary production is the formation of organic material from inorganic compounds minus losses by respiration, grazing and viral lysis. The majority of net primary production in the ocean is undertaken by the process of photosynthesis by phytoplankton. Phytoplankton are aquatic, microscopic, photosynthetic organisms. Although phytoplankton account for only ca. 1% of the Earth's living biomass, they are responsible for ca. 50% of global primary production (Field et al., 1998; Falkowski and Raven, 2007). Furthermore, they play a key role in the cycling of carbon (C), oxygen (O), nitrogen (N) and other elements between the atmosphere, oceans and geosphere, and are therefore a fundamental component of the Earth System as a whole (Sarmiento and Gruber, 2006). Phytoplankton communities are extremely diverse, which is manifested as different sizes, morphologies, functions, and pigment compositions (Collins et al., 2014).

Cyanobacteria are generally considered to be the most ancient microorganisms and the only bacteria capable of performing oxygenic photosynthesis (Lyons et al., 2014), they are thought to have been dominant in the phytoplankton community for well over a billion years and their evolution of oxygenic photosynthesis changed the atmosphere of our planet from anoxic to oxygenic (Knoll, 2003). Diazotrophs are microorganisms that are capable of N₂ fixation. Cyanobacterial diazotrophs are abundant in surface waters of the open ocean and are responsible for nearly half of natural global N fixation (Canfield et al., 2010; Zehr, 2011). Through N₂ fixation, marine cyanobacterial diazotrophs convert atmospheric N₂ into

ammonium, meanwhile fixed N can be released to surrounding waters in the form of dissolved organic N, which can be utilized by non-diazotrophic phytoplankton (Mulholland and Bernhardt, 2005). The non-heterocyst-forming cyanobacteria *Trichodesmium* (Capone et al., 1997) and the symbiotic heterocyst-forming cyanobacterium *Richelia* (Follett et al., 2018a; Foster and Zehr, 2019) were considered to be the main types of diazotrophs in the ocean. More recently, new genomics approaches have highlighted the diversity of additional diazotrophs in the ocean (Zehr and Capone, 2020). Cyanobacterial diazotrophs are now known to include not only *Trichodesmium* and the diatom symbionts *Richelia* and *Calothrix* but also the unicellular symbiont cyanobacteria UCYN-A and free-living unicellular *Crocospaera* (UCYN-B) (Zehr and Capone, 2020). Despite these recent findings, *Trichodesmium* is still recognized as a critical contributor (Carpenter and Capone, 2008), with an estimated contribution of ~50% to the total amount of N₂ fixed in the ocean (Capone et al., 1997; Mahaffey, 2005; Bergman et al., 2013).

1.2 Requirements for phytoplankton growth

In marine ecosystems, the total biomass, community composition and structure, cell physiology and growth status of phytoplankton are influenced by multiple factors, including the availability of nutrients, light, physical factors (e.g., temperature, salinity, currents, mixing of water layers) as well as ecological factors (predominantly grazing by predators and viral lysis).

Light is the ultimate source of energy for most of the biosphere (Raven, 2009). All phytoplankton photosynthesize, meaning that they have the ability to convert light energy to chemical bond energy that is stored in the form of organic carbon compounds. Light intensity influences the growth of phytoplankton through its impact on photosynthesis. Under nutrient replete and optimal temperature conditions, the growth rate of phytoplankton is maximal at

saturation light point (the point where the light intensity does not increase the photosynthesis rate is called the light saturation point; Sorokin and Krauss, 1958) even though phytoplankton can make a number of adaptations and acclimations to reduce light limitation (Mock and Kroon, 2002; Fábregas et al., 2004). Adaptation and acclimation to light by phytoplankton can occur through a series of mechanisms including adjustments in light harvesting pigment concentrations, changing the size of the functional absorption cross sections of their photosystems, changing the density of reaction centers and electron transport components and their relative proportions, and biochemical feedback in the Calvin-Benson cycle, as well as changes in the abundance of enzymes involved in carbon metabolism (Falkowski and Raven, 2007).

Temperature influences phytoplankton in both direct and indirect ways. Nearly all chemical reactions are faster under higher temperature until an optimal temperature is reached (Boyd et al., 2013; Naselli-Flores et al., 2020). Even though higher temperatures can increase chemical reactions, response to temperature is species-specific, and optimal growth is thus observed over different temperature ranges in different phytoplankton species (Reynolds, 1984). Thus, increasing temperature may lead to an increase in the metabolic rate of some phytoplankton species and a decrease in the metabolic rate of other phytoplankton species, potentially leading to a shift in the composition of the phytoplankton community (Beardall et al., 2009b; Wang et al., 2021). Temperature also plays a role in controlling water viscosity and density, thus directly influencing the sinking, floating and swimming of phytoplankton, and thereby the irradiance and nutrient conditions they encounter. Temperature also has indirect effects on phytoplankton; for example, via its influence on water column stability and nutrient supply. Increased upper-

ocean stratification due to warming has been suggested to result in reduced nutrient input from the deep ocean, indirectly affecting phytoplankton growth (Polovina et al., 2008; Boyce et al., 2010).

All phytoplankton must obtain nutrients from their external environment. Around 30 of the 92 naturally occurring elements can be found in all living organisms (Dolmella and Bandoli, 1993; Sterner and Elser, 2002). The availability of micronutrients, macronutrients and vitamins influence the biochemical composition of phytoplankton (Morris et al., 1974; Nakamura and Miyachi, 1982; Gordillo et al., 1998; Kalacheva et al., 2002; Fábregas et al., 2004). Alfred Redfield proposed that the N:P ratio of plankton (16:1) causes the ocean to have a remarkably similar ratio of dissolved NO_3^- and PO_4^{3-} (Redfield, 1934). The 'Redfield ratio' of 106C:16N:1P has since evolved into a key stoichiometric concept for scientists exploring marine biogeochemistry (Anderson and Sarmiento, 1994; Deutsch et al., 2007). Cellular elemental stoichiometry has also been extended to include other elements (Ho et al., 2003a). Although the average C:N:P in the ocean is relatively constant, the macronutrient ratios in specific marine regions and in specific phytoplankton communities can differ significantly from the canonical Redfield ratio (Geider and La Roche, 2002; Arrigo, 2005), and the stoichiometry of individual species and taxonomic groups can vary significantly (Ho et al., 2003b; Twining et al., 2010), meanwhile the stoichiometry of the same species can vary depending on its environmental conditions (Nuester et al., 2012).

As one of the macronutrients with highest requirements in phytoplankton, N can account for 7%-20% of phytoplankton cellular mass (Geider and La Roche, 2002). N plays a central role in phytoplankton metabolism as a constituent of proteins, nucleic acids, chlorophyll a, b and c,

enzymes, amino acids and N-containing osmolytes (Geider and La Roche, 2002). Even though N is the second most abundant element for life on Earth, the vast majority of N exists in a form that is not available to most organisms, N₂. Bioavailable N in the ocean is present in numerous forms: nitrate, nitrite, ammonium and organic nitrogen such as amino acids, urea, peptides, and proteins (Moore et al., 2013).

Phosphorus (P) is an essential nutrient for all life on earth (Paytan and McLaughlin, 2007). It plays essential roles in cellular structure (phospholipids), genetic information storage and transmission (DNA and RNA), energy transduction (adenosine 5-triphosphate; ATP), metabolic signaling (inositol trisphosphate, (de)phosphorylated proteins and metabolites), as well as stress response and homeostasis (inorganic polyphosphate; poly-P) (Gray and Jakob, 2015). The most common inorganic form, phosphate, is considered the most biologically available form of P in the ocean, but its concentration can be chronically low in surface waters of some tropical and subtropical ocean regions (Wu et al., 2000; Paytan and McLaughlin, 2007).

In addition to control by macronutrients, the growth, distribution and species composition of marine phytoplankton communities are also influenced by a series of trace metal nutrients (micronutrients), which are co-factors or part of co-factors for numerous enzymes mediating important cellular processes in phytoplankton (Morel et al., 2003, 2020). The major biochemical functions of some trace elements in marine microorganisms are displayed in Table 1.1. Fe is important for marine phytoplankton because Fe containing proteins are essential for photosynthetic and respiratory electron transport, and are directly involved in nitrate and nitrite reduction, N₂ fixation, chlorophyll synthesis, and a number of other biosynthetic or degradative reactions (Table 1.2; Geider and La Roche, 1994). One of the most prominent Fe-dependent

processes in phytoplankton is the photosynthetic transport chain. Fe is found within the reaction center of both photosystems, with 2–3 Fe atoms in photosystem II (PSII) and 12 Fe atoms in photosystem I (PSI) (Raven et al., 1999). In addition, Fe is a structural component of nitrate assimilation enzymes as well as in nitrogenase, the N₂ fixing enzyme, and in superoxide dismutase (Fe-SOD) which is involved in the processing of the reactive oxygen species superoxide. Zinc is an essential element for carbonic anhydrase (Badger, 2003; Kupriyanova and Pronina, 2011; Lionetto et al., 2016) and alkaline phosphatase (Dyhrman and Ruttenberg, 2006). These enzymes are responsible for carbon and phosphate uptake, respectively. Based on evidence showing decreasing silicic acid uptake rates and Si:P ratios at low dissolved inorganic Zn concentrations, Zn may be involved in silicic acid uptake and frustule deposition in diatoms (Sunda and Huntsman, 2005). The Zn finger protein is a common DNA binding domain found in many transcription factors, which is important in DNA and RNA replication (Klug, 2010). Cobalt is known to be required in the corrin-ring of the B₁₂ molecule, making it essential for vitamin-producing organisms (Banerjee and Ragsdale, 2003). Vitamin B₁₂ plays important roles in central metabolism, it can influence the growth (Droop, 1955) and potentially community composition of phytoplankton in some ocean regions (Panzeca et al., 2006).

Table 1.1 Roles of micronutrients in phytoplankton cells (adapted from Quigg et al., 2016 and Sunda, 1988)

Element	Functions	Examples of compounds
Fe	Listed separately in Table 1.2 below	
Zn	Enzymes (ca. 150 known), ribosome structure, nucleic acid replication and polymerization, hydration and dehydration of CO ₂ , hydrolysis of phosphate esters, Mehler reaction (production of superoxide)	DNA and RNA polymerases, carbonic anhydrase, alkaline phosphatase, superoxide dismutase
Mn	Electron transport in PSII, maintenance of chloroplast membrane structure, breakdown reactions and those involving halogens, superoxide dismutase, Mehler reaction	O ₂ evolving complex, catalases, peroxidases, manganin, superoxide dismutase
Cu	Electron transport (photosynthesis and respiration) enzymes, disproportionation of O ₂ radicals to O ₂ and H ₂ O ₂ in reaction	Plastocyanin, cytochrome oxidases, superoxide dismutase
Mo	Nitrogen reduction (nitrate and nitrite reduction to ammonium), ion absorption	Nitrate and nitrite reductase, nitrogenase
Co	Component of Vitamin B ₁₂ , C ₄ photosynthesis pathway, C and H transfer reactions with glycols and ribose	Vitamin B ₁₂ , carbonic anhydrase
Cd	May substitute into enzymes that typically use Zn	Carbonic anhydrase in diatoms
Ni	Hydrolysis of urea; co-factor in urease; superoxide dismutase and hydrogenase	Urease, superoxide dismutase

Table 1.2 The role of iron in phytoplankton metabolism (adapted from Geider and La Roche, 1994)

Catalyst	Reaction
cytochromes	photosynthetic and respiratory e^- transfer
cytochrome oxidase	$O_2 + 4e^- + 4H^+ \rightarrow 2H_2O$
Fe-superoxide dismutase	$2O_2^- + 2H^+ \rightarrow H_2O_2 + O_2$
catalase	$2H_2O_2 \rightarrow 2H_2O + O_2$
peroxidase	$R(HO)_2 + H_2O_2 \rightarrow RO_2 + 2H_2O$
ferredoxin	e^- to $NADP^+$, NO_3^- , SO_2 , N_2 , thioredoxin
other Fe-S centers	photosynthetic and respiratory e^- transfer
succinate dehydrogenase	$FAD + \text{succinate} \rightarrow \text{fumarate} + FADH_2$
aconitase	isomerization of citrate to isocitrate
coproporphyrinogen oxidase	oxidative decarboxylation of Mg-protoporphyrin
nitrate reductase	$NO_3^- + 2e^- \rightarrow NO_2^-$
nitrite reductase	$NO_3^- + 6e^- + 3H^+ \rightarrow NH_4^+$
nitrogenase	$N_2 + 8H^+ \rightarrow 2NH_4^+$
lipoxygenase	fatty acid oxidation, carotenoid degradation
glutamate synthetase	$\text{glutamine} + \alpha\text{-keto glutarate} \rightarrow 2 \text{ glutamate}$
xanthine oxidase	$\text{Xanthine} + H_2O + O^2 \rightarrow \text{uric acid} + O_2^-$
alkaline phosphatase (PhoD and PhoX)	$R-PO_3 \rightarrow R + PO_3^{2-}$

1.3 Nutrient limitation in the ocean

Multiple nutrients are essential for phytoplankton growth, so if the concentration of one or more of these is/are depleted to a sufficiently low level, the nutrient(s) may limit the abundance and functionality of phytoplankton (Box 1). By examining the macronutrient stoichiometry within phytoplankton, Alfred Redfield found an empirical relationship between the intracellular stoichiometry ($C_{106}N_{16}P_1$) and that of the major nutrients in the ocean interior (16 N: 1 P) (Redfield, 1958). This ratio, termed as the Redfield ratio, has been used as a diagnostic tool to

make assessments of the most deficient nutrient in the ocean relative to phytoplankton requirements (Redfield, 1934), with the amount of the most deficient nutrient limiting the biomass, or yield, of phytoplankton (von Liebig, 1841). On the other hand, the concentration of the most deficient nutrient may limit not just the amount of biomass, but also the phytoplankton growth rate (Blackman, 1905). In the last few decades, it has further been found that the phytoplankton in surface oceans can be simultaneously limited by multiple nutrients, referred to as nutrient co-limitation. Definitions of nutrient co-limitation vary (Box 1; Arrigo, 2005; Saito et al., 2008; Sperfeld et al., 2016; Moore et al., 2013; Browning et al., 2017a).

Box 1 | Concepts of nutrient (co-)limitation

Single limitation. Only addition of one of the specific nutrients leads to a growth response. The addition of other nutrients with this specific nutrient does not result in further response beyond that of the specific nutrient alone. The addition of other nutrients without this specific nutrient does not result in any response (Sperfeld et al., 2016; Browning et al., 2017a).

Serial limitation. Only addition of one or more nutrient(s) result in a positive growth response and addition of this or these nutrient(s) together with an extra nutrient result in a greater growth response (Sperfeld et al., 2016; Browning et al., 2017a).

Simultaneous co-limitation. Only addition of two or more nutrients result in a growth response, whereas the addition of any single nutrient of them does not result in a growth response (Arrigo, 2005; Saito et al., 2008; Browning et al., 2017a).

Independent co-limitation. Addition of two or more nutrients separately results in a growth response and addition of these nutrients together leads to a greater growth response.

This co-limitation can be specified to super-additive co-limitation (the extent growth response of addition of these nutrients together is greater than sum of the separately responses); additive co-limitation (the extent growth response of addition of these nutrients together is equal to the sum of the separately responses); sub-additive co-limitation (the extent growth response of addition of these nutrients together is less than the sum of the separately responses and meanwhile the extent growth response of addition of these nutrients together is greater than each of the separately response) and antagonistic co-limitation (the extent growth response of addition of these nutrients together is less than each of the separately response) according to the extent growth response of addition of these nutrients together .

Biochemically dependent co-limitation. Addition of either of two nutrients results in a growth response, with one nutrient aids the uptake or assimilation of the other nutrient (Saito et al., 2008). For example, under conditions of phosphorus limitation, supply of phosphorus, Fe, or Zn might enhance growth, with Fe and Zn potentially increasing production of alkaline phosphatase enzymes that scavenge P from the DOP pool (e.g., Mahaffey et al., 2014).

Biochemical substitution co-limitation. Addition of two nutrients separately results in a growth response, with one nutrient substituting for the other nutrient (Saito et al., 2008). For example, Fe, Ni and Zn might be interchangeable within superoxide dismutase enzymes, hence supply of any might increase growth rates (e.g. Peers and Price, 2004).

It has previously been discussed that nutrients are key factors controlling primary productivity in the oceans. Because the global distribution of nutrients in the modern ocean is regulated by a complex interplay between ocean physics, chemistry and biology, nutrient concentrations vary

geographically, seasonally and with depth, often leading to limitation of primary productivity in the surface ocean by depleted concentrations of one or more elements. Diverse studies of shipboard amendment experiments have highlighted nutrient limitation in the ocean (Fig 1.1; Moore et al., 2013; Saito et al., 2014; Browning et al., 2017a). N is typically the primary limiting nutrient in the oligotrophic ocean regions especially in the subtropical gyres of Atlantic Ocean, where most of these ocean regions are under single limitation by N, but there are also some regions in the subtropical North Atlantic with P as the secondary limiting nutrient. The main reason for this is that enhanced Fe-rich dust deposition in these regions (from the Saharan Desert) enhances N₂ fixation by diazotrophs, thereby contributes additional bioavailable N resources and drives the system into P limitation. Upwelling of high nitrate waters in combination with the lack of a Fe source to the surface waters leads to Fe as the primary limiting nutrient in the North and equatorial Pacific and the high-(macro) nutrient low- chlorophyll (HNLC) regions of the Southern Ocean.

The atmospheric concentration of CO₂ is rising due to CO₂ emissions by anthropogenic activities, seawater pH decreases as a result of ocean CO₂ uptake, leading to ocean-acidification. The decrease in pH of the surface ocean impacts phytoplankton by influencing the availability of some elements or compounds (Moore et al., 2013). For example, the availability of calcium carbonates (Fabry et al., 2008) and iron (Shi et al., 2010). As *Trichodesmium* is a dominant diazotroph species inhabiting surface waters of the low latitude oceans where phytoplankton growth is limited by low iron availability (Capone et al., 1997; Moore et al., 2001), a reduced availability of Fe due to lower pH would inevitably affect the growth of *Trichodesmium* under Fe limitation (Shi et al., 2010; Moore et al., 2009). In addition, as decrease in pH can limit the

efficiency of nitrogenase in *Trichodesmium* (Shi et al., 2012), therefore, in order to compensate for the demand for N, *Trichodesmium* needs to synthesize more nitrogenase for nitrogen fixation. As a monomer nitrogenase complex contains 38 Fe atoms (Whittaker et al., 2011), an upregulation of nitrogenase would lead to an increased demand for Fe.

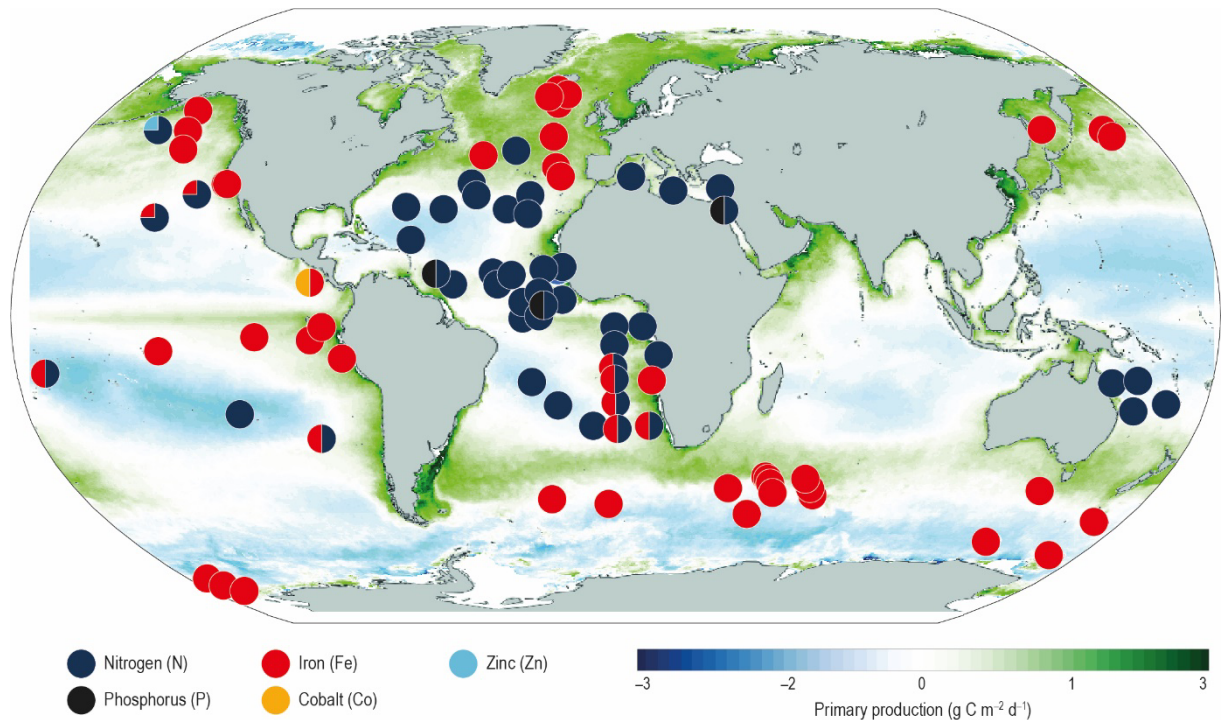


Fig 1.1 Map of the dominant limiting resource (IPCC, 2019). The background indicates depth integrated primary productivity using the Vertically Generalized Production Model algorithm. Colouring of the circles indicates the primary limiting nutrients inferred from chlorophyll and/or primary productivity increases following artificial amendment of: N (blue), P (black), Fe (red), Co (yellow) and Zn (cyan). Divided circles indicate potentially co-limiting nutrients.

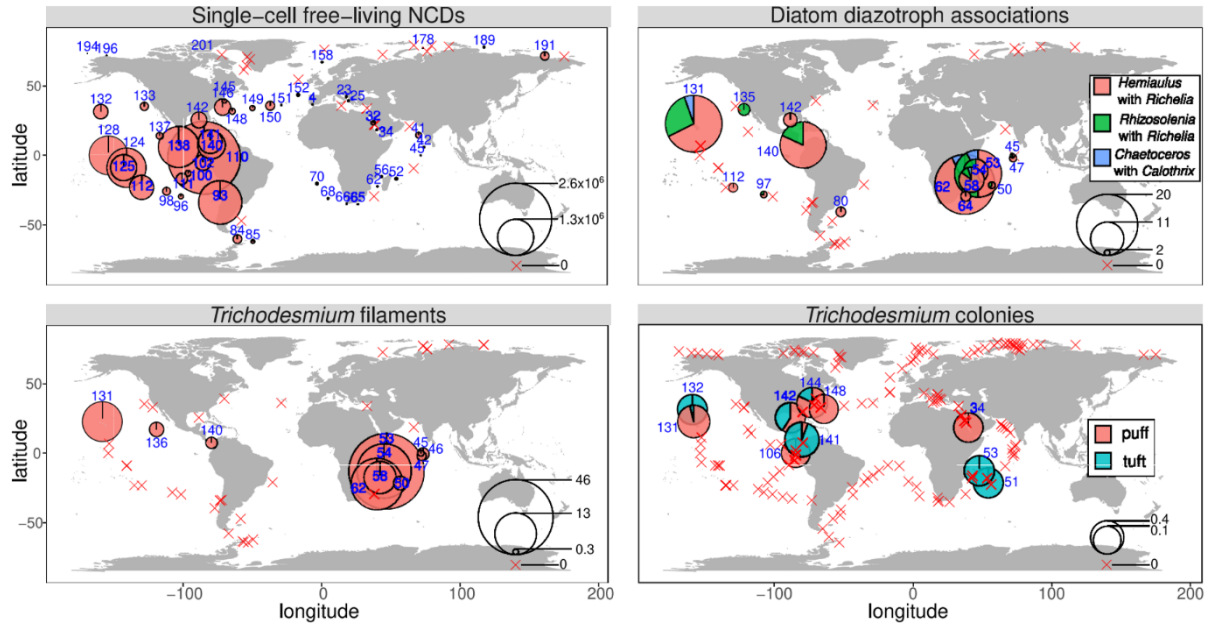
1.4 Abundance of diazotrophs in the ocean and their growth environment

The abundance of diazotroph is recognized to show latitudinal variations with higher relative abundances in tropical and subtropical regions (Fig 1.2; Langlois et al., 2008; Pierella Karlusich et al., 2021). In these regions, around 1–40 free filaments L⁻¹ and colonies referred to as ‘tufts’ or ‘puffs’ aggregated with tens to hundreds of *Trichodesmium* filaments can be observed (Fig

1.2; Pierella Karlusich et al., 2021).

The relative availabilities of P and Fe are important in determining the geographic distributions of diazotrophs. In the low-latitude oligotrophic gyres where *Trichodesmium* are abundant, DIP is typically depleted (Fig 1.3a; $<20\text{nM}$), P may therefore be the controlling factor for diazotrophic growth (e.g., North Atlantic). While in these regions DOP concentrations greatly exceed DIP (Fig 1.3b) and since *Trichodesmium* can utilize a range of metalloenzymes to obtain P in the DOP pool, DOP in these ocean regions could therefore potentially support a large fraction of microbial P demand. In the low-latitude Pacific and Indian Oceans, Fe in the surface waters is typically depleted ($<0.2\text{nM}$; Fig 1.3c), meanwhile the requirement of diazotrophs for Fe is thought to be enhanced relative to other species as they require Fe for the enzyme nitrogenase that is involved in N_2 fixation (Berman-Frank et al., 2007; Richier et al., 2012). Iron consequently appears to be a controlling factor for diazotrophic growth in some regions (e.g., South Atlantic and South Pacific; Fig 1.2; Schlosser et al., 2014).

Even though Zn limitation of phytoplankton is considered not to occur widely in the ocean, in the low-latitude oligotrophic gyres surface ocean dissolved Zn (DZn) concentrations are chronically low ($<1\text{ nmol/kg}$; Fig 1.3d Roshan et al., 2018). Zinc is a cofactor for the alkaline phosphatase PhoA (Kim and Wyckoff, 1991), and with projected increasing atmospheric N inputs there could be a shift toward more widespread and stronger P stress (Moore et al., 2013), *Trichodesmium* may therefore require more Zn by an increasing demand for alkaline phosphatase to facilitate the utilization of DOP.



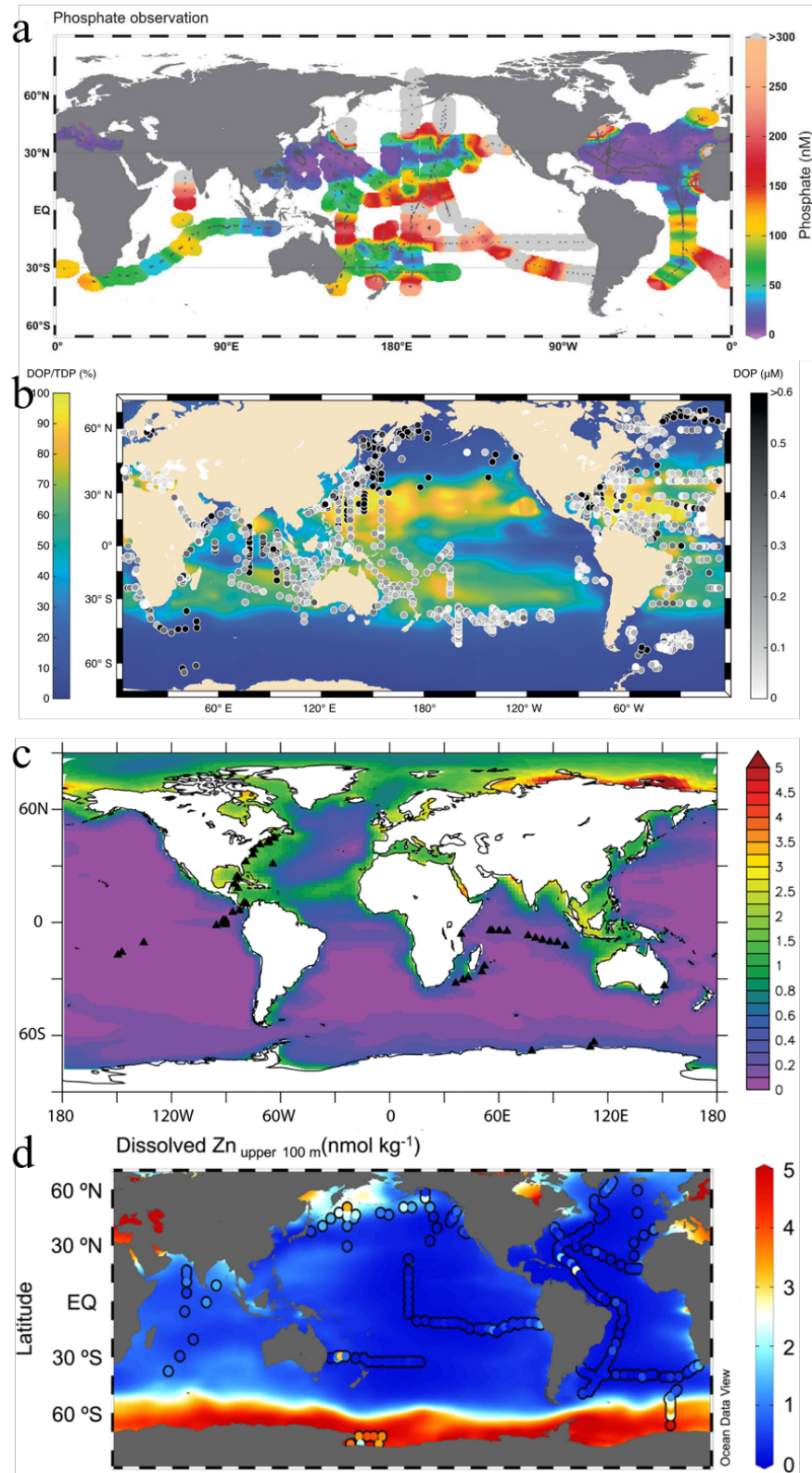


Fig 1.3 **a.** Distribution of DIP concentrations (Martiny et al., 2019); **b.** Distribution of DOP concentrations and contribution to TDP over the global ocean (**b**; Duhamel et al., 2021). Percentage contribution (colour bar) of DOP to TDP and observed DOP concentrations (greyscale circles) at 50 m depth. **c.** Annual average surface Fe concentration (0–100 m) from the NEMO-PISCES model (Toulza et al., 2012). Color scale stands for dissolved iron concentration (nM). **d.** Distributions of dissolved Zn. Concentration of observed (color-filled circles) and ANN-modeled (color map) dissolved Zn at upper 100 m (Roshan et al., 2018).

1.5 Cellular strategies to cope with nutrient stress

1.5.1 Phosphorus Physiology in Phytoplankton

Phosphorus deficiency has been recognized as an important driver of marine ecosystem functioning (Karl, 2014), influencing microbial genetic diversity and global oceanic primary productivity (Benitez-Nelson, 2000; Coleman and Chisholm, 2010). In regions where N₂ fixation is enhanced, DIP concentrations are typically strongly drawn down (Wu et al., 2000; Moore et al., 2009; Martiny et al., 2019), often becoming growth-limiting for diazotrophs and co-limiting for the rest of the phytoplankton community (Moore et al., 2013). This potentially goes on to influence the sinking export rate of P and carbon (Benitez-Nelson, 2000; Paytan and McLaughlin, 2007).

In order to cope with a DIP-deficient environment, both eukaryotic algae and prokaryotic cyanobacteria have evolved a series of sophisticated strategies (Fig 1.4). Firstly, in cyanobacteria, P stress responses are triggered by the transcription of the set of genes termed the Pho regulon (Wanner, 1996). When starved of P, expression of the Pho regulon would be upregulated in cyanobacteria, which enhances the uptake of DIP (Falkner et al., 2006; Pitt et al., 2010; Hudek et al., 2016), triggers the process of synthesis of enzymes to release P from several components such as RNA (Ray et al., 1991; Sebastian and Ammerman, 2009), and decreases the phospholipid levels in the membrane via a remodeling process (Peng et al., 2019). This pho regulon transcription is controlled by a two-component regulatory response system, which comprises an inner-membrane histidine kinase sensor protein and a cytoplasmic transcriptional response regulator. Under DIP depleted conditions, the response regulator is phosphorylated by the sensor kinase on an aspartic residue (Aspartic acid is an α -amino acid that is used in the

16

biosynthesis of proteins). Phosphorylated response regulators are able to bind to specific sequences on DNA to activate or repress the transcription of genes. These specific sequences, termed Pho boxes, were first identified in *E. coli* (Makino et al., 1988). In some marine cyanobacteria species like *Trichodesmium* and *Prochlorococcus*, Pho boxes have been identified upstream of a number of putative pho regulon genes (Sebastián et al., 2016). In addition, cyanobacteria have been reported to have other P stress sensing genes; for example, both the *Prochlorococcus* and *Synechococcus* have the *ptrA* gene (Martiny et al., 2006; Reistetter et al., 2013). Secondly, microorganisms have the ability to regulate their P requirements and thus modulate cellular P (Krauk et al., 2006). Specifically, (i) Under P stress, many groups of marine microorganisms include cyanobacteria *Trichodesmium* have the ability to substitute phospholipids with non P-containing lipids (Van Mooy et al., 2009; Merchant and Helmann, 2012); (ii) It has been observed that both marine prokaryotes and microbial eukaryotes downregulate their P-rich ribosomes and rRNA under P stress (Dyhrman et al., 2012; Kujawinski et al., 2017); (iii) It is predicted that the increase in polyphosphate prevents transient DIP accumulation and down-regulation of the P stress response and it is supported by the observation of the increase in cellular poly-P/TPP of *Trichodesmium* and *Synechococcus* under P stressed conditions (Orchard et al., 2010b; Dyhrman et al., 2012). Thirdly, microorganisms have the ability to utilize alternative P forms. For example, both *Prochlorococcus* and *Trichodesmium* were found to utilize phosphite as the sole P source (Feingersch et al., 2012; Martínez et al., 2012; Polyviou et al., 2015). In addition, microorganisms are able to access DOP via a series of enzymes (Fig 1.5). For example, microorganisms are able to utilize APs, phosphodiesterases and 5' nucleotidases to hydrolyzes DIP from phosphomonoesters (Dyhrman and Ruttenberg, 2006), phosphodiesteres (Dyhrman et al., 2012; Yamaguchi et al., 2020) and 5'

nucleotides (Dyhrman et al., 2006b, 2012), respectively, and many cyanobacteria have the ability to access DIP from phosphonates through a diverse suite of enzymes like C-P lyase (Scanlan et al., 2009; Martinez et al., 2010; Villarreal-Chiu et al., 2012; McGrath et al., 2013). Forth, upregulation of DIP transport systems is also common in microorganisms when cells are under P stress (Sowell et al., 2009; Coleman and Chisholm, 2010).

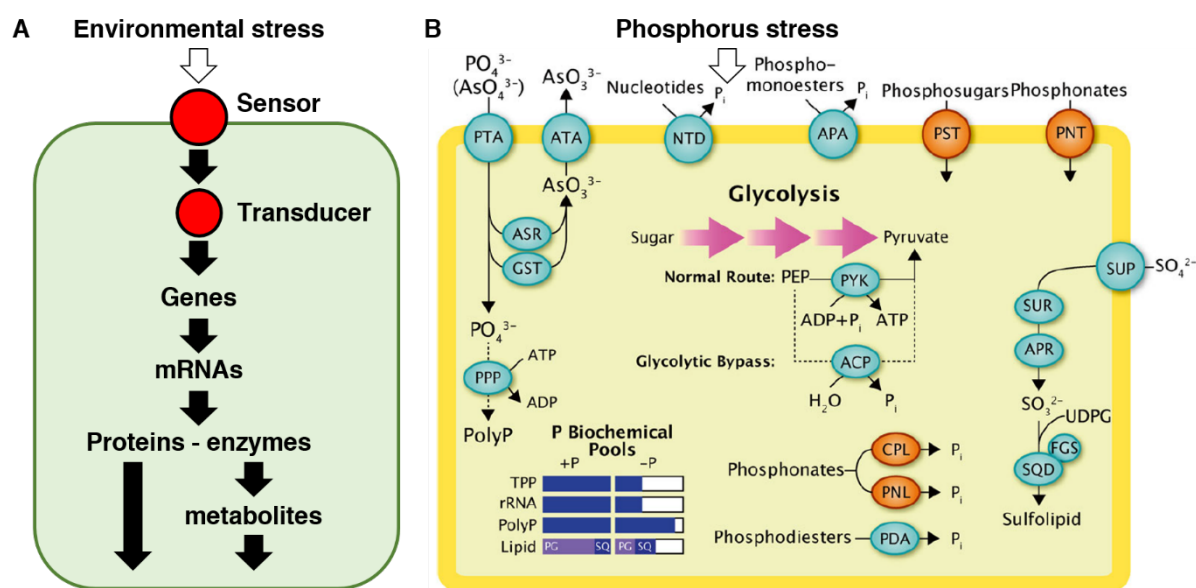


Figure 1.4 **A.** A general scheme showing the responses of a cyanobacterial cell to environmental stress Adapted from Murata and Los (Murata and Los, 2006) and Los (Los et al., 2008). **B.** A cell model illustrating common P stress responses in algae by Dyhrman (Dyhrman, 2016). Bars indicate changes in P containing biochemical pools. ACP: Acid phosphatase. APA: Alkaline phosphatase. APR: Adenosine-5'-phosphosulfate reductase. ASR: Arsenate reductase. ATA: Arsenite translocating ATPase. CPL: C-P lyase. FGS: Ferredoxin-dependent glutamate synthase. GST: Glutathione S Transferase. NTD: 5' Nucleotidase. PDA: Phosphate diesterase. PEP: Phosphoenolpyruvate. PG: Phospholipid. PNL: Generic phosphonate lyase. PNT: Phosphonate transporter. PolyP: Polyphosphate. PPP: Polyphosphate polymerase. PST: P sugar transporter. PTA: Phosphate transporter. PYK: Pyruvate kinase. rRNA: Ribosomal RNA. SQ: Sulfolipid. SQD: sulfolipid biosynthesis protein. SUP: Sulfate permease. SUR: Sulfate reductase. TPP: Total particulate phosphate. UDPG: Uridine diphosphate glucose.

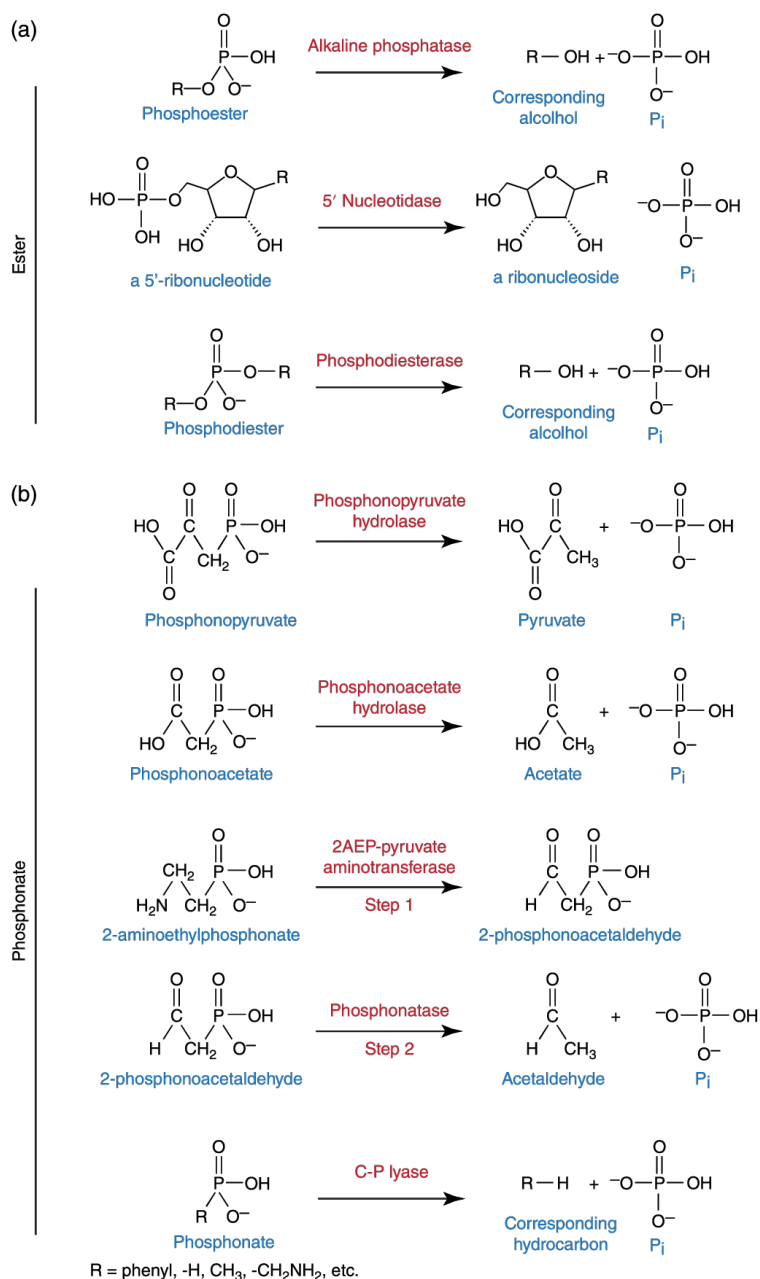


Fig 1.5 Enzymes for the hydrolysis of DOP. **(a)** Enzymes for the hydrolysis of phosphoesters. **(b)** Enzymes for the hydrolysis of phosphonate substrates. Adapted from Dyhrman (Dyhrman, 2016).

1.5.2 Iron Physiology in Phytoplankton

The role of Fe in phytoplankton has been described in the previous section (1.2; Table 1.1 and 1.2). A low supply of Fe is limiting the growth of phytoplankton in up to 30% of the global ocean (Moore et al., 2013). To cope with the low Fe availability, phytoplankton have evolved a series of response strategies. One of the obvious phenomena is the reduction in cell size of

phytoplankton under nutrient limitation (Fe included; Sunda and Huntsman, 1998). It has been reported that many phytoplankton under Fe limitation conditions can reduce their cell size to 50-80% of their cell size without impact on their growth rate (Sunda and Huntsman, 1995; Marchetti and Harrison, 2007). By reducing their cell size, phytoplankton increase their surface area to volume ratio, thus allowing for an increase in membrane transporters per unit volume and subsequently an increase in uptake rate of Fe (Luxem et al., 2017). In addition, Fe requiring proteins in phytoplankton under Fe limiting conditions can be reduced and/or substituted for proteins that do not require Fe. For example, phytoplankton under Fe limitation conditions have been shown to substitute Fe-containing protein ferredoxins, which mediate electron transfer in a series of metabolic reactions, for flavodoxins that do not require Fe (Roche et al., 1993). In addition, some diatom species are able to replace Fe-containing cytochrome c6 with Cu-containing electron transport protein plastocyanin (Peers and Price, 2006). Furthermore, phytoplankton may have the ability to adjust their photosynthesis to respond to Fe limitation. A preferential down-regulation of PSI relative to PSII has been found to occur in both prokaryotic and eukaryotic phytoplankton under Fe limiting conditions (Strzepek and Harrison, 2004; Behrenfeld and Milligan, 2013).

1.6 Metabolites and what measuring them might tell us about phytoplankton in the ocean

Metabolites are small molecules with the molecular weight < 1500 Daltons as intermediates or end products of cellular metabolism (Fiehn, 2002). Small metabolites can be major nutrient, and/or energy sources for some heterotrophs in the ocean (Johnson et al., 2016). Furthermore, metabolites can play a key role in maintaining the interactions between phytoplankton and

bacteria (Amin et al., 2015; Bertrand et al., 2015; Durham et al., 2015; Heal et al., 2017). Metabolomics is a powerful tool to explore the physiology and chemical ecology of marine organisms, especially marine organisms under laboratory conditions (Johnson et al., 2016; Durham et al., 2017; Kujawinski et al., 2017; Heal et al., 2019; Dawson et al., 2020; Johnson, 2021). Cell metabolism is highly plastic, responding to environmental conditions in marine eukaryotic phytoplankton under variable P availability (Kujawinski et al., 2017). Moreover, the composition of metabolites in phytoplankton cells is regulated by their growth phase (Barofsky et al., 2009, 2010; Vidoudez and Pohnert, 2012; Fiore et al., 2015; Matusz and Pohnert, 2015). Whilst the abundance of intracellular proteins, lipids and nucleic acids in *Trichodesmium* has been demonstrated to be regulated by P and Fe limitation (Walworth et al., 2016; Kujawinski et al., 2017), metabolites such as some specific nucleic acids remain uninvestigated.

1.7 The exponentially fed batch culture

Batch culture or semi-continuous culture methods are commonly used to investigate nutrient requirements and limitation of marine phytoplankton (e.g. Sunda, 2012; Walworth et al., 2016; Boatman et al., 2018). These culture methods are usually easier to maintain than other methods and can provide opportunities to take relatively large sample volume periodically, while the pulsed supply of medium with the limiting nutrient may alter the competitive outcome in experiments (Tilman, 1981; Sommer, 1986). A few studies applied continuous culture methods on the investigation of nutrient limitation in marine phytoplankton (Wilhelm and Trick, 1995; Pickell et al., 2009; Trick et al., 2010; Spackeen et al., 2018). The continuous culture methods such as the chemostat method have the disadvantage that they cannot produce large volumes of sample and are difficult to maintain, which may lead to contamination during the experiment

(Bull, 2010).

The exponentially fed batch (EFB) culture is a good alternative method to chemostats (Fig 1.6; Fischer et al., 2014). The EFB culture system has a continuous inflow but no outflow. The culture medium is added proportionally to the culture bottles and the speed of medium supply increases exponentially over time to compensate for the larger overall culture volume and maintain constant dilution (Fischer et al., 2014). As there is no outflow in the EFB culture system, the volume of the medium thus increases exponentially until sampling, as long as a constant dilution rate is set, thus a relatively large volume of samples can be obtained by using this method. Furthermore, the EFB culture system allows for strict control of trace metal contamination (Marki et al., 2020), which is important for the study of nutrient limitation in phytoplankton. I therefore applied trace metal clean conditions with EFB cultures throughout the experiments presented in this thesis.

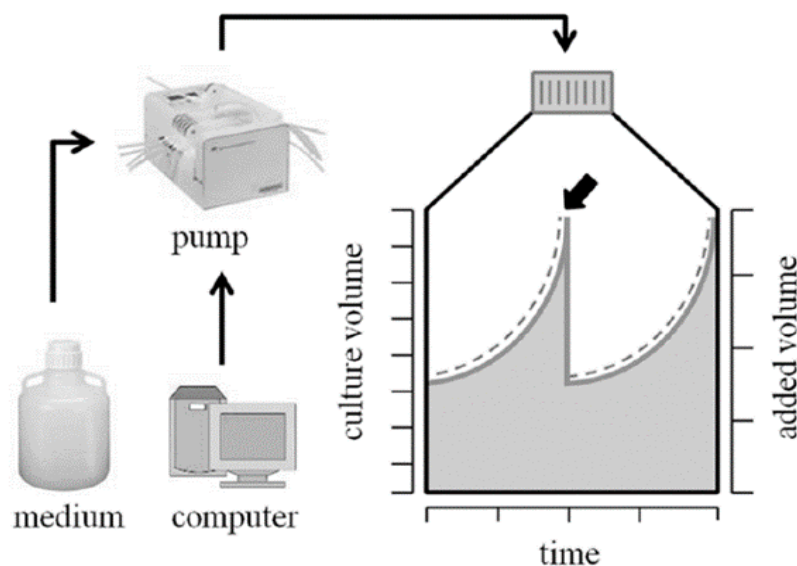


Fig 1.6 The exponentially fed batch culture (Fischer et al., 2014).

1.8 Thesis objectives

My aim throughout this thesis was to explore the relative roles of DOP, Fe and Zn on the growth

and responses of *Trichodesmium*. *Trichodesmium* is a colonial diazotrophic cyanobacterium that occurs in the oligotrophic (sub-)tropical ocean. It is likely that P and/or Fe limit the growth and N₂ fixation rate of *Trichodesmium*, and it has been hypothesized that the limiting nutrient differs between ocean basins. Phosphorus is an essential nutrient for all life on earth, but in some (sub-)tropical regions the concentrations of DIP can be depleted, potentially to limiting levels. In these regions, marine microbes, including *Trichodesmium* are able to utilize the more replete DOP pool with the participation of a series of enzymes such as AP. AP is a metalloenzyme, requiring either Zn (Kim and Wyckoff, 1991), or more recently discovered, Fe (Rodriguez et al., 2014; Yong et al., 2014). Alkaline phosphorus activity might therefore be limited by the availability of these trace metals (Mahaffey et al., 2014; Browning et al., 2017b). Other than AP, many other P-metabolizing enzymes are also metalloenzymes, requiring metal cofactors (Duhamel et al., 2021). Through this, an emerging view is that the oceanic cycles of P and trace elements are intimately connected. In turn, the level of P stress might be a major factor regulating the oceanic cycles of trace elements. This is expected to be particularly important for N₂ fixing microbes, diazotrophs, as they are often under P limitation when the rest of the community is N limited. To date, however, there is relatively limited evidence demonstrating how trace element quotas of oceanic microbes respond to P limitation (Liu et al., 2011). I therefore undertook a project to conduct EFB of *Trichodesmium*, varying the supply of P sources, Fe and Zn. Chapter 2 presents the effects of different P sources on the growth of the diazotrophic cyanobacteria *Trichodesmium* and the discussion on our finding of P limitation shows a more than trebling of zinc requirements in *Trichodesmium*. Chapter 3 presents the impact of the relative availability of P and Fe sources on cellular elemental quotas, APA and particulate metabolites in *Trichodesmium*. Chapter 4 presents the impact of the relative

availability of P sources and Zn on cellular elemental quotas and APA.

Chapter 2. Phosphorus limitation enhances diazotroph zinc quotas

This chapter was published as: Wang, X., Browning, T. J., Achterberg, E. P., and Gledhill, M. (2022). Phosphorus Limitation Enhances Diazotroph Zinc Quotas. *Front. Microbiol.* 13, 1–9. doi:10.3389/fmicb.2022.853519.

Abstract

Trichodesmium spp. is a colonial diazotrophic cyanobacterium found in the oligotrophic (sub)tropical oceans, where dissolved inorganic phosphorus (DIP) can be depleted. To cope with low P concentrations, P can be scavenged from the dissolved organic P (DOP) pool. This requires deployment of multiple enzymes that are activated by trace metals, potentially enhancing metal requirements under stronger P limitation. To test this, I grew *Trichodesmium* under trace-metal-controlled conditions, where P was supplied as either DIP or DOP (methylphosphonic acid). Mean steady state biomass under the DOP treatment was only 40% of that grown under equivalent DIP supply, carbon normalized alkaline phosphorus activity was elevated 4-fold, and the zinc (Zn): carbon ratio was elevated 3.5-fold. This finding matches the known, dominant Zn requirement across a diversity of enzymes involved in P stress responses and supports an important interaction in the oceanic cycles of these two nutrients.

2.1 Introduction

Bioavailable nitrogen (N) is the limiting factor for phytoplankton growth throughout the majority of the (sub)tropical oceans (Moore et al., 2013). Diazotrophs, N₂ fixing microbes, supply new bioavailable N to such environments, thereby increasing productivity of the whole community (Mahaffey, 2005). In regions where N₂ fixation is enhanced, dissolved inorganic phosphorus (DIP) is typically strongly drawn down (Martiny et al., 2019), often becoming growth-limiting for diazotrophs and co-limiting for the rest of the phytoplankton community (Moore et al., 2013).

In addition to DIP, P is also available as dissolved organic P (DOP), which accounts for up to 70-90% of the total dissolved P in surface waters of low DIP regions (Karl and Björkman, 2002). DOP utilization is mediated by enzymes that liberate DIP (Dyhrman et al., 2006a); these include phosphoester hydrolyzing enzymes (e.g., alkaline phosphatase (AP), phosphodiesterase and 5' nucleotidase) and phosphonate catabolic enzymes (e.g., C-P lyase, substrate-specific enzymes including phosphonoacetate hydrolase and phosphonatase). Among these, several are metalloenzymes, requiring metal cofactors (Duhamel et al., 2021). Specifically, (i) AP enzymes require zinc (Zn) and magnesium (PhoA; Kim and Wyckoff 1991), or calcium and iron (Fe) (PhoD/X; Yong et al. 2014; Rodriguez et al. 2014); (ii) Phosphonoacetate hydrolases require Zn (McGrath et al., 2013); and (iii) C-P lyases contain Zn and Fe (Stosiek et al., 2020).

Alongside playing a role in regulating the rate of P acquisition from the DOP pool (Mahaffey et al., 2014; Browning et al., 2017b), the trace element requirement for P releasing enzymes will hence also control the quotas of these elements in phytoplankton as a function of P

limitation status. Altered trace element quotas should in turn feedback to the inventories and cycling of these elements in seawater (Duhamel et al., 2021). Clear evidence for this is however lacking. In this study, a new, trace-metal-clean culturing approach was used to examine effects of different P sources on growth of the diazotrophic cyanobacteria *Trichodesmium*. The findings provide evidence for changes in micronutrient requirements, which are consistent with the diverse array of mechanisms employed by marine microbes to alleviate P stress.

2.2 Materials and methods

Cultures. To examine effects of different P sources on growth of the diazotrophic cyanobacteria *Trichodesmium* ISM101, I cultured *Trichodesmium* ISM101 with 5 μM DIP and 5 μM methylphosphonate acid (MPA) separately in triplicates using exponentially fed batch (EFB) culture system for 30 days. EFB cultures were carried out as described by Marki et al. (2020) and Fischer et al. (2014). For both treatments, *Trichodesmium* was cultured with 5 μM DIP prior to the start of this experiment. At the beginning of the experiment, the medium for one treatment was replaced with medium with 5 μM MPA as the sole P source, the other treatment being kept at 5 μM DIP. Throughout the study I followed trace metal clean protocols (Sunda and Huntsman, 2005). The cultures were maintained in EFB cultures at 25°C on a 12h/12h light/dark cycle at 140 $\mu\text{mol photons m}^{-2} \text{ s}^{-1}$ in YBCII media (Chen et al., 1996) with amendment phosphorus concentration (5 μM) and Fe concentration (40 nM). YBCII medium was prepared with ultrapure water (Ultrapure, MQ; $\leq 18 \text{ M}\Omega \text{ cm}^{-1}$; Millipore) and analytical reagent grade salts (Table 2.1). YBCII medium was adjusted to pH 7.8-8.1 by addition of 0.01 M sodium hydroxide and filter sterilised with disposable rapid flow filter units (PES, 0.1 μm , Nalgene). 10 L high density polyethylene carboys (Nalgene) were used for the YBCII culture medium reservoir. The

initial volume of the culture was 1400 mL. Fresh medium was pumped into sterile polycarbonate culture bottles (2000 mL, Nalgene) maintaining a constant dilution rate of 0.1 d^{-1} through narrow bore polypropylene tubing (inner diameter 0.51 mm, Ismaprene, Pharmed) using a peristaltic pump (IPC-N, Ismatec). The peristaltic pump was controlled by a programmable microcontroller (Raspberry Pi3), which automatically increased the flow rate each hour in relation to the real time culture volume. The dilution rate employed together with the starting volume allowed a single time point recovery of ~500 mL of sample every three days. All sample collection and medium preparation was carried out in a laminar flow hood equipped with a high efficiency particulate air filter, located within a trace-metal-clean laboratory.

Table 2.1 Modified YBCII media recipe used in the experiment

Components	Concentration in media (mol L ⁻¹)
Major salts	
NaCl	0.42
KCl	0.01
NaHCO ₃	0.0025
H ₃ BO ₃	0.00058
KBr	0.00097
NaF	0.00007
MgSO ₄	0.025
MgCl ₂	0.02
CaCl ₂	0.01
SrCl ₂	0.000065
LiCl	0.03
Macronutrients	
Na ₂ EDTA·2H ₂ O	2.0×10 ⁻⁶
CuSO ₄ ·5H ₂ O	8.0×10 ⁻⁹
ZnSO ₄ ·7H ₂ O	2.0×10 ⁻⁸
CoCl ₂ ·6H ₂ O	8.0×10 ⁻⁹
MnCl ₂ ·4H ₂ O	1.8×10 ⁻⁸
Na ₂ MoO ₄ ·2H ₂ O	1.0×10 ⁻⁷
NiSO ₄ ·6H ₂ O	2.0×10 ⁻⁸
Na ₂ SeO ₃	1.0×10 ⁻⁸
FeEDTA	4.0×10 ⁻⁸
NaH ₂ PO ₄	
Vitamins	
Thiamine	3.0×10 ⁻⁷
Biotin	2.0×10 ⁻⁹
Cyanocobalamin	3.7×10 ⁻¹⁰

Fast Repetition Rate fluorescence. Fast Repetition Rate fluorometry of *Trichodesmium* ISM101 cultures was conducted throughout the whole culture period with a FASTOcean sensor equipped with a FASTAct laboratory system (Chlesea Technologies Group). Samples were dark acclimated for 20–30 minutes in the culture cabinet prior to measurements. Recovery of minimum fluorescence (F_o) and maximum fluorescence (F_m) allowed determination of the potential photochemical efficiency of photosystem II (PSII) ($F_v/F_m = (F_m - F_o)/F_m$).

Alkaline phosphatase activities (APA). Whole water APA rates were measured using the fluorometric substrate MUF-P (Sigma-Aldrich) following the protocol of Ammerman (1993). 100 mM concentrated MUF-P and MUF (Sigma-Aldrich) stock solution was prepared by dissolving MUF-P and MUF into 2-methoxyethanol. Working stocks (100 μ M) were made daily by diluting this concentrated stock with ultrapure water. The assays were started by adding 100 μ L of MUF-P to 5 mL samples in replicate 15 mL tubes to yield a final substrate concentration of 2 μ M. A 150 μ L subsample was transferred into a 96 well plate immediately from the mixed sample. 50 μ L of filtered 50 mM borate buffer (pH 10.8) was added to the subsample in the well plate and mixed to a final pH >10. APA was measured on a temperature-controlled (25 °C) plate reader (FLX800TBI, BioTek) with Gen 5 software using an excitation wavelength of 365 nm and an emission wavelength of 455 nm. Fluorescence measurements were performed at $t=0$, 1, and 2 h. APA (h^{-1}) was calculated as the fluorescence of a 2 μ M MUF divided by the initial ($t=0$ to $t=2$ h) slope of fluorescence time course (fluorescence per hour). Regular ultrapure blanks and paraformaldehyde-killed controls were conducted and generally yielded fluorescence values similar to $t = 0$ readings.

Chlorophyll A. 20 mL of sample was filtered onto glass fiber filters (25 mm, 0.7 μ m,

Fisherbrand) and stored in a -80°C freezer until analysis. Samples were extracted for 24 hours in 10 mL 90% acetone in a -20°C freezer in the dark. Samples were brought to room temperature in the dark before measurement on a calibrated Turner Designs trilogy fluorometer following the method of Welschmeyer (1994).

Nutrients. Samples for analysis of dissolved inorganic nitrate + nitrite and P (15 mL) were filtered through glass fiber filters (25 mm, $0.7\ \mu\text{m}$, Fisherbrand) under low pressure (200 mpa). Samples were stored in polypropylene tubes (15 mL, Fisherbrand) at -20°C until analysis and then analysed using a SEAL QuAAtro nutrient autoanalyser system (SEAL Analytical). Samples for analysis of total dissolved P (TDP; 50 mL) were filtered through sterile PES syringe filters ($0.2\ \mu\text{m}$, Fisherbrand). Samples were stored in polypropylene tubes (50 mL, Fisherbrand) at -20°C . Prior to analysis, TDP samples and blanks were digested under elevated pressure (1.5 bar) and temperature (120°C) for 30 min following addition of the oxidizing reagent Oxisolv (Merck), and then analysed using a SEAL QuAAtro nutrient autoanalyser system (SEAL Analytical). The DOP concentration was subsequently calculated as $\text{DOP} = \text{TDP} - \text{DIP}$. After measuring 10 samples of YBCII medium with a fixed TDP concentration of $5\ \mu\text{M}$, I determined that the mean oxidation efficiency of TDP during the measurement was $86.35 \pm 11.24\ \%$. The DOP data were therefore corrected upwards for this oxidation efficiency.

Particulate organic C/N. Particulate organic C/N concentrations were determined by filtering 50 mL sample through pre-combusted (500°C , 12 h) glass fiber filters (25 mm, $0.7\ \mu\text{m}$, Fisherbrand) under low pressure (200 mpa). Filters were stored frozen at -20°C . Prior to analysis, filters were dried at 50°C for 12 hours. After drying, filters were wrapped in tin boats ($8 \times 8 \times 15\ \text{mm}$) and put in a well plate and stored in desiccator. Samples and blanks were

analyzed using an elemental analyzer (Eurovector EA3000 Elemental Analyzer) with Callidus version 5.1 software.

Particulate element concentrations. 50 mL of sample was filtered onto acid-cleaned (10% HCl) polyethersulfone (PES) membrane filters (25 mm, 0.8 μm , PALL). Filters were frozen and stored at -20 °C until digestion. Cell digestions were carried out as described by Honey et al. (2013): filters were placed in acid-washed (20% HNO_3) 15 mL PFA digestion vials with 2 mL of concentrated redistilled HNO_3 (Savillex, QMX) and heated to 120°C for 24 h. The filter was removed from the vial and the HNO_3 evaporated off (75°C, overnight). The residue was dissolved in 3 mL of 1% HNO_3 and spiked with indium (4 $\mu\text{g L}^{-1}$) as an internal standard. The samples were then centrifuged at 14,000 rpm (Centrifuge 5430R, Eppendorf) for 10 minutes and the upper supernatant was taken for determination by inductively coupled plasma mass spectrometry (Element XR, ThermoFisher), using prepared elemental standard calibrations for quantification.

2.3 Results and Discussion

I tested for interactions between P limitation, DOP availability, and cellular elemental quotas in *Trichodesmium* ISM101 under two P supply treatments: (i) 5 μM DIP and (ii) 5 μM MPA, a phosphonate synthesized by marine microbes (Metcalf et al., 2012). Experiments were conducted using high volumes (2 L) in triplicate under trace-metal-clean conditions using an exponentially fed batch culture approach (Fischer et al., 2014; Marki et al., 2020), which allows for regular harvesting of sufficient biomass required for bulk phytoplankton elemental analysis. *Trichodesmium* biomass (particulate organic carbon (POC)) within the DIP treatment increased 1.4-fold over 18 days and showed no significant changes from day 12 (Quade post hoc test;

$p < 0.05$. Fig 2.1a), whereupon I assumed that growth had reached an approximate steady state matching the dilution rate of the culture (0.1 d^{-1}) and biomass concentration was dictated by the concentration of the most deficient nutrient in the culture medium (Fischer et al., 2014). The biomass of the MPA treatment showed a more complex trend, with POC ultimately decreasing to 0.7 times the initial value within 21 days, after which no significant changes were observed and steady state was assumed (Quade post hoc test; $p < 0.05$. Fig 2.1a).

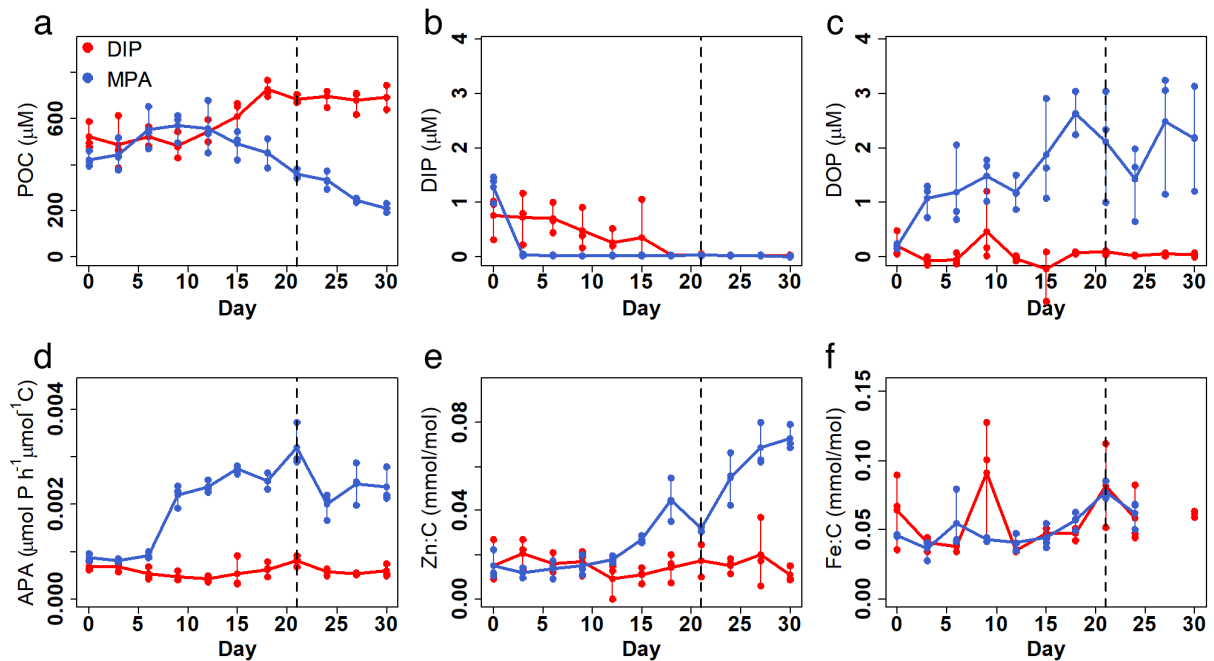


Fig 2.1 Responses of *Trichodesmium* ISM101 to DIP and MPA treatment. **a**, Particulate organic carbon (POC). **b**, dissolved inorganic phosphorus (DIP). **c**, dissolved organic phosphorus (DOP). **d**, POC-normalized APA. **e**, Fe:C ratio. **f**, Zn:C ratio. Points show triplicate measurements every three days, lines map the change in the mean value with time. Time period to the right side of the dashed line is considered to be the steady state.

Concentrations of DIP for both treatments were fully depleted at steady state (0.03 ± 0.01 and $0.02 \pm 0.01 \mu\text{M}$; Fig 2.1b), implying that for both sets of cultures the low P availability limited biomass. Nevertheless, three lines of evidence suggested that (i) the level of P stress in the MPA treatments was higher than that of the DIP treatment, and (ii) that this was due to a situation approaching P-Fe co-limitation in the DIP treatment. Firstly, APA was 4-fold higher in the MPA

treatment, implying stronger P stress in this treatment (Fig 2.1d; Mahaffey et al. 2014). Secondly, the apparent photochemical PSII efficiency (F_v/F_m) was significantly lower in the DIP treatment (Fig 2.3b). F_v/F_m has been previously demonstrated to remain high under steady state P limitation (Kruskopf and Flynn, 2006), whereas under steady state Fe limitation large decreases are observed (Schrader et al., 2011). Thirdly, mean steady state POC per filament in the DIP treatment was 45% lower than the MPA treatment (pairwise Wilcox test, $p < 0.05$), which I hypothesize was related to filament length, as *Trichodesmium* filaments have been shown to be significantly smaller under limitation by Fe in comparison to P (Tzubari et al., 2018). Fourth, the mean steady state particulate Fe concentration in DIP treatment was 46 ± 16 nM, indicating that all of the supplied Fe in the medium (40 nM) was taken up by *Trichodesmium*. In turn, stronger P limitation in the MPA treatment could be ascribed to lower accessibility of this P source (Dyhrman and Haley, 2006; Sosa et al., 2019), with dissolved MPA concentrations in this treatment remaining at around 40% of the supplied concentration (2.05 ± 0.93 μ M; Fig 2.1c).

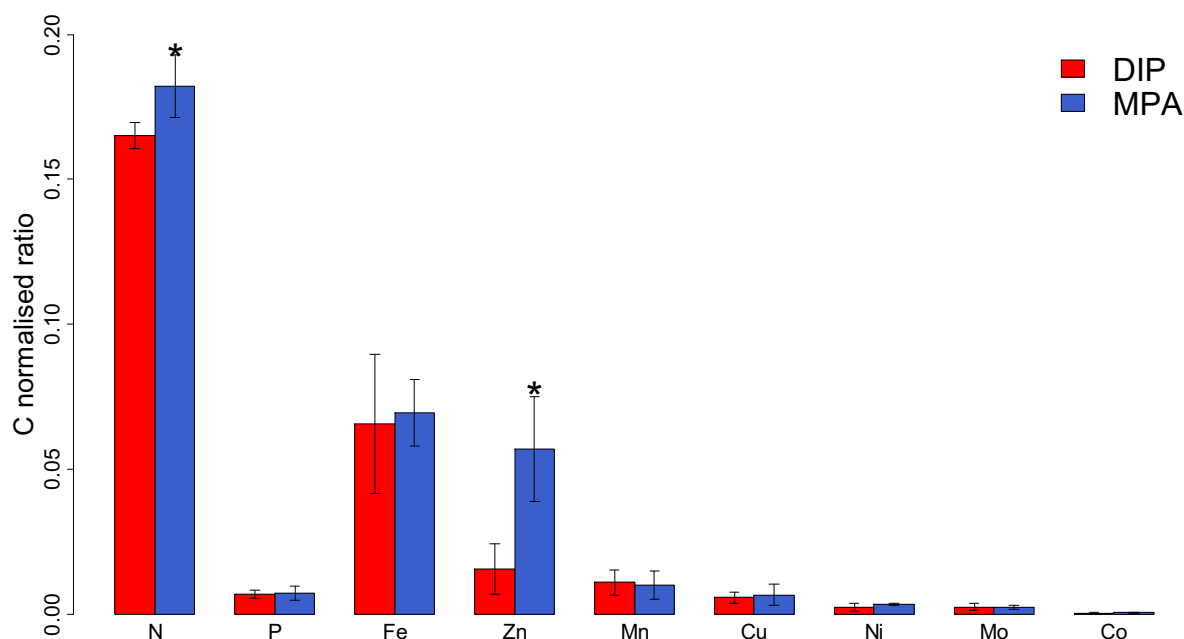


Fig 2.2 Elemental composition of *Trichodesmium* ISM101 at steady state (day \geq 21) grown under supply of DIP and MPA. Bars show the mean steady state elemental ratios, error bars are the standard deviation (n=7–12). N and P are in units of mol:mol; all others are in units of mmol:mol. * Indicates statistically significant differences between treatments (pairwise Wilcox test, $p < 0.05$). I note that mean steady state particulate Fe: C ratios were similar to those found in the literature for *Trichodesmium* (65.6 ± 24 μ mol:mol in comparison to 69.5 ± 3.48 μ mol:mol in Berman-Frank et al., 2001).

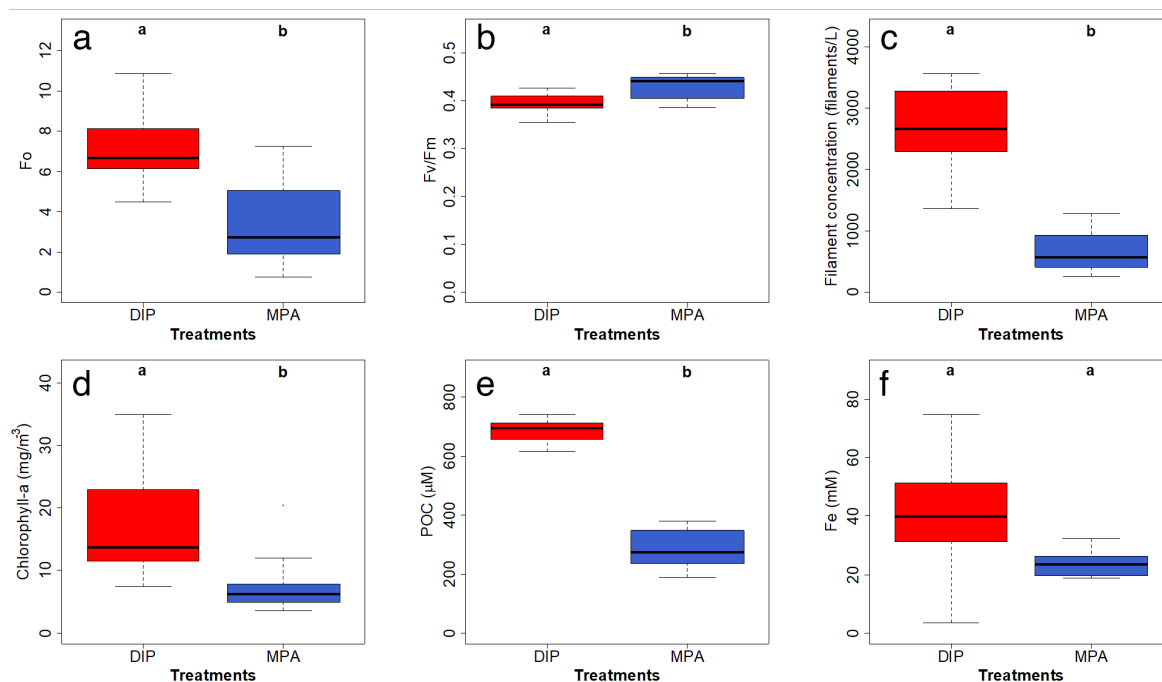


Fig 2.3 Parameters determined at steady state (day \geq 21) for *Trichodesmium* ISM101 growing with a constant dilution rate of 0.1 d^{-1} with 2 different P sources (DIP and MPA). **a**, F_0 . **b**, F_v/F_m . **c**, Filament concentration. **d**, Chlorophyll a concentration. **e**, POC. **f**, particulate Fe concentration. Letters indicate statistically significant differences between treatments (pairwise Wilcox test, $p < 0.05$).

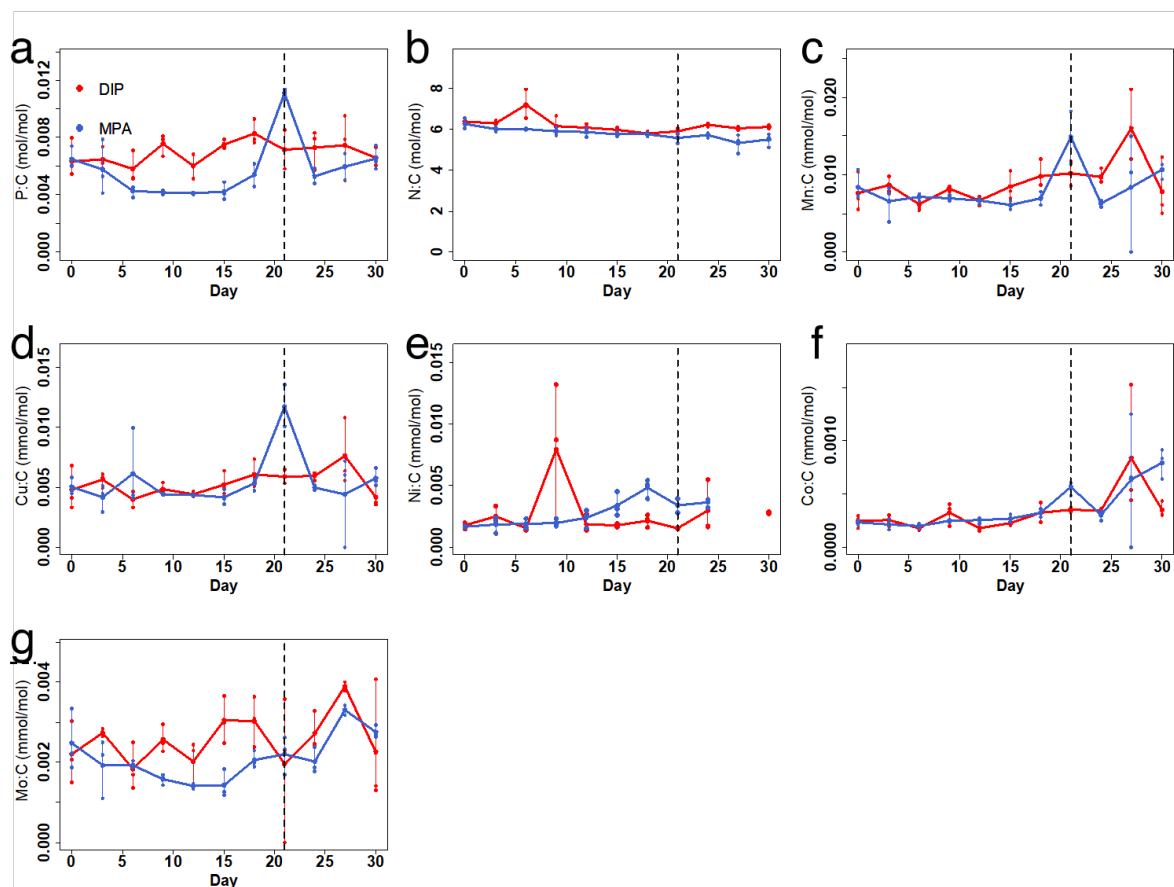


Fig 2.4 Elemental ratios determined throughout the duration of the exponentially fed batch culture at steady state (day \geq 21) for *Trichodesmium* ISM101 growing with a constant dilution rate of 0.1 d $^{-1}$ with 2 different P sources (DIP and MPA). Points show triplicate measurements every three days, lines map the change in the mean value with time, right side of the dashed line is considered to be the steady state.

Differences in elemental composition between the two treatments at steady state were minimal for all elements apart from Zn (Fig 2.2 and 2.4), which in contrast showed 3.5-fold elevated Zn:C in the MPA treatment (0.057 ± 0.018 mmol/mol C in comparison to 0.016 ± 0.009 mmol/mol C in the DIP treatment). This finding is consistent with a recent evaluation of trace element requirements for mechanisms to cope with P limitation (Duhamel et al., 2021): of all the trace elements assessed, Zn stands out as having the greatest demand, with elevated requirements in comparison to all other metals across a diversity of transferases, hydrolases, lyases, isomerases, ligases and translocases (Duhamel et al., 2021). With these set of observations, I cannot decouple the specific cellular sinks for Zn that occurred within the MPA

treatment. However, notable was that APA in MPA treatment increased from day 6 and stabilized from day 9 (Fig 2.1d), whereas the increase in Zn:C was later, from day 12, and did not reach a clear plateau over the experiment duration (30 days; Fig 2.1f). The latter observation suggests that the Zn enhancement was not simply due to the well-characterized enhanced production of AP enzymes under greater P stress (and specifically, Zn-requiring PhoA; (Mahaffey et al., 2014)), but rather to a diversity of strategies to cope with stronger P limitation (Wei et al., 2018; Duhamel et al., 2021). Furthermore, the lack of increase in Fe requirements under stronger P limitation is inconsistent with the expectation of more dominant roles of PhoX and PhoD over PhoA (Luo et al., 2011), but is consistent with (i) the Fe requirement for these enzymes being relatively minor in comparison to overall cellular Fe demands and, (ii) the lower Fe—but dominant Zn—requirement in a variety of other, non-AP, enzymes produced in response to low P (Duhamel et al., 2021).

Our observations of enhanced Zn quotas under stronger P limitation in culture are consistent with available field observations (Tovar-Sanchez et al., 2006; Twining et al., 2010). Tovar-Sanchez et al. (2006) found Zn:P quotas of *Trichodesmium* in the low P eastern Subtropical North Atlantic were $\sim 8.6 \text{ mmol mol}^{-1}$, very close to mean steady state Zn:P quota I observed in the MPA treatment ($8 \pm 3.7 \text{ mmol mol}^{-1}$). Additionally, Twining et al. (2010) found that the Zn quotas of *Synechococcus* in Sargasso Sea eddies with lower DIP supply were roughly 20 times higher than those with higher DIP supply. Together, our observations in culture and these findings in the field suggest a crucial level of interaction between the cycles of these two nutrients in the ocean. The impacts of such an interaction might be exacerbated in a future ocean, where increasing atmospheric N inputs could drive a shift towards more widespread and

stronger P stress (Moore et al., 2013).

Chapter 3. Phosphorus sources affect the elemental stoichiometry of *Trichodesmium* under Fe limitation

Abstract

Trichodesmium spp. is a colonial diazotrophic cyanobacterium found in the oligotrophic (sub)tropical oceans, where the distribution of *Trichodesmium* is strongly regulated by the availability of phosphorus (P) and iron (Fe). The bulk carbon (C): nitrogen (N): P elemental composition of phytoplankton has previously been shown to depart from classical 'Redfield' values under nutrient limitation conditions. I hypothesized that the abundance of intracellular metabolites and the extended elemental stoichiometry of *Trichodesmium*, including a range of trace elements, is variable in response to different conditions of P and Fe limitation that are found in the ocean. To test this, I grew *Trichodesmium* under trace-metal-controlled conditions, where P was supplied as either dissolved inorganic P (DIP) or dissolved organic P (DOP; methylphosphonic acid) from Fe depleted to elevated levels. I found that the steady state elemental stoichiometry of *Trichodesmium* under the Fe depleted condition was $(C_{106}N_{15.82}P_{0.62})_{1000}Fe_{2.26}Zn_{2.37}Mn_{1.68}Cu_{0.68}Ni_{0.31}Mo_{0.42}Co_{0.03}$ for the DIP treatment where *Trichodesmium* was under Fe limitation and $(C_{106}N_{13.89}P_{0.49})_{1000}Fe_{3.38}Zn_{2.51}Mn_{0.97}Cu_{0.52}Ni_{0.42}Mo_{0.33}Co_{0.03}$ for the MPA treatment where *Trichodesmium* was under Fe-P co-limitation. Mean steady state Fe: carbon in the DIP treatment was only 50% of that in the control treatment, and the zinc (Zn): carbon ratio was elevated 2-fold. The average elemental stoichiometry following Fe recovery was

$(C_{106}N_{16.8}P_{0.7})_{1000}Fe_{4.41}Zn_{1.44}Mn_1Cu_{0.52}Ni_{0.19}Mo_{0.3}Co_{0.03}$ for the DIP treatment and $(C_{106}N_{15.9}P_{0.73})_{1000}Fe_{7.36}Zn_{2.24}Mn_{1.08}Cu_{0.71}Ni_{0.63}Mo_{0.38}Co_{0.02}$ for the MPA treatment. No significant changes were observed in the carbon-normalized abundance of targeted metabolites produced by *Trichodesmium*, whether in the Fe depleted, Fe replete condition or transition phase from Fe depleted to Fe replete condition. These results suggest *Trichodesmium* employs different strategies to cope with Fe/P limitation, which is reflected in its elemental stoichiometry that are potentially related to changes in the abundance of Fe acquisition proteins.

3.1 Introduction

The low availability of bioavailable nitrogen (N) in surface waters of the subtropical and tropical oceans is generally considered the main limiting factor for phytoplankton growth, thus limiting the primary production, which facilitates ocean carbon sequestration (Falkowski, 1997; Moore et al., 2013). Diazotrophs, N₂ fixing microbes, can supply new bioavailable N to such environments, thereby increasing productivity. *Trichodesmium* is a dominant diazotroph species inhabiting surface waters of the low latitude oceans (Capone et al., 1997). Although recent genomic discoveries have highlighted the diversity of additional diazotrophs in the ocean (Zehr and Capone, 2020), *Trichodesmium* is still recognized as a critical contributor (Carpenter and Capone, 2008), with an estimated contribution of ~50% to the total N₂ fixed in the ocean (Capone et al., 1997; Mahaffey, 2005; Bergman et al., 2013).

In low latitude N depleted ocean regions, the distribution of *Trichodesmium* is regulated by the availability of phosphorus (P) and iron (Fe) (Moore et al. 2009; Sohm et al. 2011; Snow et al. 2015; Rouco et al., 2018; Cerdan-Garcia et al., 2021). Furthermore, recent evidence suggests that *Trichodesmium* becomes more abundant with a more strongly upregulated expression of nitrogenase genes and higher N₂ fixation rates when it is co-limited by Fe-P compared to single limitation by Fe or P (Garcia et al., 2015; Walworth et al., 2016, 2018; Held et al., 2020; Cerdan-Garcia et al., 2021). An important part of the development of this co-limitation condition is the ability of *Trichodesmium* to access a broad range of dissolved organic P (DOP) compounds with enzymes including alkaline phosphatases (APs) and C-P lyases (Dyhrman et al. 2006; Orchard et al. 2010; Morrissey and Bowler 2012; Cerdan-Garcia et al. 2021).

Previous studies have focused mainly on the availability of Fe and P in relation to growth rate, N₂ fixation rate, distribution, alkaline phosphatase activity (APA), major elemental stoichiometry, transcriptomics and proteomics of *Trichodesmium* (Chen et al., 1996; Hynes et al., 2009; Ho, 2013; Yamaguchi et al., 2016; Tzubarri et al., 2018; Frischkorn et al., 2019; Cerdan-Garcia et al., 2021). However, studies on the elemental stoichiometry which include trace metal stoichiometry of *Trichodesmium* under Fe and/or P-limited conditions are scarce (White et al., 2006a; Nuester et al., 2012). Trace metals are essential cofactors for many of the enzymes involved in the acquisition and utilization of N and P, and include Fe and Mo for N₂ fixation (Dominic et al., 2000; Tuit et al., 2004), Zn and/or Fe in APs (Kim and Wyckoff, 1991; Rodriguez et al., 2014; Yong et al., 2014), Ni for hydrogenases and superoxide dismutase (Ho et al., 2013; Tuo et al., 2020), and Cu for reductive deamination of amines and amino acids and plastocyanin (Palenik and Morel, 1991). Therefore, there is a complex set of linkages between the biological use of N, P, and trace metals in *Trichodesmium*. Determining how the elemental stoichiometry of *Trichodesmium* changes in response to changes in Fe and P limitation and under growth on different P sources is therefore critical for understanding, and ultimately, accurate modelling of N₂ fixation in the ocean.

Metabolomics is a powerful tool to explore the physiology and chemical ecology of marine organisms (Johnson et al., 2016; Durham et al., 2017; Kujawinski et al., 2017; Heal et al., 2019; Dawson et al., 2020; Johnson, 2021). Cell metabolism is highly plastic, responding to environmental conditions in marine eukaryotic phytoplankton under variable P availability (Kujawinski et al., 2017). Moreover, the composition of metabolites in phytoplankton cells is regulated by their growth phase (Barofsky et al., 2009, 2010; Vidoudez and Pohnert, 2012;

Fiore et al., 2015; Mausz and Pohnert, 2015). Whilst the abundance of intracellular proteins, lipids and nucleic acids in *Trichodesmium* have been demonstrated to be regulated by P and Fe limitation (Walworth et al., 2016; Kujawinski et al., 2017), metabolites such as some specific nucleic acids remain uninvestigated.

I tested for the impact of the relative availability of P sources and Fe on cellular elemental quotas and particulate metabolites in *Trichodesmium* ISM101. Two P sources were utilized: (i) 5 μM dissolved inorganic P (DIP) and (ii) 5 μM methylphosphonate acid (MPA), a phosphonate synthesized by marine microbes (Metcalf et al., 2012). Experiments were conducted at high volume (2 L) with triplicate replication under trace-metal-clean conditions using an exponentially fed batch culture approach (Fischer et al., 2014; Marki et al., 2020), which allows for regular harvesting of sufficient biomass required for bulk phytoplankton elemental and metabolite analysis.

3.2 Materials and methods

Cultures. To examine effects of different iron (Fe) concentrations on growth of the diazotrophic cyanobacteria *Trichodesmium* ISM101, I cultured *Trichodesmium* with 5 μM DIP and 5 μM MPA separately in triplicate under supply of Fe depleted media (4 nM; 33 days) and then Fe replete media (40 nM; 21 days) using a trace-metal-clean exponentially fed batch (EFB) culture system (Fischer et al., 2014; Marki et al., 2020). In a control treatment I cultured *Trichodesmium* with a constant media supply of 5 μM DIP and 40 nM Fe. The cultures were maintained in EFB cultures at 25°C on a 12h/12h light/dark cycle at 140 $\mu\text{mol photons m}^{-2} \text{ s}^{-1}$ in YBCII media (Chen et al., 1996). YBCII medium was prepared with ultrapure water (Ultrapure, MQ; $\leq 18 \text{ M}\Omega \text{ cm}^{-1}$; Millipore) and analytical reagent grade salts (Table 2.1). YBCII medium was

adjusted to pH 7.8-8.1 by addition of 0.01 M sodium hydroxide and filter sterilised with disposable rapid flow filter units (PES, 0.1 μm , Nalgene). Ten L high density polyethylene carboys (Nalgene) were used for the YBCII culture medium reservoir. Cultures were grown in sterile polycarbonate culture bottles (2 L, Nalgene). The initial volume of the cultures was 1400 mL into which fresh medium was pumped using narrow bore polypropylene tubing (inner diameter 0.51 mm, Ismaprene, Pharmed) with a peristaltic pump (IPC-N, Ismatec) via a filter (0.2 μm ; Sterivex). The peristaltic pump was controlled by a programmable microcontroller (Raspberry Pi3), which automatically increased the flow rate each hour in relation to the real time culture volume, thereby maintaining a constant culture dilution rate of 0.1 d⁻¹. The dilution rate employed together with the starting volume allowed a single time point recovery of ~500 mL of sample every three days. All sample collection and medium preparation was carried out in a laminar flow hood equipped with a high efficiency particulate air filter, located within a trace-metal-clean laboratory.

Fast Repetition Rate fluorometry. Fast Repetition Rate fluorometry of *Trichodesmium* ISM101 cultures was conducted throughout the whole culture period with a FASTOcean sensor equipped with a FASTAct laboratory system (Chlsea Technologies Group). Samples were dark acclimated for 20–30 minutes in the culture cabinet prior to measurements. Recovery of minimum fluorescence (F_0) and maximum fluorescence (F_m) allowed determination of the potential photochemical efficiency of photosystem II (PSII; $F_v/F_m = (F_m - F_0)/F_m$).

Alkaline phosphatase activity (APA). Whole water APA rates were measured using the fluorometric substrate MUF-P (Sigma-Aldrich) following the protocol of Ammerman (1993).

100 mM concentrated MUF-P and MUF (Sigma-Aldrich) stock solution was prepared by

dissolving MUF-P and MUF into 2-methoxyethanol. Working stocks (100 μM) were made daily by diluting this concentrated stock with ultrapure water. The assays were started by adding 100 μL of MUF-P to 5 mL samples in replicate 15 mL tubes to yield a final substrate concentration of 2 μM . A 150 μL subsample was transferred into a 96 well plate immediately from the mixed sample. 50 μL of filtered 50 mM borate buffer (pH 10.8) was added to the subsample in the well plate and mixed to a final pH >10. APA was measured on a temperature-controlled (25 $^{\circ}\text{C}$) plate reader (FLX800TBI, BioTek) with Gen 5 software using an excitation wavelength of 365 nm and an emission wavelength of 455 nm. Fluorescence measurements were performed at $t=0$, 1, and 2 h. APA (h^{-1}) was calculated as the fluorescence of a 2 μM MUF divided by the initial ($t=0$ to $t=2$ h) slope of fluorescence time course (fluorescence per hour). Regular ultrapure blanks and paraformaldehyde-killed controls were conducted and generally yielded fluorescence values similar to $t = 0$ readings.

Nutrients. Samples of dissolved inorganic nitrate + nitrite and P (15 mL) were filtered through glass fiber filters (25 mm, 0.7 μm , Fisherbrand) under low pressure (200 mpa). Samples were stored in polypropylene tubes (15 mL, Fisherbrand) at -20°C until analysis and then analysed using a SEAL QuAAtro nutrient autoanalyser system (SEAL Analytical). Samples of total dissolved P (TDP; 50 mL) were filtered through sterile PES syringe filters (0.2 μm , Fisherbrand). Samples were stored in polypropylene tubes (50 mL, Fisherbrand) at -20°C . Prior to analysis, TDP samples and blanks were digested under elevated pressure (1.5 bar) and temperature (120 $^{\circ}\text{C}$) for 30 min following addition of the oxidizing reagent Oxisolv (Merck), and then analysed using a SEAL QuAAtro nutrient autoanalyser system (SEAL Analytical). DOP concentration was subsequently calculated as $\text{DOP} = \text{TDP} - \text{DIP}$.

Particulate organic C/N. Particulate organic C/N concentrations were determined by filtering 50 mL sample through pre-combusted (500°C, 12 h) glass fiber filters (25 mm, 0.7 µm, Fisherbrand) under low pressure (200 mpa). Filters were stored frozen at -20 °C. Prior to analysis, filters were dried at 50 °C for 12 hours. After drying, filters were wrapped in tin boats (8×8×15 mm) and put in a well plate and stored in desiccator. Samples and blanks were analyzed using an elemental analyzer (Eurovector EA3000 Elemental Analyzer) with Callidus version 5.1 software.

Particulate element concentration. 50 mL of sample was filtered onto acid-cleaned (10% HCl) PES membrane filters (25 mm, 0.8 µm, PALL). Filters were frozen and stored at -20 °C until digestion. For cell digestion, filters were placed in acid-washed (20% HNO₃) 15 mL PFA digestion vials with 2 mL of concentrated redistilled HNO₃ (Savillex, QMX) and heated to 120°C for 24 h. The filter was removed from the vial and the HNO₃ evaporated off (75°C, overnight). The residue was dissolved in 3 mL of 1% HNO₃ and spiked with indium (4 µg L⁻¹) as an internal standard. The samples were then centrifuged at 14,000 rpm (Centrifuge 5430R, Eppendorf) for 10 minutes and the upper supernatant was taken for determination by inductively coupled plasma mass spectrometry (Element XR, ThermoFisher), using prepared elemental standard calibrations for quantification.

Metabolite concentration. 250 mL of sample was transferred to bioprocessing bag (Standard Flexboy, 500 mL). Before filtration, 250 µL optima grade formic acid together with 25 µL internal standard (860 µg/L D6 biotin, 630 µg/L C13N15 Riboflavin) was added to 250 mL of sample. Sterivex filter unit was connected to bioprocessing bag via a PharMed BPT tubing (PharMed, 1m). The bioprocessing bag was then suspended two meters above the ground to

complete the filtration using gravity. Filters were frozen and stored at -80 °C until elution. For sample elution, 2 mL of cold (-20 °C) extraction solvent was added to each sterivex to cover the filter pieces (40:40:20 acetonitrile: methanol: 0.1 M formic acid), ultrapure water was used throughout, methanol, acetonitrile and formic acid were of LCMS grade (Optima, Fisher Scientific). Sterivex filter units with Luer ends capped with Luer stoppers were placed in ultrasonic bath filled with ice with the Luer lock end down, the ultra-sonication lasted for 20 min at 4 °C. After ultra-sonication, sample was pushed into 2 mL pre-weighed Eppendorf vial and vials were placed in centrifugal evaporator and the solvents evaporated overnight, the weight of the sample after evaporation ranged from 0.1g to 0.4 g. 50 µL sample was transferred to a HPLC vial and spiked with 5 µL Yeast extract containing ¹³C labelled metabolites (U-13C, Cambridge Isotope Laboratories, 98%). Additional samples for quality control (QC) were analyzed in all experiments (Kido Soule et al., 2015). These QC samples consisted of a mixed standard of authentic metabolites and a pooled sample consisting of aliquots of each sample (50 µL). Metabolites were separated by reversed phase high performance liquid chromatography (HPLC; Synergi Fusion 4 µm, 2×150 mm) and detected by electrospray ionization mass spectrometry (ESI-MS; ThermoFisher Q-Exactive). Solvents were (A) 10 mM ammonium formate: 5% methanol and (B) methanol. Metabolites were separated using a delayed linear gradient elution that started at 100% A, ramped from 100 to 50% A at 9 min and then to 100% B at 12 min. Elution of metabolites was followed by a column wash with 100% B (2 min), and then a return to starting conditions and a 4 min column equilibration prior to injection of the next sample. Peak areas and retention times for known metabolites were processed in mzmime (<http://mzmime.github.io/>) using a targeted feature detection approach, targeted metabolites are listed in Table 3.1. The concentrations of ¹³C labelled metabolites in the yeast extract was

quantified for each sample batch with unlabeled standards and this concentration was then used to determine the concentration of each metabolite in the sample from the ratio of the isotopes. For compounds lacking unlabeled standards, I used the ^{13}C labelled metabolite to normalize the response across all the samples.

Table 3.1 Targeted metabolites and their class

Name	Class
Adenosine diphosphate	Nucleotide
Adenosine monophosphate	Nucleotide
Arginine	Amino acid
Adenosine	Nucleoside
Choline	Nutrient
Flavin mononucleotide	Vitamin
Glutamate	Amino acid
Guanine	Nucleotide
Guanosine	Nucleoside
Histidine	Amino acid
Isoleucine	Amino acid
Kynurenine	Amino acid
Leucine	Amino acid
5'-Deoxy-5'-methylthioadenosine	Nucleo
Nicotinamide	Vitamin
NAD ⁺	Vitamin
Phenylalanine	Amino acid
Proline	Amino acid
Riboflavin	Vitamin
Thiamine	Vitamin
Tryptophan	Amino acid

3.3 Results and Discussion

3.3.1 *Trichodesmium* responses to Fe availability

Trichodesmium carbon biomass under the Fe depleted condition decreased to 0.55 and 0.61 times the initial values within 24 days in the DIP and MPA treatments respectively, after which no significant changes were observed (Quade post hoc test; $p < 0.05$. Fig 3.1a). At this point (days 24–33) I assumed that growth had reached an approximate steady state matching the dilution rate of the culture (0.1 d^{-1}). The biomass concentration at this point is dictated by the concentration of the most limiting nutrient in the culture medium (Fischer et al., 2014), which in the case of the Fe depletion experiment was Fe (DIP treatment), or both Fe and bioavailable P (MPA treatment; see discussion below). After restoring the Fe concentration in the medium to 40 nM on day 33, *Trichodesmium* biomass within both treatments increased gradually to 1.9 and 1.02 fold of the steady state Fe limited values, respectively (Fig 3.1a). After day 42 (DIP) and 48 (MPA), no significant biomass changes were observed and *Trichodesmium* was assumed to have recovered from Fe limitation (Quade post hoc test; $p < 0.05$. Fig 3.1a). The *Trichodesmium* recovery time from the Fe depletion was therefore 9 and 15 days for DIP and MPA, respectively (Fig 3.1a).

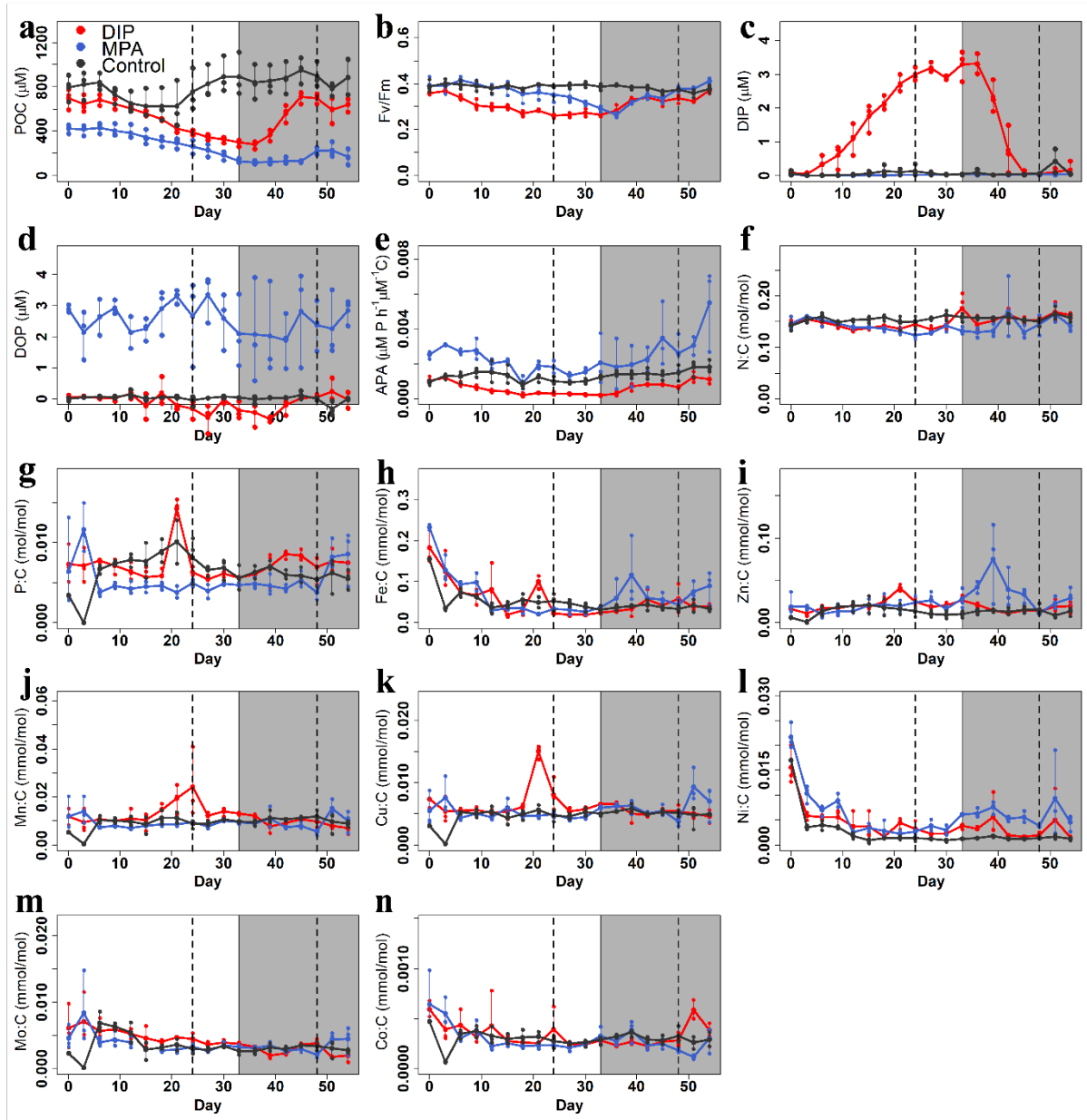


Fig 3.1 Responses of *Trichodesmium* ISM101 under DIP and MPA phosphorus sources to variations in Fe supply. Points show triplicate measurements every three days, lines map the change in the mean value with time. The left part without shading indicates period where Fe depleted (4 nM) media was supplied. The shaded region indicates where the high Fe (40 nM) media was supplied. The time period to the right side of the dashed line for each condition is considered here to be at steady state (Quade post hoc test; $p < 0.05$).

The nutrient limitation status of each treatment through the Fe depletion and Fe recovery phases could be dissected via observed changes in DIP concentrations, F_v/F_m and APA (Fig 3.1b, c and e). At time $t=0$, *Trichodesmium* in both the DIP and MPA treatments were assumed to be under P limitation, with both treatments having fully depleted DIP concentrations ($< 0.1 \mu\text{M}$; Fig 3.1c).

Carbon-normalized APA was however elevated 2.5-fold in the MPA treatment over the DIP treatment, suggesting this treatment was under stronger P limitation than the DIP treatment, consistent with a lower availability of this P source (Duhamel et al. 2010; Mahaffey et al. 2014; Fig 3.1e). In addition, F_v/F_m values in the DIP treatment were lower than the control or MPA treatments (0.36; Fig 3.1b), suggesting that the DIP treatment was potentially under a co-limitation situation by DIP and Fe, as previously found under steady state when supplying this media to *Trichodesmium* (Wang et al., 2022). Application of the Fe depleted media led to a steady rise in DIP concentrations for the DIP treatment, reaching to $3.09 \pm 0.28 \mu\text{M}$ at steady state (day 24). This DIP increase was accompanied by an 0.26-fold decrease in F_v/F_m and 0.75-fold decrease in APA, both further pointing towards a shift from P limitation, or P-Fe co-limitation, into stronger Fe limitation (Schrader et al. 2011; Mahaffey et al. 2014; Wang et al., 2022). The MPA treatment contrasted with the DIP treatment upon application of the Fe depleted media in showing no DIP accumulation, a more gradual F_v/F_m reduction, and APA levels that remained elevated. Together this demonstrated that this treatment was shifting from strong P limitation through to Fe-P co-limitation.

After restoring the Fe concentration back to 40 nM (Fe recovery phase), *Trichodesmium* in both DIP and MPA treatments reverted back to the original condition: DIP remained depleted in the MPA treatment but decreased steadily in the DIP treatment to full depletion by day 48 ($0.06 \pm 0.07 \mu\text{M}$); F_v/F_m increased in both treatments, but to a lower value in the DIP treatment; and APA increased in both but was 3.7-fold lower in the DIP treatment at steady state. Together these indicated a return to P limitation in the MPA treatment and a situation of P-Fe co-limitation in the DIP treatment.

3.3.2 Elemental stoichiometry

The overall average, steady state elemental stoichiometry of *Trichodesmium* under the Fe depleted condition was $(C_{106}N_{15.82}P_{0.62})_{1000}Fe_{2.26}Zn_{2.37}Mn_{1.68}Cu_{0.68}Ni_{0.31}Mo_{0.42}Co_{0.03}$ for the DIP treatment and $(C_{106}N_{13.89}P_{0.49})_{1000}Fe_{3.38}Zn_{2.51}Mn_{0.97}Cu_{0.52}Ni_{0.42}Mo_{0.33}Co_{0.03}$ for the MPA treatment. The average elemental stoichiometry following Fe recovery was $(C_{106}N_{16.8}P_{0.7})_{1000}Fe_{4.41}Zn_{1.44}Mn_1Cu_{0.52}Ni_{0.19}Mo_{0.3}Co_{0.03}$ for the DIP treatment and $(C_{106}N_{15.9}P_{0.73})_{1000}Fe_{7.36}Zn_{2.24}Mn_{1.08}Cu_{0.71}Ni_{0.63}Mo_{0.38}Co_{0.02}$ for the MPA treatment.

The MPA treatment showed small decreases in N:C ratios under Fe limited condition (0.11-fold; Fig 3.1f). The mean steady state N:C ratio under the Fe depleted condition for both the DIP and MPA treatments was significantly lower than that in the control treatment (0.149 ± 0.024 , 0.131 ± 0.010 and 0.157 ± 0.008 mol/mol for DIP, MPA and control treatments respectively; Fig 3.2a; Table 3.2). Declining N:C ratios under Fe limitation were consistent with previous studies (Beversdorf et al. 2010; Shi et al. 2012). The nitrogenase complex of *Trichodesmium* has been predicted to host 19 to 53% of cellular Fe (Kustka et al., 2004), with the abundance of nitrogenase and rates of N_2 fixation reducing under Fe limitation (Shi et al., 2007; Snow et al., 2015). Therefore, I suggest that lowered Fe availability limited N_2 fixation, in turn reducing N:C quotas. Under Fe recovery, the N:C ratio increased for both the treatments, and at steady state no significant differences in N:C ratios from the control treatment were observed (0.161 ± 0.012 , 0.15 ± 0.019 and 0.157 ± 0.011 mol/mol for DIP, MPA and control treatments respectively; Fig 3.2b; Table 3.2).

Table 3.2 Mean steady state carbon normalized elemental ratios of *Trichodesmium* ISM101 under Fe depleted (upper) and Fe recovery (bottom area with shading) conditions. Standard deviations are shown in the smaller font.

Treatment	N (mol/mol)	P (mol/mol)	Fe (mmol/mol)	Zn (mmol/mol)	Mn (mmol/mol)	Cu (mmol/mol)	Ni (mmol/mol)	Mo (mmol/mol)	Co (mmol/mol)
DIP	0.149 0.024	0.0058 0.0006	0.0213 0.0037	0.022 0.005	0.0158 0.0082	0.0064 0.0016	0.0029 0.0010	0.0039 0.0006	0.00029 0.00011
MPA	0.131 0.010	0.0046 0.0006	0.0319 0.0062	0.024 0.010	0.0092 0.0012	0.0049 0.0008	0.0039 0.0016	0.0031 0.0005	0.00025 0.00006
Control	0.157 0.008	0.0068 0.0018	0.0424 0.0013	0.011 0.004	0.0096 0.0012	0.0049 0.0006	0.0012 0.0003	0.0030 0.0005	0.00027 0.00004
DIP	0.161 0.012	0.0073 0.0013	0.0457 0.0206	0.0171 0.0062	0.0084 0.0023	0.0050 0.0010	0.0028 0.0032	0.0025 0.0012	0.00042 0.00015
MPA	0.15 0.019	0.0068 0.0031	0.0695 0.0320	0.0211 0.0115	0.0103 0.0051	0.0067 0.0031	0.0060 0.0051	0.0037 0.0017	0.00020 0.00011
Control	0.157 0.011	0.0057 0.0015	0.0366 0.0097	0.0125 0.0055	0.0103 0.0029	0.0049 0.0010	0.0014 0.0003	0.0031 0.0008	0.00029 0.00007

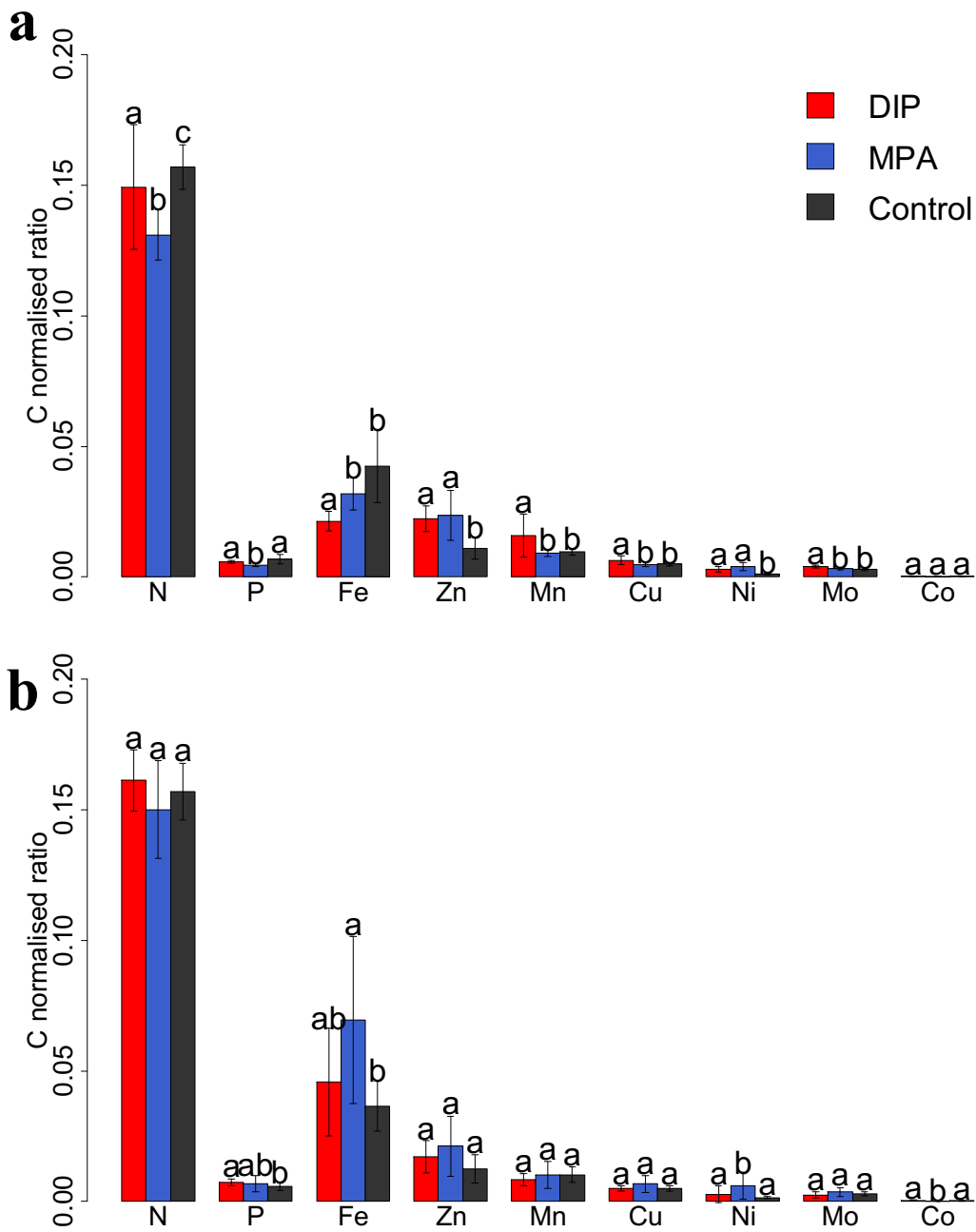


Fig 3.2 Elemental composition of *Trichodesmium* ISM101 at steady state for **a**, Fe depleted media (4 nM) and **b**, Fe replete media (40 nM). Bars show the mean steady state elemental ratios, error bars are the standard deviation (n=7–12). N and P are in units of mol:mol; all others are in units of mmol:mol. Bars labeled with the same letter have means that are statistically indistinguishable between treatments with the applied statistical test (pairwise Wilcoxon test, $p < 0.05$).

No significant differences were observed between the mean steady state P:C ratio in the DIP and control treatments under the Fe depleted condition, but both were significantly higher than in the MPA treatment ($(5.8 \pm 0.6) \times 10^{-3}$, $(4.6 \pm 0.6) \times 10^{-3}$ and $(6.8 \pm 1.8) \times 10^{-3}$ mol/mol in DIP,

MPA and control treatments respectively; Fig 3.2a; Table 3.2). This is consistent with the expectation of lowest P availability in the MPA treatment under this condition (Fig 3.1c and e). Interestingly, *Trichodesmium* in both the DIP and MPA treatments increased their P:C ratio upon Fe-recovery (1.26-fold and 1.48-fold, respectively). This occurred despite a situation of strengthening P limitation (Fig 3.1c and e), but the values were consistent with my previous work (Wang et al., 2022).

Fe quotas for both DIP and MPA treatments declined in response to reduced Fe availability, consistent with previous findings (Kustka et al., 2004; Berman-Frank et al., 2007; Nuester et al., 2012; Shi et al., 2012), but showed subtle differences depending on the degree of Fe limitation (Fig 3.2a; Table 3.2). Specifically, under the steady state Fe depleted condition, the DIP treatment was under strongest Fe limitation and it had the lowest Fe:C ratio (0.0213 ± 0.0037 mmol:mol), the control treatment was under no Fe limitation and it had the highest Fe:C ratio (0.0424 ± 0.0013 mmol:mol), whilst the MPA treatment was under Fe-P co-limitation and had an Fe:C ratio in between (0.0319 ± 0.0062 mmol:mol). The 1.5 times higher Fe:C ratios in the MPA treatment compared to the DIP treatment under the steady state, Fe depleted condition, could be a consequence of weaker Fe limitation due to co-limitation by P as well as Fe; however enhanced cellular Fe quotas under lower P availability could also play a role. Specifically, although MPA can not be hydrolysed by AP, mean steady state APA in MPA treatment was roughly 8.5 fold of that in DIP treatment (Fig 3.1e), suggesting much higher production of AP enzymes which include the Fe-containing forms PhoX and PhoD (Yong et al., 2015; Rodriguez et al., 2014). In addition, MPA is utilized by *Trichodesmium* via C-P lyases, which also contain Fe (Stosiek et al., 2020). Upon Fe recovery, steady state Fe:C ratios in the DIP and MPA

treatments increased 2.14-fold and 1.69-fold over the Fe depleted condition respectively (Fig 3.2b, Table 3.2), consistent with increased Fe availability in both treatments.

No significant differences were observed between mean steady state Zn:C ratio in the DIP and MPA treatments under the Fe depleted condition, while both of them were significantly higher than in the control treatments (0.022 ± 0.005 , 0.0024 ± 0.01 and 0.011 ± 0.004 mmol:mol in the DIP, MPA and control treatments respectively; Fig 3.2a; Table 3.2). In the steady state Fe recovery phase Zn quotas showed decreases in both DIP and MPA treatments. This contrasts with previous work (Wang et al., 2022) that showed 3.5-fold increases in Zn quotas under strong P limitation under growth on MPA in comparison to DIP. However, closer inspection of the Fe recovery phase showed Zn quotas in the MPA treatment increased 3.1-fold over 6 days, but then decreased moving into steady state (Fig 3.1i), suggesting that Zn accumulation under P limitation could be time scale dependant.

The quotas of several other trace elements increased under strongest Fe limitation found in the DIP treatment in the Fe depletion phase: mean steady state ratios of Mn:C, Cu:C and Mo:C in were significantly higher (1.65, 1.31, and 1.3-fold) than that in the control treatment (Fig 3.2a; Table 3.2; Quade post hoc test; $p < 0.05$). These decreased in the Fe recovery phase (Fig 3.2b; Table 3.2). The absolute requirement for Mn in photosynthesis is well known (Raven et al., 1999) with increased requirements for Mn under low Fe availability reported for diverse phytoplankton including cyanobacteria as well as diatoms, likely due to a substitutable Fe or Mn requirement for superoxide dismutase enzymes (Peers and Price, 2004; Salomon and Keren, 2011, 2015; Sharon et al., 2014; Kaushik et al., 2015; Marki et al., 2020). Enhanced Cu requirements under stronger Fe limitation could potentially be ascribed to the substitution of

Fe-containing c6 with Cu-containing plastocyanin within the photosynthetic electron transport chain (Peers et al., 2005; Peers and Price, 2006; Schoffman et al., 2016). The mechanism leading to enhanced Mo quotas is more difficult to ascribe, although its requirement in nitrogenase alongside Fe could conceivably lead to enhanced assimilation into different forms of nitrogenase or enhanced uptake due to reduced competition for Fe uptake sites at low Fe concentrations (Pau, 2004; Hernandez et al., 2009).

3.3.3 Particulate metabolites

Adenosine is a purine nucleoside serving as a building block for adenosine triphosphate (ATP), and its levels increase when ATP is metabolised to produce energy when energy demands increase (Kujawinski et al., 2017). The adenosine:C in the MPA treatment increased 1.34-fold initial values under the Fe depleted condition, this might be related to *Trichodesmium* under Fe limitation condition may require more energy to support the acquisition of Fe. The adenosine:C in MPA treatment showed a decreasing and increasing trend under the Fe depleted condition, with no significant differences detected between the mean steady state adenosine:C in DIP and MPA treatments, while both of them were significantly higher than in control treatment (Fig 3.3). Upon initiation of the Fe recovery phase, adenosine:C continued to increase 1.5-fold in the MPA treatment over the first three days (day 33 - day 36). I suggest that this reflects a continued strengthening of Fe limitation in the MPA treatment, as shown by decreases in F_v/F_m over this time period and despite initiation of supply of the high Fe media (Schrader et al., 2011). Following this time lag, adenosine:C ratio in both of the DIP and MPA treatments decreased, while the mean steady state adenosine:C ratio was still significantly higher than that in the control treatment (0.013 ± 0.01 , 0.014 ± 0.08 and 0.005 ± 0.01 mmol/mol in the DIP, MPA and

control treatments respectively).

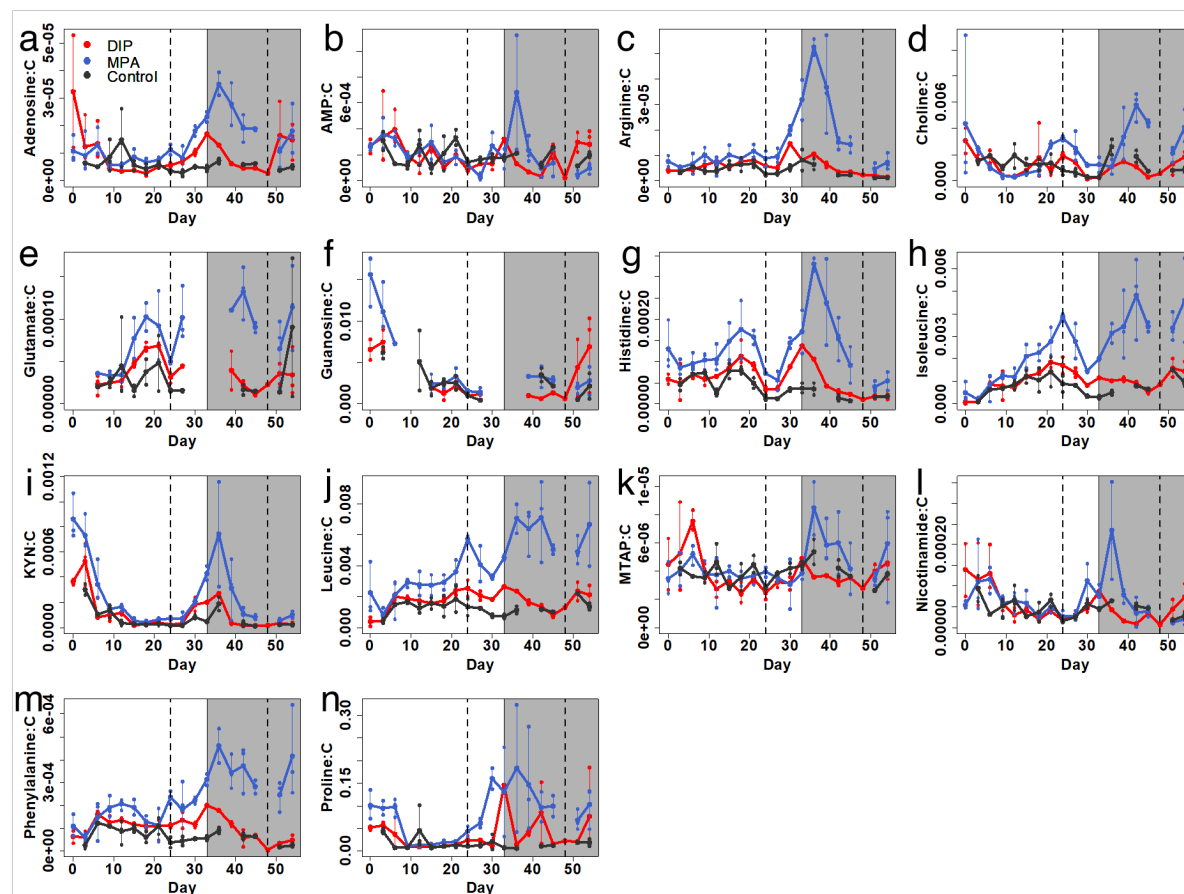


Fig 3.3 Particulate metabolite responses in *Trichodesmium* ISM101 for DIP and MPA treatments to different Fe supply concentrations. All metabolites are normalized to POC. Points show triplicate measurements every three days, lines map the change in the mean value with time. The shaded region indicates where the high Fe (40 nM) media was introduced. The time period to the right side of the dashed line for each condition is considered here to be at steady state.

Variations in the biomass-normalized abundances of some amino acids were also detected (Fig 3.3). Under the Fe depleted condition, significantly increased abundances of arginine, glutamate, histidine, isoleucine, leucine, phenylalanine and proline were detected in both the DIP and MPA treatments, with abundances in the MPA treatment always significantly higher than those in DIP treatments. As for adenosine, the initial portion of the Fe recovery phase for the MPA treatment was characterized by further increases in amino acids, potentially related to continued strengthening of Fe limitation in this treatment. Following this time lag, amino acids decreased or remained stable, with abundances always remaining higher for the MPA than for the DIP

treatment, which were statistically indistinguishable from the control treatment. The fixed N in *Trichodesmium* is assimilated via the glutamine synthetase–glutamate synthase (GS-GOGAT) pathway. In the first step, GS catalyzes the ATP-dependent condensation of glutamate with ammonium to glutamine (Liaw et al., 1995). Since Fe deficiency can limit N₂ fixation rate (Shi et al., 2007; Snow et al., 2015), *Trichodesmium* in Fe depleted condition may lead to a reduction in the amount of ammonium involved in glutamine synthesis due to the limitation of N₂ fixation by Fe depletion, resulting in the accumulation of glutamate. Furthermore, proline synthesis from glutamate, so the accumulation of glutamate may be the reason for the accumulation of the amount of proline (Verslues and Sharma, 2010). The increase in the abundance of leucine and isoleucine was likely due to an increase in the abundance of pyruvate and threonine in *Trichodesmium*.

To compare changes in metabolite production by *Trichodesmium* in response to different nutrient concentrations and different P sources, I projected the carbon-normalized abundance of targeted metabolites into a lower-dimensional space using non-metric dimensional scaling (NMDS; Fig 3.4). Surprisingly, there were no significant changes in the carbon-normalized abundance of targeted metabolites produced by *Trichodesmium*, whether in the Fe depleted, Fe replete condition or transition phase from Fe depleted to Fe replete condition. The putative reason might be that the changes in the abundance of proteins of *Trichodesmium* brought by Fe limitation may not account for a significant amount of the proteome, resulting in insignificant changes in abundance of metabolites. For example, a recent study indicated the proteins that were upregulated under N or P limitation of *E.huxleyi* accounted for only 1.7% and 5.7% of the total spectral counts, respectively (McKew et al., 2015).

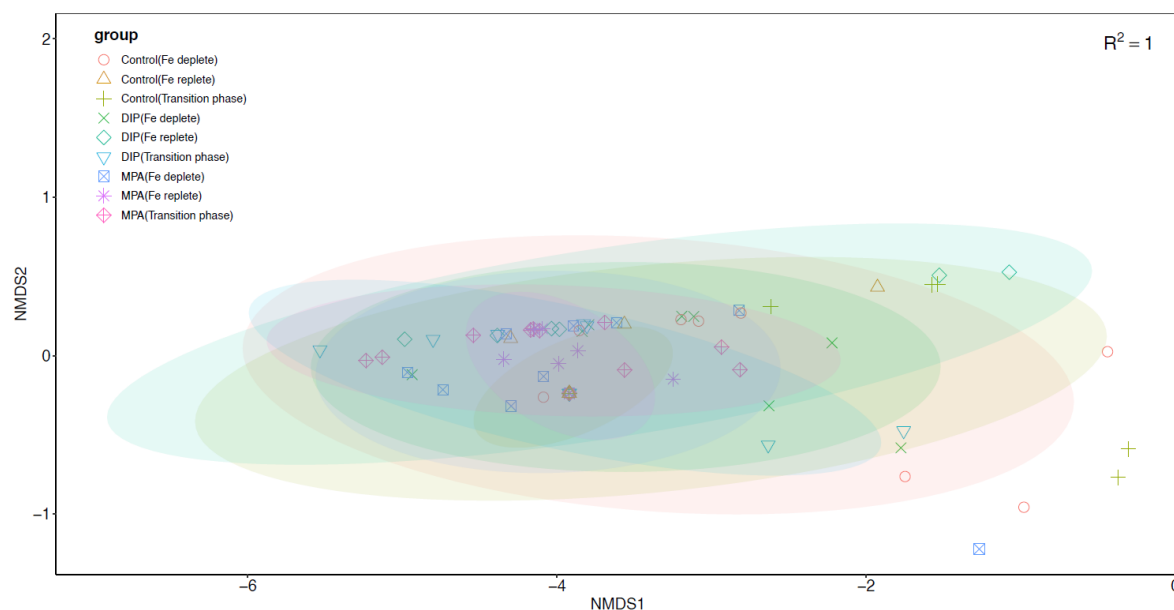


Fig 3.4 Non-metric multidimensional scaling (NMDS) of metabolites comparing treatment effects across sampling days (Fe deplete = day 24-33, Transition phase = day 36-45, Fe replete = day 48-54).

3.4 Conclusions

I determined the elemental stoichiometry in *Trichodesmium* ISM101 under different Fe levels whilst supplying different P sources. I observed a significant decrease in carbon biomass in the DIP and MPA treatments under Fe depleted condition, suggesting growth was limited by Fe availability. When DIP was the supplied P source, reduced Fe supply resulted in increased Zn:C, Mn:C, Cu:C and Mo:C ratios and a decreased Fe:C ratio. Conversely, when MPA was the supplied P source, reduced Fe supply resulted in an increased Zn:C ratio and decreased Fe:C, P:C and N:C ratios. These results suggest *Trichodesmium* employs different strategies to cope with Fe-limitation reflected in its elemental stoichiometry. No significant changes were observed in the carbon-normalized abundance of targeted metabolites produced by *Trichodesmium*, whether in the Fe depleted, Fe replete condition or transition phase from Fe depleted to Fe replete condition. A putative reason for the lack of significant difference in the metabolome is that the changes in the abundance of proteins of *Trichodesmium* brought by Fe

limitation may not account for a significant amount of the total proteome, resulting in insignificant changes in abundance of metabolites.

Chapter 4. Zinc limitation enhances nickel quotas of *Trichodesmium*

Abstract

Zinc (Zn) serves as a cofactor in several phosphorus (P) acquisition enzymes. In oligotrophic oceans where *Trichodesmium* spp. is abundant, both the concentrations of dissolved inorganic P (DIP) and Zn can be at low levels. To access P from the dissolved organic P (DOP) pool, *Trichodesmium* can utilize multiple enzymes such as alkaline phosphatase (AP), which can have Zn as a cofactor. Thus, the lack of Zn could affect the ability of *Trichodesmium* to access P from the DOP pool. To test this, I grew *Trichodesmium* under Zn limitation conditions, where P was supplied as either DIP or DOP (methylphosphonic acid). Mean steady state biomass under the Zn depleted DIP treatment was only 62% of that Zn replete control treatment, suggesting that Zn-limiting conditions were achieved. The elemental stoichiometry of *Trichodesmium* under Zn limited conditions was $(C_{106}N_{17.6}P_{0.95})_{1000}Fe_{5.6}Zn_{2.27}Mn_{1.07}Cu_{0.6}Ni_{1.7}Mo_{0.28}Co_{0.07}$. The mean steady state nickel (Ni): carbon ratio in the Zn depleted DIP and MPA treatments was 11.4 and 10 times respectively that of the Zn replete control treatment. I hypothesize that this was either related to (i) biochemical usage of the Ni under conditions of low Zn availability, for example, enhanced usage of Ni under low Zn could be related to a substitution of Zn-containing superoxide dismutase (SOD) enzymes by Ni-containing ones or (ii) mistaken accumulation of Ni by upregulated cation transport proteins, which could be linked to the relative position of these two

cations in the Irving–Williams series and the restricted ability to distinguish uptake between the two metals. This observation presented in this chapter provided a novel perspective on the relatively high Ni demand for *Trichodesmium*.

4.1 Introduction

Zinc (Zn) is an essential element for phytoplankton in the ocean, serving as a metal cofactor for many important cellular processes (Vallee and Auld, 1990; Morel et al., 2003). For example, Zn is required for nucleic acid repair and transcription proteins (Montsant et al., 2007; Twining and Baines, 2013), carbonic anhydrase (Badger, 2003; Kupriyanova and Pronina, 2011; Lionetto et al., 2016), alkaline phosphatase (AP; Dyhrman and Ruttenberg 2006) and some other P-metabolizing enzymes such as transferases and lyases (Duhamel et al., 2021). Different phytoplankton species show variable responses to Zn depletion due to their specific biological requirements (Sunda and Huntsman, 1992). Therefore, Zn availability has been suggested to influence phytoplankton community composition in the ocean (Crawford et al., 2003; Cullen and Sherrell, 2005; Sinoir et al., 2016).

Diazotrophs, N_2 fixing microbes, supply new bioavailable N to the open ocean, thereby increasing productivity of the whole community (Mahaffey, 2005). In regions where N_2 fixation is enhanced, dissolved inorganic phosphorus (DIP) is typically strongly drawdown (Martiny et al., 2019), often becoming growth-limiting for diazotrophs and co-limiting for the rest of the phytoplankton community (Moore et al., 2013). *Trichodesmium* is a filamentous cyanobacterium, which has long been thought to be an important contributor to N_2 fixation, with an estimated contribution of ~50% to the total N_2 fixed in the ocean (Capone et al., 1997; Mahaffey, 2005; Bergman et al., 2013). *Trichodesmium* occurs in the oligotrophic (sub-)tropical oceans where Fe supplies are elevated (Capone et al., 2005; Mahaffey, 2005; Mark Moore et al., 2009). In addition to DIP, P is also available to *Trichodesmium* as dissolved organic P (DOP), which accounts for up to 70-90% of the total dissolved P in surface waters of

low DIP regions (Karl and Björkman, 2002). To obtain P from DOP pool, *Trichodesmium* uses enzymes such as alkaline phosphatase (AP), which hydrolyses phosphoesters, and C-P lyase, which is responsible for the hydrolysis of phosphonate. Both AP and C-P lyase are metalloenzymes, specifically, (i) AP enzymes require zinc (Zn) and magnesium (PhoA; Kim and Wyckoff 1991), or calcium and iron (Fe) (PhoD/X; Yong et al. 2014; Rodriguez et al. 2014); and (ii) C-P lyases contain Zn and Fe (Stosiek et al., 2020).

It has been reported that up to one third of the total proteome of microbes and half of the enzymes contain metal cofactors (Andreini et al., 2008; Waldron et al., 2009; Cvetkovic et al., 2010). The general affinity of divalent metals for organic ligands applies to a wide range of compounds such as proteins, consistent with the description of the Irving-Williams series ($Mn < Fe < Co < Ni < Cu > Zn$; Irving and Williams 1953). In addition, marine phytoplankton are able to make use of alternative sources of essential elements and have evolved to substitute some elements by others in various biochemical processes (Morel et al., 2020). Therefore, in the absence of certain metals in the surroundings, transporter proteins of organisms may increase the uptake of other metals.

My previous experiments tested the impact of the relative availability of P sources and Fe availability on cellular elemental quotas and particulate metabolites in *Trichodesmium* (Chapter 2 and 3). To investigate the effect of Zn deficiency on the growth and physiological status of *Trichodesmium* under conditions with different P sources, the impact of the relative availability of P sources and Zn on cellular elemental quotas in *Trichodesmium* ISM101 was tested, the results of which are presented and discussed in this chapter 4. As for Chapters 2 and 3, two P sources were utilized: (i) 5 μ M DIP and (ii) 5 μ M methylphosphonate acid (MPA), a

phosphonate synthesized by marine microbes (Metcalf et al., 2012). The experiments were conducted at high volume (2 L) with triplicate replication under trace-metal-clean conditions using an exponentially fed batch culture approach (Fischer et al., 2014; Marki et al., 2020), which allows for regular harvesting of sufficient biomass required for bulk phytoplankton elemental analysis.

4.2 Materials and methods

Cultures. To examine effects of different Zn concentrations on growth of the diazotrophic cyanobacteria *Trichodesmium* ISM101, I cultured *Trichodesmium* with 5 μM DIP and 5 μM MPA separately in triplicate using Zn depleted media (0 nM; 24 days) using a trace-metal-clean exponentially fed batch (EFB) culture system (Fischer et al., 2014; Marki et al., 2020). In a control treatment I cultured *Trichodesmium* with a constant media supply of 5 μM DIP and 20 nM Zn. The cultures were maintained at 25°C on a 12h/12h light/dark cycle at 140 $\mu\text{mol photons m}^{-2} \text{ s}^{-1}$ in YBCII media (Chen et al., 1996). It should be noted that I did not add EDTA when I was configuring the Zn-free YBCII medium (experimental error). The YBCII medium was prepared with ultrapure water (Ultrapure, MQ; $\leq 18 \text{ M}\Omega \text{ cm}^{-1}$; Millipore) and analytical reagent grade salts (Table 2.1). YBCII medium was adjusted to pH 7.8-8.1 by addition of 0.01 M sodium hydroxide and filter sterilised with disposable rapid flow filter units (PES, 0.1 μm , Nalgene). Ten-litre high density polyethylene carboys (Nalgene) were used for the YBCII culture medium reservoir. Cultures were grown in sterile polycarbonate culture bottles (2000 mL, Nalgene). The initial volume of the cultures was 1400 mL, into which fresh medium was pumped using narrow bore polypropylene tubing (inner diameter 0.51 mm, Ismaprene, Pharmed) using a peristaltic pump (IPC-N, Ismatec) via a filter (0.2 μm ; Sterivex). The

peristaltic pump was controlled by a programmable microcontroller (Raspberry Pi3), which automatically increased the flow rate each hour in relation to the real time culture volume, thereby maintaining a constant culture dilution rate of 0.1 d^{-1} . The dilution rate employed together with the starting volume allowed a single time point recovery of ~500 mL of sample every three days. All sample collection and medium preparation was carried out in a laminar flow hood equipped with a high efficiency particulate air filter, located within a trace-metal-clean laboratory.

Fast Repetition Rate fluorometry. Fast Repetition Rate fluorometry of *Trichodesmium* ISM101 cultures was conducted throughout the whole culture period with a FASTOcean sensor equipped with a FASTAct laboratory system (Chlesea Technologies Group). Samples were dark acclimated for 20–30 minutes in the culture cabinet prior to measurements. Recovery of minimum fluorescence (F_0) and maximum fluorescence (F_m) allowed determination of the potential photochemical efficiency of photosystem II (PSII; $F_v/F_m = (F_m - F_0)/F_m$).

Alkaline Phosphatase Activity (APA). Whole water APA rates were measured using the fluorometric substrate MUF-P (Sigma-Aldrich) following the protocol of Ammerman (1993). 100 mM concentrated MUF-P and MUF (Sigma-Aldrich) stock solution was prepared by dissolving MUF-P and MUF into 2-methoxyethanol. Working stocks (100 μM) were made daily by diluting this concentrated stock with ultrapure water. The assays were started by adding 100 μL of MUF-P to 5 mL samples in replicate 15 mL tubes to yield a final substrate concentration of 2 μM . A 150 μL subsample was transferred into a 96 well plate immediately from the mixed sample. 50 μL of filtered 50 mM borate buffer (pH 10.8) was added to the subsample in the well plate and mixed to a final pH >10. APA was measured on a temperature-controlled (25 °C)

70

plate reader (FLX800TBI, BioTek) with Gen 5 software using an excitation wavelength of 365 nm and an emission wavelength of 455 nm. Fluorescence measurements were performed at $t=0$, 1, and 2 h. APA (h^{-1}) was calculated as the fluorescence of a 2 μM MUF divided by the initial ($t=0$ to $t=2$ h) slope of fluorescence time course (fluorescence per hour). Regular ultrapure blanks and paraformaldehyde-killed controls were conducted and generally yielded fluorescence values similar to $t = 0$ readings.

Nutrients. Samples of dissolved inorganic nitrate + nitrite and P (15 mL) were filtered through glass fiber filters (25 mm, 0.7 μm , Fisherbrand) under low pressure (<200 mPa). Samples were stored in polypropylene tubes (15 mL, Fisherbrand) at -20 °C until analysis and then analysed using a SEAL QuAAtro nutrient autoanalyser system (SEAL Analytical). Samples of total dissolved P (TDP; 50 mL) were filtered through sterile PES syringe filters (0.2 μm , Fisherbrand). Samples were stored in polypropylene tubes (50 mL, Fisherbrand) at -20 °C. Prior to analysis, TDP samples and blanks were digested under elevated pressure (1.5 bar) and temperature (120 °C) for 30 min following addition of the oxidizing reagent Oxisolv (Merck), and then analysed using a SEAL QuAAtro nutrient autoanalyser system (SEAL Analytical). DOP concentration was subsequently calculated as $\text{DOP} = \text{TDP} - \text{DIP}$.

Particulate organic C/N. Particulate organic C/N concentrations were determined by filtering 50 mL sample through pre-combusted (500°C, 12 h) glass fiber filters (25 mm, 0.7 μm , Fisherbrand) under low pressure (<200 mPa). Filters were stored frozen at -20 °C. Prior to analysis, filters were dried at 50 °C for 12 hours. After drying, filters were wrapped in tin boats (8×8×15 mm) and put in a well plate and stored in desiccator. Samples and blanks were analyzed using an elemental analyzer (Eurovector EA3000 Elemental Analyzer) with Callidus

version 5.1 software.

Particulate element concentration. 50 mL of sample was filtered onto acid-cleaned (10% HCl) PES membrane filters (25 mm, 0.8 μm , PALL). Filters were frozen and stored at $-20\text{ }^{\circ}\text{C}$ until digestion. For cell digestion, filters were placed in acid-washed (20% HNO_3) 15 mL PFA digestion vials with 2 mL of concentrated redistilled HNO_3 (Savillex, QMX) and heated to 120°C for 24 h. The filter was removed from the vial and the HNO_3 evaporated off (75°C , overnight). The residue was dissolved in 3 mL of 1% HNO_3 and spiked with indium ($4\text{ }\mu\text{g L}^{-1}$) as an internal standard. The samples were then centrifuged at 14,000 rpm (Centrifuge 5430R, eppendorf) for 10 minutes and the upper supernatant was taken for determination by inductively coupled plasma mass spectrometry (Element XR, Thermo), using prepared elemental standard curves for quantification.

4.3 Results and Discussion

4.3.1 Absence of EDTA in the culture media

It should be noted that I did not add EDTA when I was preparing the Zn-free YBCII medium (experimental error), so during the culture process the YBCII medium for the control treatment contained EDTA, while the YBCII medium for both the MPA and DIP treatments did not contain EDTA. The metal chelator EDTA is a component of the medium YBCII, which is commonly used to grow *Trichodesmium* (Chen et al., 1996). The addition of EDTA to the medium appears to stimulate N_2 fixation and growth in *Trichodesmium* (Paerl et al., 1994), potentially via chelating metals and reducing the toxic stress in *Trichodesmium* or preventing the precipitation of Fe, which is poorly soluble in oxygenated seawater (Anderson and Morel,

1978, 1982). In this experiment, the mean steady state POC concentration in both the DIP and MPA treatments without EDTA was significantly lower than in the control treatment containing EDTA (pairwise Wilcox test, $p < 0.05$; Fig 4.1a), they were 516 ± 55.8 , 551 ± 86.5 and 828 ± 79.3 μM for the DIP, MPA and control treatments respectively, demonstrating that *Trichodesmium* was under stronger limitation in both the EDTA free treatments than in the control treatment containing EDTA. One possible reason could be Fe availability was reduced because of the low solubility, however, values of the apparent photochemical efficiency, F_v/F_m , remained elevated throughout all treatments and at all timepoints (Fig 4.1b) indicating that growth of *Trichodesmium* was not limited by the availability of Fe (see discussion below). In the following results and discussion, I therefore consider that the lack of EDTA did not influence the growth of *Trichodesmium* in either the DIP and MPA treatments.

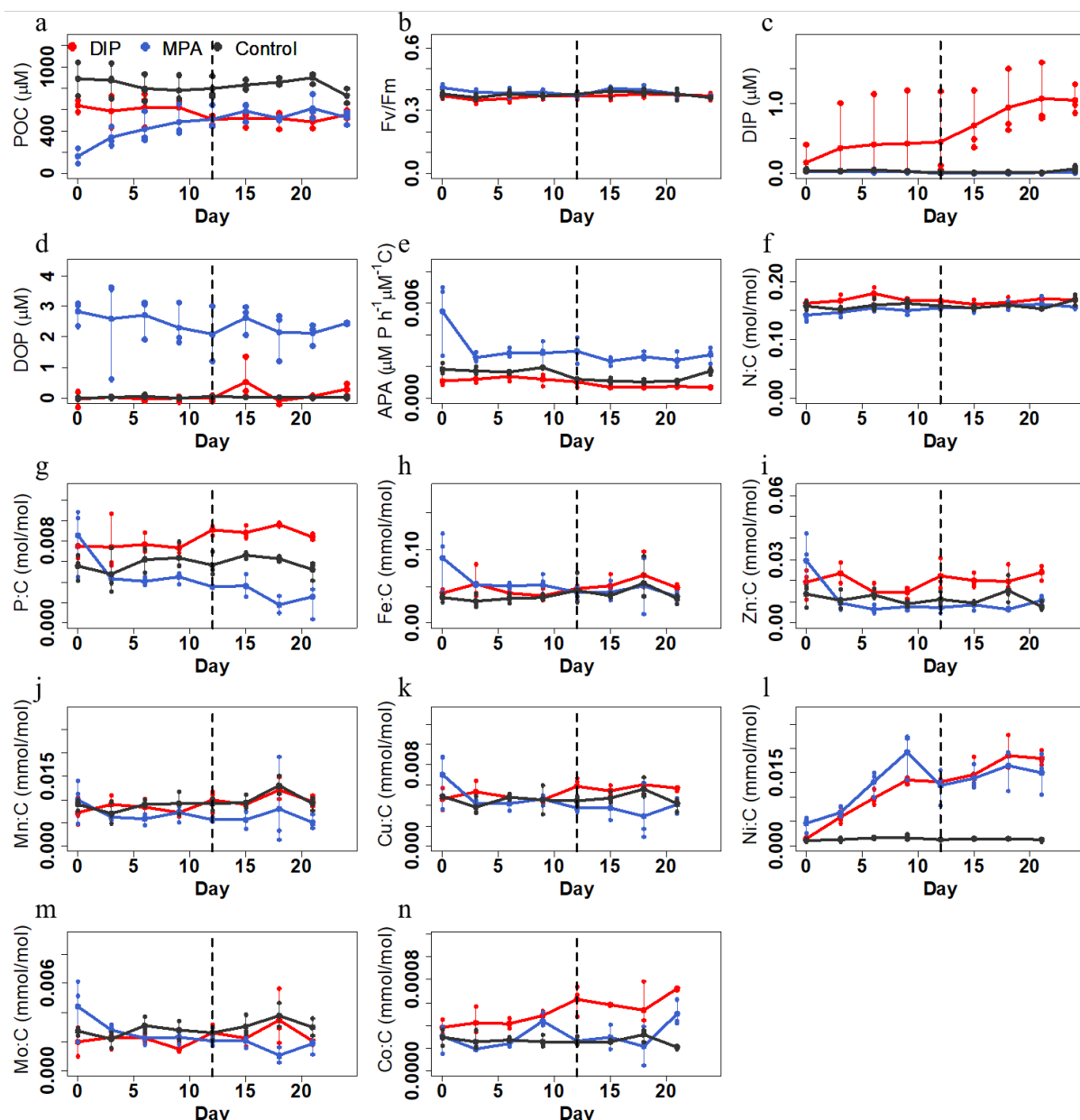


Fig 4.1 Responses of *Trichodesmium* ISM101 under DIP and MPA phosphorus sources to low Zn (0 nM) supply. Points show triplicate measurements every three days, lines map the change in the mean value with time. The time period to the right side of the dashed line is considered here to be at steady state (Quade post hoc test; $p < 0.05$).

4.3.2 *Trichodesmium* responses to Zn depletion

Trichodesmium carbon biomass within the MPA treatment increased 3.57-fold from 165 ± 70.9 to $482 \pm 148 \mu\text{M}$ over 15 days and showed no significant changes from day 9 (Quade post hoc test; $p < 0.05$; Fig 4.1a). In contrast, the biomass of the DIP treatment showed a decreasing trend,

with POC ultimately decreasing to 0.8 times the initial value within 12 days, after which no significant changes were observed and steady state was assumed (Quade post hoc test; $p < 0.05$; Fig 4.1a). At this point (days 12–24) I assumed that growth had reached an approximate steady state matching the dilution rate of the culture (0.1 d^{-1}). The biomass concentration at this point is dictated by the concentration of the most limiting nutrient in the culture medium (Fischer et al., 2014), which in the case of the Zn depletion experiment was Zn (DIP treatment), or bioavailable P (MPA treatment; see discussion below).

Values of the apparent photochemical efficiency, F_v/F_m , remained elevated throughout all treatments and at all timepoints (Fig 4.1b), they were 0.37 ± 0.02 , 0.39 ± 0.02 and 0.38 ± 0.02 for the DIP, MPA and control treatments respectively, demonstrating that *Trichodesmium* was under steady state nutrient limitation rather than starvation (Parkhill et al., 2001). Under this condition, the continuous supply of the limiting nutrient results in limitation of growth rates but does not lead to a buildup of dysfunctional reaction centers, which is associated with nutrient starvation and accompanying F_v/F_m reductions (Geider et al., 1993). The nutrient limitation status of each treatment through the Zn depletion phase could be dissected via observed changes in DIP concentrations and APA (Fig 4.1c and e). At time $t=0$, *Trichodesmium* under both the DIP and MPA treatments were assumed to be under P limitation, with both having fully depleted DIP concentrations ($< 0.1 \text{ } \mu\text{M}$; Fig 4.1c; but note that one of the DIP treatment triplicates had a DIP concentration of $0.41 \text{ } \mu\text{M}$). Mean, steady state carbon-normalized APA was however elevated 3.7-fold in the MPA treatment over the DIP treatment, suggesting this treatment was under stronger P limitation than the DIP treatment, consistent with a lower availability of this P source (Duhamel et al. 2010; Mahaffey et al. 2014; Fig 4.1e). Application of the Zn depleted

media led to a steady rise in DIP concentrations for the DIP treatment, reaching to 0.84 ± 0.46 μM at steady state (day 12). This DIP increase accompanied with a biomass decrease and a slight reduction in APA (Fig 4.1a and e) pointed towards a shift from P limitation into Zn limitation. The MPA treatment contrasted with the DIP treatment upon application of the Zn depleted media in showing no DIP accumulation, whilst DOP concentrations and rates of APA remained elevated (Fig 4.1d and e). Together this demonstrated that this treatment was constantly under P limitation.

4.3.3 Elemental quotas of *Trichodesmium* response to Zn depletion

The MPA treatment showed a decreasing trend in P:C ratios under the Zn depleted condition (2.9-fold; Fig 4.1g). The mean steady state P:C ratio was significantly lower than in the DIP and control treatments; conversely, the DIP treatment retained an elevated P:C ratio and its mean steady state value was significantly higher than that in the control treatment ($(8.9 \pm 0.5) \times 10^{-3}$, $(2.9 \pm 1.2) \times 10^{-3}$ and $(5.9 \pm 0.9) \times 10^{-3}$ mol/mol in DIP, MPA and control treatments, respectively; Fig 4.2; Table 4.1). This finding is consistent with the expectation of a gradient in P availability: lowest P availability in the MPA treatment (Fig 4.1c and d), highest P availability in the Zn-limited DIP treatment, and intermediate values in the Zn-replete, DIP-containing control treatment. This flexibility in P quotas is consistent with the known ability of *Trichodesmium* to accumulate and store P, or initiate mechanisms to reduce P requirements (Romans et al. 1994; Orchard et al. 2010; Van Mooy et al. 2009). *Trichodesmium* takes up excess P when available (so called ‘luxury uptake’), storing it in the form of polyphosphate (Romans et al., 1994; Orchard et al., 2010b). This is consistent with what I observed in the Zn depleted DIP treatment, which had the highest DIP availability among the three treatments. On

the other hand, *Trichodesmium* can also substitute the non-P containing sulfolipid for the P-rich phospholipid to modulate their P requirements thus reducing cellular P quotas under P limitation (Van Mooy et al., 2009), potentially explaining why the MPA treatment for lowest P availability had the lowest P:C ratio among these treatments. The Zn depleted DIP treatment had significantly higher mean steady state N:C ratio than in the Zn depleted MPA and Zn-replete control treatments (Fig 4.2; pairwise Wilcox test, $p < 0.05$). This could be consistent with the Zn uptake, with evidence suggesting that in Zn depleted conditions, cyanobacteria are able to upregulate a number of N-rich proteins to enhance the acquisition and transport of Zn from the surrounding environment (Barnett et al., 2014). However, it is difficult to assess if such protein transporters, whilst potentially strongly regulated by Zn availability, ever constitute a large enough fraction of *Trichodesmium*'s proteome to drive these bulk N:C changes (e.g., McKew et al. 2015; see also Chapter 5 'Conclusions and Future Directions').

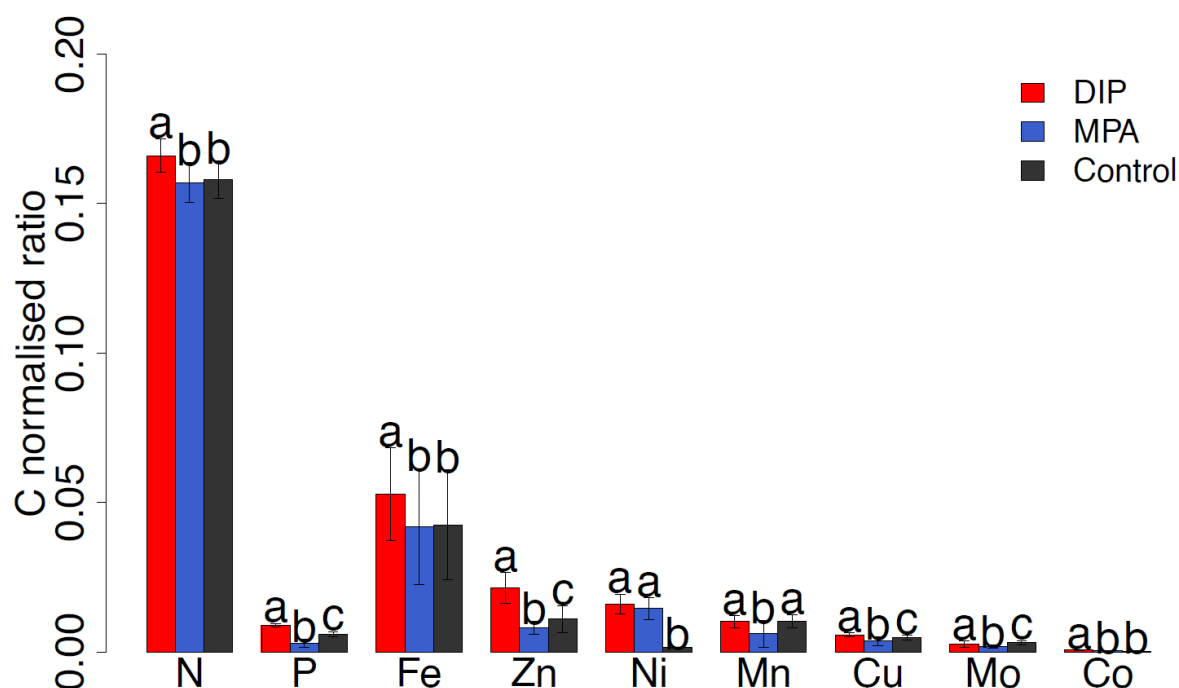


Fig 4.2 Elemental composition of *Trichodesmium* ISM101 at steady state for low Zn media (0 nM). Bars show the mean steady state elemental ratios, error bars are the standard deviation (n=8–15). N and P are in units of mol:mol; all others are in units of mmol:mol. Bars labeled with the same letter have means that are statistically indistinguishable between treatments with the applied statistical test (pairwise Wilcox test, $p < 0.05$).

Table 4.1 Mean steady state carbon normalized elemental ratios of *Trichodesmium* ISM101 under Zn depleted condition. Standard deviations are shown in the smaller font.

Treatment	N (mol/mol)	P (mol/mol)	Fe (mmol/mol)	Zn (mmol/mol)	Mn (mmol/mol)	Cu (mmol/mol)	Ni (mmol/mol)	Mo (mmol/mol)	Co (mmol/mol)
DIP	0.166 0.006	0.009 0.0006	0.0528 0.0155	0.0214 0.005	0.0101 0.002	0.0057 0.0006	0.016 0.0033	0.0026 0.0011	0.00062 0.00013
MPA	0.157 0.007	0.003 0.0013	0.042 0.006	0.008 0.002	0.0061 0.0044	0.0036 0.0014	0.014 0.0036	0.0017 0.0006	0.00032 0.00015
Control	0.158 0.006	0.006 0.0009	0.0425 0.0184	0.011 0.004	0.0102 0.0022	0.0047 0.0008	0.0014 0.0002	0.0031 0.0007	0.00026 0.00005

The MPA treatment showed small decreases in Fe:C ratios under the Zn depleted condition (0.31-fold; Fig 4.1h), and the mean steady state Fe:C ratio for the DIP treatment was significantly higher than that in both the MPA treatment and Zn-replete control treatment (0.053

± 0.014 , 0.042 ± 0.019 and 0.042 ± 0.018 mmol/mol for DIP, MPA and control treatments respectively; Fig 4.2). The MPA treatment showed trends of decreasing Zn:C ratios, with a mean steady state Zn:C ratio 2.7-fold lower of its initial value (day 0; Fig 4.1i). The mean steady state Zn:C ratio for the MPA treatment was significantly lower than the Zn-replete control treatment and both of them were significantly lower than in Zn depleted DIP treatment (0.021 ± 0.005 , 0.008 ± 0.002 and 0.011 ± 0.004 mmol/mol in the DIP, MPA and control treatments respectively; Fig 4.2). Therefore, although the Zn depleted DIP treatment was expected to be under Zn limitation, decreases in Zn quotas were not observed relative to the Zn replete control, and P-limited MPA, treatments.

The most dramatic changes in elemental stoichiometry were for Ni, with both Zn depleted MPA and DIP treatments showed trends of increasing Ni:C ratios (Fig 4.11). No significant differences were observed between mean steady state Ni:C ratio in the DIP and MPA treatments, while both of them were significantly higher than in the Zn-replete control treatments (0.016 ± 0.0033 , 0.014 ± 0.0036 and 0.0014 ± 0.0002 mmol/mol in the DIP, MPA and control treatments respectively; Fig 4.2; pairwise Wilcox test, $p < 0.05$), where the mean steady state Ni:C ratio in the DIP and MPA was 11.4 and 10 times respectively that of the control treatment. This observation is consistent with cellular accumulation of Ni under low Zn availability. This was either related to (i) biochemical usage of the Ni under the conditions of low Zn availability, or (ii) mistaken accumulation of Ni by upregulated cation transport proteins. For example, enhanced usage of Ni under low Zn could be related to a substitution of Zn-containing superoxide dismutase (SOD) enzymes by Ni-containing ones (Miller, 2012). In contrast, mistaken accumulation of Ni under low Zn could be linked to the relative position of these two

cations in the Irving–Williams series (Irving and Williams, 1953). Therefore, since Zn and Ni are almost equal in the Irving–Williams series, Ni uptake is not favored when Zn is at elevated concentrations. However, when in the Zn depleted state, the binding sites could be increasingly occupied by other metals, and since Ni has higher position than Co, Fe(II) and Mn in the Irving–Williams series, it is therefore possible that Ni wins the competition for the binding sites, resulting in an increase in the Ni:C ratios in the Zn depleted state. In addition, the low mean steady state Ni:C quota (Fig 4.2) observed in this study might be due to the use of the high concentration of organic ligand (EDTA) added to the medium, which complexed Ni making it less available for biological interactions.

The DIP treatment also showed an increasing trend in Co:C ratios under Zn depleted conditions (1.6-fold; Fig 4.1n) and the mean steady state Co:C ratio was 1.93 and 2.35-fold of that in the MPA and control treatments respectively; they were $(6.16 \pm 1.34) \times 10^{-4}$, $(3.2 \pm 1.5) \times 10^{-4}$ and $(2.62 \pm 0.52) \times 10^{-4}$ mmol/mol in DIP, MPA and control treatments respectively. Co potentially can substitute for Zn as the metal co-factor of APs (Gong et al., 2005; Jakuba et al., 2008; Saito and Goepfert, 2008). However, during observations, the APA:C values for the Zn depleted DIP treatment remained low ($< (9.7 \pm 3.3) \times 10^{-4} \mu\text{mol P h}^{-1} / \text{mol C}$), consistent with the elevated DIP concentrations (Fig 4.1c). Whilst this role cannot be ruled out, I therefore suggest that the increase in Co:C that I observed was not due to the substitution of Zn on APs. *Trichodesmium* has been demonstrated to have an absolute Co requirement, partially in vitamin B₁₂ but potentially also in methionine aminopeptidase, prolidase, nitrile hydratase, glucose isomerase, methylmalonyl-CoA carboxytransferase, aldehyde decarbonylase, lysine-2,3-aminomutase, and bromoperoxidase (Kobayashi and Shimizu, 1999; Rodriguez and Ho, 2015). In addition,

based on the Irving-Williams series, Co is one place lower than Ni. Therefore, it will also preferentially bind to cation transporters over other metals such as Fe(II) and Mn, but potentially less than that of Ni, and the Co:Ni ratio in the medium is 2:5, then Ni may therefore occupy the position of binding to cation transporters after Ni, thereby increasing the Co:C quota, consistent with observations (Fig 4.1h, j, l, n).

At time = 0, ratios of the mean Mo:C and Cu:C were significantly higher than at other time points in the MPA treatment, and no significant differences were observed in the ratios from day 3 onwards and the mean steady state ratio of the experiment (Fig 4.1j and k; Quade post hoc test; $p < 0.05$). However, the mean steady ratios of the Mo:C, Mn:C and Cu:C in the MPA treatment was significantly lower than in both the DIP and control treatments (Fig 4.2; pairwise Wilcox test, $p < 0.05$). Mo is an essential micronutrient for N_2 fixation because it is a cofactor of both the nitrogenase and nitrate reductase enzymes (Raven et al., 1999; Hoffman et al., 2014). Mn is required for the water-splitting reaction in oxygenic photosynthesis in photosynthetic organisms and a redox-active cofactor of some central enzymes such as Mn-SOD, oxalate oxidase, glycosyl transferases and pyruvate carboxylase (Da Silva and Williams, 2001; Schmidt and Husted, 2019). Cu is known as an important redox element required in the photosynthetic electron transport chain from the cytochrome b6f complex of PSII to PSI that use the metallo-protein plastocyanin (Raven et al., 1999). Although the mechanism leading to these decreased quotas is difficult to ascribe, all of these elements are associated with photosynthesis or N_2 fixation in *Trichodesmium*, it is therefore possible that the stronger P limitation of *Trichodesmium* in the MPA treatment may have affected the growth state and thus N_2 fixation and photosynthesis even though F_v/F_m remained elevated throughout all treatments.

4.4 Conclusions

I determined the elemental stoichiometry in *Trichodesmium* ISM101 under Zn depleted condition whilst supplying different P sources. Markedly elevated Ni:C ratios in both Zn-depleted MPA and DIP treatments were observed in the experiment which is consistent with cellular accumulation of Ni under low Zn availability. Zn limitation caused a shift in rank order which Ni:C leapfrogged Mn:C, Cu:C and Mo:C in both DIP and MPA treatments and was more abundant than Zn:C in the MPA treatment while Ni:C only leapfrogged Co:C in the control treatment. Even though this experiment could not decouple the specific cellular sinks for Ni that occurred within the Zn depleted treatments, biochemical usage of the Ni under the conditions of low Zn availability, such as substitution of Zn-containing SOD by Ni-containing ones, or mistaken accumulation of Ni by upregulated cation transport proteins (under conditions of low Zn) could be potential options (Sunda and Huntsman, 1995; Jakuba et al., 2008; Sinoir et al., 2016; Shire and Kustka, 2021). This would be an important finding, as currently *Trichodesmium* is thought to have a relatively high Ni requirement, due to NiSOD, which might be involved in protecting nitrogenase from superoxide inhibition of *Trichodesmium* (Ho, 2013). My observation presented in this chapter therefore provided a novel perspective on the relatively high Ni demand for *Trichodesmium*, while what the exact cause of the enhanced Zn quota of *Trichodesmium* under the stronger P limitation remains unknown, warranting further research. Finally, in the work presented in this chapter, the elemental stoichiometry of *Trichodesmium* under Zn depleted conditions was shown for the first time, ultimately providing a useful resource for ocean biogeochemical models that may in the future resolve Zn (Weber et al., 2018)

Chapter 5. Conclusions and future directions

5.1 Overall conclusions

The primary aim of this thesis was to explore the relative roles of phosphate, DOP, Fe and Zn in the growth, physiology, and elemental composition of the diazotrophic cyanobacterium *Trichodesmium*. This has been achieved by applying an EFB culture system under trace-metal-controlled conditions whilst varying the supply of different P sources, under replete and scarce Fe and Zn availability.

Chapter 2 presented interactions between P limitation, DOP availability, and cellular elemental quotas in *Trichodesmium* under two P supply treatments: (i) 5 μ M DIP and (ii) 5 μ M MPA, a DOP source. This experiment showed a 3.5-fold elevated Zn:C of *Trichodesmium* in the MPA treatment, which was under stronger P limitation. Whilst this is the first time this observation has been made, it is consistent with a known, major Zn requirement for DOP acquisition: a recent evaluation of trace element requirements for mechanisms to cope with P limitation demonstrated elevated Zn requirements in comparison to all other metals across a diversity of transferases, hydrolases, lyases, isomerases, ligases and translocases (Duhamel et al., 2021). Even though this experiment could not decouple the specific cellular sinks for Zn that occurred within the P-limited MPA treatment, the results suggest that the Zn enhancement was not simply due to the well-characterized enhanced production of AP enzymes under greater P stress (Mahaffey et al., 2014), but rather to a diversity of strategies to cope with stronger P limitation (Wei et al., 2018). This was because APA in MPA treatment increased from day 6 and stabilized from day 9 (Fig 2.1d), whereas the increase in Zn:C was later, from day 12, and did not reach a clear plateau over the experiment duration (30 days). This observation of enhanced Zn quotas under stronger P limitation in culture is consistent with limited available field observations,

which show elevated *Trichodesmium* Zn quotas in lower P waters (Tovar-Sanchez et al., 2006) and suggests a crucial level of interaction between the cycles of these two nutrients in the ocean (Mahaffey et al., 2014; Duhamel et al., 2021).

Chapter 3 presented the results of an experimental test for interactions between DOP and Fe availability on cellular elemental quotas and particulate metabolites in *Trichodesmium*. As in Chapter 2, two P supply treatments were conducted: (i) 5 μ M DIP and (ii) 5 μ M MPA; however, in this experiment Fe availability ranged over a gradient from depleted (4 nM) through to elevated levels (20 nM). Several lines of evidence were found for the low Fe levels leading Fe limitation of *Trichodesmium*; specifically, a significant decrease in the overall carbon biomass concentrations, reduced F_v/F_m and reduced APA. However, it was found that *Trichodesmium* was more Fe limited under the DIP treatment in comparison to the MPA treatment (F_v/F_m slightly more elevated in the MPA treatment, APA slightly higher) suggesting that the MPA treatment was under Fe-P co-limitation. Under the strongest Fe limitation, the low Fe, DIP treatment resulted in increased Zn:C, Mn:C, Cu:C and Mo:C ratios and a decreased Fe:C ratio. Conversely, under the Fe-P co-limited low Fe, MPA treatment, reduced Fe supply resulted in an increased Zn:C ratio and decreased Fe:C, P:C and N:C ratios. These results suggest *Trichodesmium* employs different strategies to cope with Fe limitation reflected in its elemental stoichiometry; specifically, the significantly higher Fe:C ratio of *Trichodesmium* in MPA treatment compared to in DIP treatment was likely due to *Trichodesmium* in the MPA treatment being under dual Fe and P limitation, both reducing the overall intensity of Fe limitation for this treatment as well as potentially leading to an increase in some Fe containing enzymes related to P metabolism, such as AP (PhoA; Kim and Wyckoff 1991) and C-P lyase (Stosiek et al.,

2020). This work demonstrates how elemental composition in *Trichodesmium* is dynamic, depending on the availability of different nutrients. Ultimately, these data could be of strong value in informing ocean biogeochemical models that currently typically rely on fixed elemental stoichiometry in phytoplankton (Follett et al., 2018b; Anugerahanti et al., 2021).

Chapter 4 presented the impact of the relative availability of different P sources and Zn on cellular elemental quotas in *Trichodesmium*. The experimental design replicated that used to investigate Fe in Chapter 3, but here investigated the availability of Zn. As for Chapters 2 and 3, two P supply treatments, (i) 5 μ M DIP and (ii) 5 μ M MPA, were utilized, with Zn varying from high to low availability. The experiment appeared successful in generating Zn limiting conditions in the DIP treatment, where carbon biomass concentrations and APA both declined. As for the low Fe condition presented in Chapter 3, although experiencing low Zn availability, APA remained elevated in the MPA treatment, suggesting this treatment was still under P limitation, or possibly P-Zn co-limitation. One of the clearest findings in this experiment was markedly elevated Ni:C ratios in both Zn depleted MPA and DIP treatments. This observation is consistent with cellular accumulation of Ni under low Zn availability (Miller, 2012). Even though this experiment could not decouple the specific cellular sinks for Ni that occurred within the Zn depleted treatments, biochemical usage of the Ni under the conditions of low Zn availability, such as substitution of Zn-containing SOD by Ni-containing ones, or mistaken accumulation of Ni by upregulated cation transport proteins (under conditions of low Zn) could be potential options (Sunda and Huntsman, 1995; Jakuba et al., 2008; Sinoir et al., 2016; Shire and Kustka, 2021). This would be an important finding, as currently *Trichodesmium* is thought to have a relatively high Ni requirement, which is due to NiSOD, which might be involved in

protecting nitrogenase from superoxide inhibition of *Trichodesmium* (Ho, 2013). The observation presented in this chapter therefore provided a novel perspective on the relatively high Ni demand for *Trichodesmium*, while the exact cause for the enhanced Ni quota of *Trichodesmium* under the stronger P limitation remains unknown, warranting further research. Finally, in the work presented in this chapter, the elemental stoichiometry of *Trichodesmium* under Zn depleted conditions was shown for the first time, ultimately providing a useful resource for ocean biogeochemical models that may in the future resolve Zn (Weber et al., 2018).

5.2 Future directions

Although the work presented in Chapters 2-4 has made a significant contribution to the understanding of the growth and physiological changes in *Trichodesmium* in response to different nutrient conditions, a number of important questions related to this research remain to be answered. Some of these questions are considered below.

What are the positive and negative aspects of the EFB culture system for culturing *Trichodesmium* under trace-metal-clean conditions? One initial laboratory study has highlighted the EFB culture system as a good alternative to other culture systems for trace metal limitation studies of phytoplankton (Marki et al. 2020). With the EFB culture system, with a continuous inflow but no continuous outflow, culture medium is added proportionally to the culture bottles and the speed of medium supply increases exponentially over time to compensate for the larger overall culture volume and maintain constant dilution (Fischer et al., 2014). As there is no outflow in the EFB culture system, the volume of the medium thus increases exponentially until sampling as long as a constant dilution rate is set. Within the 2 L bottle setup used for this research, this technique provided approximately 500 mL of sample every three

88

days for analysis of a suite of samples requiring sufficient microbial biomass. *Trichodesmium* was growing well during these experiments, for example, the mean steady state POC in the control treatment exceeded 800 μM . Furthermore, the EFB culture system strictly controlled trace metal contamination, which was essential to address the questions posed in this thesis (Chapter 3 and 4).

In the course of the experiment, I noted the following negative aspects of the EFB approach: (i) the medium requirements were high (approximately 500 mL day⁻¹ for each treatment over the triplicate replicates), therefore a relatively high volume (>2 L) of medium needs to be stored in the source media carboy for the system to be operated for a few days continuously. I also set up a treatment with 5 μM ATP as the sole P source during the experiment. However, during the experiment I found that ATP degrades very quickly in the medium. Therefore, it is important to avoid using chemicals that degrade easily when using EFB as the culture method. Furthermore, although I followed strict aseptic procedures (Sunda et al., 2005), completely avoiding the growth of bacteria is still challenging. Specifically, *Trichodesmium* is known to host a number of associated bacteria, with which they exchange nutrients and organic molecules and act together to optimize the growth of the whole consortium (Sheridan et al., 2002; Hmelo et al., 2012; Van Mooy et al., 2012; Gradoville et al., 2017; Frischkorn et al., 2018b). As a result, the changes I observed in *Trichodesmium* in response to P, Fe or Zn limitation could be the result of a combination of *Trichodesmium* and bacteria, and furthermore, the species of bacteria attached to *Trichodesmium* in laboratory conditions may not be exactly the same as in the open ocean, which may lead to some deviation in the application of the laboratory data presented here to open ocean. (ii) The medium was dripped into the culture flask from the top (Fig 1.6),

therefore during the experimental steady state, especially when one metal was depleted, the way the medium was dropping in may cause some *Trichodesmium* to colonize the surface to ensure that they can access the nutrients from the fresh medium. This might be a common aspect in all culture systems of continuous supply with fresh medium by dripping in.

What exactly caused the enhanced Zn quota of *Trichodesmium* under the stronger P limitation? Preliminary work presented in Chapter 2 indicated enhanced Zn quotas under stronger P limitation (MPA treatment), but I could not decouple the specific cellular sinks for this accumulated Zn. A recent evaluation of trace element requirements for mechanisms to cope with P limitation suggests a widespread need for and importance of Zn: of all the trace elements assessed, Zn stands out as having the greatest demand, with elevated requirements in comparison to all other metals across a diversity of transferases, hydrolases, lyases, isomerases, ligases and translocases (Duhamel et al., 2021). Transcriptomics and proteomics could help to track phytoplankton physiology (Snow et al., 2015; Walworth et al., 2016, 2018; Wilson et al., 2017; Frischkorn et al., 2018a, 2019; Zhang et al., 2019). Although transcriptomics and proteomics are distinct in their experimental approaches, the fundamental aim of both methods is to obtain the expression of genes. From the biological point of view, mRNA levels can reflect the intermediate state of gene expression and represent potential protein expression, however, proteins are the direct functional performers and therefore have an indispensable role in the detection of protein level expression (Walworth et al., 2022). Combining the two will enable a comprehensive analysis of mRNA and protein expression levels in organisms grown under a particular condition and would increase our ability to precisely determine the cause of the enhanced Zn quota of *Trichodesmium* under stronger P limitation. The experiment in Chapter 2

could have utilized transcriptomic and proteomic approaches to track the changes in gene expression and protein abundance of *Trichodesmium* over the course of the experiment. Changes in abundance of proteins known to have Zn in them (e.g., PhoA and others) could be tracked to see if the change in abundance in that Zn based protein could account for the overall bulk cellular Zn quota changes in *Trichodesmium*. Notably, recent studies combining transcriptomics and proteomics have shown that transcript levels were less correlated with corresponding protein levels (Swalwell et al., 2011; Welkie et al., 2014). This might be because of the timing of sampling, with the mRNA potentially degraded by the time the protein peaks or the protein content may still be changing by the time the mRNA peaks (Walworth et al., 2022). As such I propose application of proteomics, alongside the measurements conducted here, would be optimal for a more comprehensive and in-depth understanding of the molecular mechanisms underpinning the changes in cellular elemental quotas.

Why was MPA not fully utilized by *Trichodesmium*? MPA is a DOP compound characterized by a highly stable C–P bond and is enriched in marine DOM (Metcalf et al., 2012). Many cyanobacteria are reported to have the ability to access DIP from phosphonates through a diverse suite of enzymes such as C-P lyase (Scanlan et al., 2009; Martinez et al., 2010; Villarreal-Chiu et al., 2012; McGrath et al., 2013). Work presented in Chapter 2 demonstrated that MPA can be utilized as a P source by *Trichodesmium* (that is, no other P source was supplied but *Trichodesmium* still managed to grow), but was never fully utilized as measured residual DOP concentrations in cultures were always at around 40% of the supplied MPA concentration. Since *Trichodesmium* can use MPA as their P source, why was the MPA not fully utilized by *Trichodesmium* in the experiments when it was clearly under P limitation?

Just as AP enzymes require Zn and Mg (PhoA; Kim and Wyckoff 1991), or Ca and Fe (PhoD/X; Yong et al. 2014; Rodriguez et al. 2014), C-P lyases require Zn and Fe (Stosiek et al., 2020). MPA was not fully utilized even when all these metals were at replete levels (Chapter 2). This suggests incomplete utilization of MPA was not due to the limitation by trace metal availability. The C-P lyase pathway requires several multi-protein complexes which are encoded by a suite of genes denoted phnGHIJKLM (White and Metcalf, 2004, 2007). However, the synthesis of this series of proteins would increase the demand for N in *Trichodesmium*, thereby forcing *Trichodesmium* to increase N₂ fixation. Since *Trichodesmium* in MPA treatment was under P limitation, however, it was likely to be unable to enhance N₂ fixation rates, potentially causing the bottleneck on MPA utilization. Although *Trichodesmium* are diazotrophs, they have a capability to utilize inorganic N sources as well (Saino and Hattori, 1978; Post et al., 2012). In order to verify this hypothesis, it would be possible to use MPA as the P source with trace metals at replete levels, with one treatment without a pre-fixed N source and the other treatment with the addition of DIN (e.g., ammonium, nitrate, or nitrite) as the additional N source for *Trichodesmium*. This will help us to discover if the availability of N influences *Trichodesmium* to access to P from phosphonate.

Could the observed increase in Ni:C ratios for both treatments in Chapter 4 be caused by the lack of EDTA? The two treatments under Zn depleted conditions in the experimental work in Chapter 4 had no addition of EDTA. The mean steady state Ni:C ratios in both Zn depleted DIP and MPA treatments were approximately 16 and 15 times of that in the Zn-replete control treatment, respectively. In Chapter 4, I put forward the hypothesis that this was due to an increase in Ni accumulation due to a combination of (i) increased density of cation transporters

under the low Zn availability, and (ii) mistaken identity of Ni for Zn at the cation uptake sites. However, I recognize that the lack of EDTA have played a determining role in this.

The metal chelator EDTA is a component of the medium YBCII, which is commonly used to grow *Trichodesmium* (Chen et al., 1996). The addition of EDTA to the medium appears to stimulate N₂ fixation and growth in *Trichodesmium* (Paerl et al., 1994) and may chelate metals and reduce the toxic stress in *Trichodesmium* (Anderson and Morel, 1978). Ni can be essential for *Trichodesmium* as it is contained within Ni-SOD (Palenik et al., 2003; Dupont et al., 2008). Specifically, *Trichodesmium* is known to perform photosynthesis and N₂ fixation simultaneously during the daytime, however, the nitrogenase is susceptible to damage by molecular oxygen and reactive oxygen species (Gallon, 1981). Even though it is still unclear how *Trichodesmium* protects nitrogenase from damage by oxygen, the work of Ho (2013) suggests that increasing Ni availability elevates both cellular SOD activities and N₂ fixation rates, suggesting that Ni-SOD may be involved in the protection of nitrogenase from damage by oxygen (Ho, 2013). Therefore, in order to ensure the finding of elevated Ni quotas under Zn limitation is robust and reproducible, it would be important to consider running the experiment again with the addition of EDTA.

Do metalloproteins, whilst potentially strongly regulated by elemental availability, ever constitute a large enough fraction of *Trichodesmium*'s proteome to drive the measured changes in cellular N:C? Work presented in Chapter 4 showed that *Trichodesmium* grown with 5 µM DIP under Zn depleted conditions had a significantly higher (1.05-fold) N:C ratio than the Zn replete condition (20 nM). Meanwhile work in Chapter 2 showed the steady state N:C ratio in *Trichodesmium* under P depleted condition (MPA treatment) was significantly higher

(1.1-fold) than grown with P replete condition (DIP treatment). One possible reason for this is that cyanobacteria are able to upregulate a number of N-rich proteins to enhance the acquisition and transport of Zn/P from the surrounding environment (Barnett et al., 2014).

The biochemical basis for the change in N:C ratios is critical to resolve. In low latitude N depleted surface oceans, the distribution of *Trichodesmium* is thought to be strongly regulated by the availability of P and Fe (Moore et al. 2009; Sohm et al. 2011; Snow et al. 2015; Rouco et al., 2018; Cerdan-Garcia et al., 2021). Within these regions under nutrient limitation, *Trichodesmium* might be then obliged to adjust their proteins in order to obtain nutrient from their surrounding environment (Walworth et al., 2016, 2018). Changes in N:C ratios brought by element availability could be determined by tracking changes in protein abundance of *Trichodesmium* and the relative content of some specific proteins related to uptake of this specific element during laboratory incubation. For example, changes in protein abundance in *Trichodesmium* could be tracked in MPA treatments in the work of Chapter 2, meaning that changes in the abundance of some of the proteins associated with P acquisition such as AP, C-P lyase and DIP pathways could then be observed. This could then be compared with the change in the N:C ratios to obtain a profile of the change in N:C ratios due to the change in the abundance of proteins brought about by P deficiency. A recent study indicated that even though increases in the abundance of proteins of *E. huxleyi* under N or P limitation involved in inorganic nutrient transport and both the scavenging and internal remobilization of organic forms of N and P were remarkable, but the limited overall contribution to the proteome, these proteins that were upregulated under N or P limitation accounted for only 1.7% and 5.7% of the total spectral counts, respectively (McKew et al., 2015). However, these changes of proteins that are

upregulated as a percentage of the proteome under nutrient limitation are unknown in *Trichodesmium* and exploring these changes will bring new insights into how *Trichodesmium* adapts to low nutrient environments.

What is the potential impact of monoculture conditions? The work in this thesis focused on a single species, *Trichodesmium* ISM101, and followed stringent procedures to avoid contamination by bacteria in the laboratory procedures. In contrast, in the real ocean *Trichodesmium* hosts many associated bacteria that are distinct from the free-living bacteria (Hmelo et al., 2012; Gradoville et al., 2017). *Trichodesmium* and these associated bacteria share nutrients and organic molecules to cope with environmental changes (Van Mooy et al., 2012; Frischkorn et al., 2018a; Basu et al., 2019). While the interactions between *Trichodesmium* and its associated bacteria have long been recognized (Paerly et al., 1989; O’Neil and Roman, 1992), the extent to which they regulate host physiology, how they help each other to obtain nutrients and the exchange of substances between them is still poorly resolved.

A recent study suggested that different members of the marine microbial community exhibit asynchronous diurnal cycles in the expression of uptake receptors for various organic substrates, suggesting that multiple physiological mechanisms may play a role in overcoming community-wide nitrogen limitation (Muratore et al., 2022). So, would *Trichodesmium* and associated bacteria or other microorganisms in the community then exhibit asynchronous diurnal cycles in the expression of uptake receptors for various organic substrates?

Trichodesmium were cultured and analyzed as the sole model organism in the experiments in chapter 2 to 4. *Trichodesmium* are considered to be notoriously difficult to maintain in culture

(Paerly et al., 1989; Waterbury, 2006). Inter-organismal comparative genomics between *Trichodesmium* and other bacteria revealed potential interactions involving Fe and P acquisition, exchange of vitamin B₁₂, C catabolism, and detoxification of reactive oxygen (Lee et al., 2018). Analysis of *Trichodesmium* as the sole species may therefore have ignored the intricate network with bacteria that exists in the natural ocean. Microbial community composition of *Trichodesmium* colonies in the open ocean can be obtained by high-throughput sequencing technology (Jo et al., 2020). Inter-organismal comparative genomics approaches could then be applied to identify potential interactions between *Trichodesmium* and some specific dominant species in microbial community (Lee et al., 2017).

Is *Trichodesmium* buoyancy nutrient regulated? I observed an interesting phenomenon during the experiments: most of the *Trichodesmium* floated to the surface of the medium in both the MPA and Fe depleted treatments, whereas most of the *Trichodesmium* in the DIP treatment was suspended in the medium. This phenomenon is likely associated with the buoyancy of *Trichodesmium*. *Trichodesmium* contains gas vesicles which provide buoyancy (Walsby et al., 1995). Previous studies have suggested that *Trichodesmium* use buoyancy to migrate vertically to acquire nutrients such as P (Letelier and Karl, 1998; Villareal and Carpenter, 2003; White et al., 2006b; Beardall et al., 2009a). *Trichodesmium* floating on the surface that I observed in the MPA and Fe depleted treatments also seems to be aiming to keep themselves closer to the supplied medium to ensure they take a stronger position to the supply of the limiting nutrient. Although the mechanisms by which *Trichodesmium* regulates buoyancy remains uncertain, recent studies have found some possible explanations. For example, the study of Tzubari et al. (2018) suggested that P depletion induces colony formation, which enlarges the effective cell

size then enhances vertical migration of *Trichodesmium* (Tzubari et al., 2018); Held et al. (2022) analyzed diel proteomes of field and cultured populations of *Trichodesmium* in comparison with the marine diazotroph *Crocosphaera watsonii* WH8501 and suggested daytime N₂ fixation characteristics of *Trichodesmium* allows the direct shunt of electrons from the photosystems to nitrogenase, and may reduce the production of glycogen which accounts for a large proportion of the intracellular carbohydrate ballast that affects *Trichodesmium* cell density (Romans et al., 1994; Villareal and Carpenter, 2003), thereby helping *Trichodesmium* to remain neutrally buoyant (Held et al., 2022).

For the study of the buoyancy mechanism of *Trichodesmium*, the previous work on P limitation and Fe limitation in chapter 2 and 3 could be repeated. One reason is to ensure that variations in the buoyancy of *Trichodesmium* can be observed, another reason is that the EFB culture system ensures that large volumes of samples can be harvested for omics analysis. Position of *Trichodesmium* in the culture flask could then be tracked throughout automated photographs taken by camera and *Trichodesmium* could then be sampled and analyzed according to their position in the culture flask. Proteomics can help to identify changes in protein associated with nutrient limitation. For example, *Trichodesmium* floating on the surface under P limitation may have a greater abundance of AP enzymes as well as DIP transport-related proteins than the *Trichodesmium* that sink to the bottom.

Utility of particulate metabolites. In Chapter 3 I determined the changes in particulate metabolites concentrations of *Trichodesmium* grown under different P sources and Fe availability. Variations in the biomass-normalized abundances of some amino acids were detected (Fig 3.3). Under the Fe depleted condition, significantly increased abundances of

arginine, glutamate, histidine, isoleucine, leucine, phenylalanine, and proline were detected in both the DIP and MPA treatments, with abundances in the MPA treatment always significantly higher than those in DIP treatments. Even though these changes in amino acids cannot be explained sufficiently without having accompanying proteomics/transcripts, these significant changes can be used as parameters to help explain the intracellular changes in physiology of *Trichodesmium* under nutrient limitation.

Cell metabolism is highly plastic in its response to various environmental conditions (Kujawinski et al., 2017). Moreover, the composition and release of metabolites from phytoplankton depend on the growth phase (Barofsky et al., 2009, 2010; Vidoudez and Pohnert, 2012; Fiore et al., 2015; Mausz and Pohnert, 2015). Although changes in metabolite concentrations in individual cells may be negligible under environmental stress or at different stages of growth, the amount of metabolites produced by phytoplankton in the open ocean in response to environmental stresses or growth states might be dramatic. Tracking the changes of metabolites, alongside accompanying changes in genomics, proteomics and environmental variables, will improve our understanding of the function and regulation of ocean metabolism and its interactions with nutrient cycling, which is aligned with the pursuit of the recently started international project BioGeoSCAPES (www.biogeoscapes.org). In addition, applying metabolomics to phytoplankton could help to unravel the metabolic networks, functions of some metabolic pathways and some physiological changes made in response to different environmental conditions.

Given the recent developments in genetic, protein and metabolite assay techniques and related projects, we will soon have a wealth of genetic, protein and metabolite related data on marine

phytoplankton. A combined approach of these data and mathematical modelling will greatly enhance our understanding of their metabolic processes as they interact with their environment and the evolution of their underlying metabolic pathways.

References

- Amin, S. A., Hmelo, L. R., Van Tol, H. M., Durham, B. P., Carlson, L. T., Heal, K. R., et al. (2015). Interaction and signalling between a cosmopolitan phytoplankton and associated bacteria. *Nature* 522, 98–101. doi:10.1038/nature14488.
- Ammerman, J. W. (1993). “Microbial cycling of inorganic and organic phosphorus in the water column,” in *Handbook of methods in aquatic microbial ecology* (CRC Press), 649–660.
- Anderson, D. M., and Morel, F. M. M. (1978). Copper sensitivity of *Gonyaulax tamarensis*. *Limnol. Oceanogr.* doi:10.4319/lo.1978.23.2.0283.
- Anderson, L. a, and Sarmiento, J. L. (1994). Redfield ratios of remineralization determined by nutrient data analysis. *Global Biogeochem. Cycles* 8, 65–80. doi:10.1029/93GB03318.
- Anderson, M. A., and Morel, F. M. M. (1982). The influence of aqueous iron chemistry on the uptake of iron by the coastal diatom *Thalassiosira weissflogii*. *Limnol. Oceanogr.* 27, 789–813. doi:10.4319/lo.1982.27.5.0789.
- Andreini, C., Bertini, I., Cavallaro, G., Holliday, G. L., and Thornton, J. M. (2008). Metal ions in biological catalysis: From enzyme databases to general principles. *J. Biol. Inorg. Chem.* 13, 1205–1218. doi:10.1007/s00775-008-0404-5.
- Anugerahanti, P., Kerimoglu, O., and Smith, S. L. (2021). Enhancing Ocean Biogeochemical Models With Phytoplankton Variable Composition. *Front. Mar. Sci.* 8, 1–20. doi:10.3389/fmars.2021.675428.
- Arrigo, K. R. (2005). Marine microorganisms and global nutrient cycles. *Nature* 437, 349–355. doi:10.1038/nature04159.
- Badger, M. (2003). The roles of carbonic anhydrases in photosynthetic CO₂ concentrating mechanisms. *Photosynth. Res.* doi:10.1023/A:1025821717773.
- Banerjee, R., and Ragsdale, S. W. (2003). The Many Faces of Vitamin B₁₂: Catalysis by Cobalamin-Dependent Enzymes. *Annu. Rev. Biochem.* 72, 209–247. doi:10.1146/annurev.biochem.72.121801.161828.
- Barnett, J. P., Scanlan, D. J., and Blindauer, C. A. (2014). Identification of major zinc-binding proteins from a marine cyanobacterium: Insight into metal uptake in oligotrophic environments. *Metallomics* 6, 1254–1268. doi:10.1039/c4mt00048j.
- Barofsky, A., Simonelli, P., Vidoudez, C., Troedsson, C., Nejstgaard, J. C., Jakobsen, H. H., et al. (2010). Growth phase of the diatom *Skeletonema marinoi* influences the metabolic profile of the cells and the selective feeding of the copepod *Calanus* spp. *J. Plankton Res.* 32, 263–272. doi:10.1093/plankt/fbp121.
- Barofsky, A., Vidoudez, C., and Pohnert, G. (2009). Metabolic profiling reveals growth stage variability in diatom exudates. *Limnol. Oceanogr. Methods* 7, 382–390. doi:10.4319/lom.2009.7.382.
- Basu, S., Gledhill, M., de Beer, D., Prabhu Matondkar, S. G., and Shaked, Y. (2019). Colonies of marine cyanobacteria *Trichodesmium* interact with associated bacteria to acquire iron from dust. *Commun. Biol.* 2, 284. doi:10.1038/s42003-019-0534-z.

- Beardall, J., Allen, D., Bragg, J., Finkel, Z. V., Flynn, K. J., Quigg, A., et al. (2009a). Allometry and stoichiometry of unicellular, colonial and multicellular phytoplankton. *New Phytol.* 181, 295–309. doi:10.1111/j.1469-8137.2008.02660.x.
- Beardall, J., Stojkovic, S., and Larsen, S. (2009b). Living in a high CO₂ world: Impacts of global climate change on marine phytoplankton. *Plant Ecol. Divers.* 2, 191–205. doi:10.1080/17550870903271363.
- Behrenfeld, M. J., and Milligan, A. J. (2013). Photophysiological expressions of iron stress in phytoplankton. *Ann. Rev. Mar. Sci.* 5, 217–246. doi:10.1146/annurev-marine-121211-172356.
- Benitez-Nelson, C. R. (2000). The biogeochemical cycling of phosphorus in marine systems. *Earth Sci. Rev.* 51, 109–135. doi:10.1016/S0012-8252(00)00018-0.
- Bergman, B., Sandh, G., Lin, S., Larsson, J., and Carpenter, E. J. (2013). Trichodesmium - a widespread marine cyanobacterium with unusual nitrogen fixation properties. *FEMS Microbiol. Rev.* 37, 286–302. doi:10.1111/j.1574-6976.2012.00352.x.
- Berman-Frank, I., Cullen, J. T., Shaked, Y., Sherrell, R. M., and Falkowski, P. G. (2001). Iron availability, cellular iron quotas, and nitrogen fixation in Trichodesmium. *Limnol. Oceanogr.* 46, 1249–1260. doi:10.4319/lo.2001.46.6.1249.
- Berman-Frank, I., Quigg, A., Finkel, Z. V., Irwin, A. J., and Haramaty, L. (2007). Nitrogen-fixation strategies and Fe requirements in cyanobacteria. *Limnol. Oceanogr.* 52, 2260–2269. doi:10.4319/lo.2007.52.5.2260.
- Bertrand, E. M., McCrow, J. P., Moustafa, A., Zheng, H., McQuaid, J. B., Delmont, T. O., et al. (2015). Phytoplankton-bacterial interactions mediate micronutrient colimitation at the coastal Antarctic sea ice edge. *Proc. Natl. Acad. Sci. U. S. A.* 112, 9938–9943. doi:10.1073/pnas.1501615112.
- Beverford, L. J., White, A. E., Björkman, K. M., Letelier, R. M., and Karl, D. M. (2010). Phosphonate metabolism by Trichodesmium IMS101 and the production of greenhouse gases. *Limnol. Oceanogr.* 55, 1768–1778. doi:10.4319/lo.2010.55.4.1768.
- Blackman, F. F. (1905). Optima and limiting factors. *Ann. Bot.* 19, 281–295.
- Boatman, T. G., Oxborough, K., Gledhill, M., Lawson, T., and Geider, R. J. (2018). An integrated response of Trichodesmium erythraeum IMS101 growth and photo-physiology to Iron, CO₂, and light intensity. *Front. Microbiol.* 9, 1–12. doi:10.3389/fmicb.2018.00624.
- Borowitzka, M. A., and Editors, J. A. R. (2016). *The Physiology of Microalgae*. doi:10.1007/978-3-319-24945-2.
- Boyce, D. G., Lewis, M. R., and Worm, B. (2010). Global phytoplankton decline over the past century. *Nature* 466, 591–596. doi:10.1038/nature09268.
- Boyd, P. W., Rynearson, T. A., Armstrong, E. A., Fu, F., Hayashi, K., Hu, Z., et al. (2013). Marine Phytoplankton Temperature versus Growth Responses from Polar to Tropical Waters - Outcome of a Scientific Community-Wide Study. *PLoS One* 8. doi:10.1371/journal.pone.0063091.

- Browning, T. J., Achterberg, E. P., Engel, A., and Mawji, E. (2021). Manganese co-limitation of phytoplankton growth and major nutrient drawdown in the Southern Ocean. *Nat. Commun.* 12, 884. doi:10.1038/s41467-021-21122-6.
- Browning, T. J., Achterberg, E. P., Rapp, I., Engel, A., Bertrand, E. M., Tagliabue, A., et al. (2017a). Nutrient co-limitation at the boundary of an oceanic gyre. *Nature* 551, 242–246. doi:10.1038/nature24063.
- Browning, T. J., Achterberg, E. P., Yong, J. C., Rapp, I., Utermann, C., Engel, A., et al. (2017b). Iron limitation of microbial phosphorus acquisition in the tropical North Atlantic. *Nat. Commun.* 8, 15465. doi:10.1038/ncomms15465.
- Bull, A. T. (2010). The renaissance of continuous culture in the post-genomics age. *J. Ind. Microbiol. Biotechnol.* 37, 993–1021. doi:10.1007/s10295-010-0816-4.
- Canfield, D. E., Glazer, A. N., and Falkowski, P. G. (2010). The evolution and future of earth's nitrogen cycle. *Science* (80-.). 330, 192–196. doi:10.1126/science.1186120.
- Capone, D. G., Burns, J. A., Montoya, J. P., Subramaniam, A., Mahaffey, C., Gunderson, T., et al. (2005). Nitrogen fixation by *Trichodesmium* spp.: An important source of new nitrogen to the tropical and subtropical North Atlantic Ocean. *Global Biogeochem. Cycles* 19, 1–17. doi:10.1029/2004GB002331.
- Capone, D. G., Zehr, J. P., Paerl, H. W., Bergman, B., and Carpenter, E. J. (1997). *Trichodesmium*, a globally significant marine cyanobacterium. *Science* (80-.). 276, 1221–1229. doi:10.1126/science.276.5316.1221.
- Carpenter, E. J., and Capone, D. G. (2008). “Nitrogen Fixation in the Marine Environment,” in *Nitrogen in the Marine Environment* doi:10.1016/B978-0-12-372522-6.00004-9.
- Cerdan-Garcia, E., Baylay, A., Polyviou, D., Woodward, E. M. S., Wrightson, L., Mahaffey, C., et al. (2021). Transcriptional responses of *Trichodesmium* to natural inverse gradients of Fe and P availability. *ISME J.* doi:10.1038/s41396-021-01151-1.
- Chen, Y. B., Zehr, J. P., and Mellon, M. (1996). Growth and nitrogen fixation of the diazotrophic filamentous nonheterocystous cyanobacterium *Trichodesmium* sp. IMS 101 in defined media: Evidence for a circadian rhythm. *J. Phycol.* 32, 916–923. doi:10.1111/j.0022-3646.1996.00916.x.
- Coleman, M. L., and Chisholm, S. W. (2010). Ecosystem-specific selection pressures revealed through comparative population genomics. *Proc. Natl. Acad. Sci. U. S. A.* 107, 18634–18639. doi:10.1073/pnas.1009480107.
- Collins, S., Rost, B., and Rynearson, T. A. (2014). Evolutionary potential of marine phytoplankton under ocean acidification. *Evol. Appl.* 7, 140–155. doi:10.1111/eva.12120.
- Crawford, D. W., Lipsen, M. S., Purdie, D. A., Lohan, M. C., Statham, P. J., Whitney, F. A., et al. (2003). Influence of zinc and iron enrichments on phytoplankton growth in the northeastern subarctic Pacific. *Limnol. Oceanogr.* 48, 1583–1600. doi:10.4319/lo.2003.48.4.1583.
- Cullen, J. T., and Sherrell, R. M. (2005). Effects of dissolved carbon dioxide, zinc, and manganese on the cadmium to phosphorus ratio in natural phytoplankton assemblages.

- Limnol. Oceanogr.* doi:10.4319/lo.2005.50.4.1193.
- Cvetkovic, A., Menon, A. L., Thorgersen, M. P., Scott, J. W., Poole, F. L., Jenney, F. E., et al. (2010). Microbial metalloproteomes are largely uncharacterized. *Nature* 466, 779–782. doi:10.1038/nature09265.
- Da Silva, J. J. R. F., and Williams, R. J. P. (2001). *The biological chemistry of the elements: the inorganic chemistry of life*. Oxford University Press.
- Dawson, H. M., Heal, K. R., Boysen, A. K., Carlson, L. T., Ingalls, A. E., and Young, J. N. (2020). Potential of temperature- And salinity-driven shifts in diatom compatible solute concentrations to impact biogeochemical cycling within sea ice. *Elementa* 8. doi:10.1525/elementa.421.
- Deutsch, C., Sarmiento, J. L., Sigman, D. M., Gruber, N., and Dunne, J. P. (2007). Spatial coupling of nitrogen inputs and losses in the ocean. *Nature* 445, 163–167. doi:10.1038/nature05392.
- Dolmella, A., and Bandoli, G. (1993). The biological chemistry of the elements. The inorganic chemistry of life. *Inorganica Chim. Acta*. doi:10.1016/s0020-1693(00)85610-8.
- Dominic, B., Zani, S., Chen, Y., Mellon, M. T., and Zehr, J. P. (2000). ORGANIZATION OF THE *nif* GENES OF THE NONHETEROCYSTOUS CYANOBACTERIUM TRICHODESMIUM SP. IMS101. *J. Phycol.* 36, 693–701. doi:10.1046/j.1529-8817.2000.99208.x.
- Droop, M. R. (1955). A pelagic marine diatom requiring cobalamin. *J. Mar. Biol. Assoc. United Kingdom*. doi:10.1017/S0025315400027600.
- Duhamel, S., Diaz, J. M., Adams, J. C., Djaoudi, K., Steck, V., and Waggoner, E. M. (2021). Phosphorus as an integral component of global marine biogeochemistry. *Nat. Geosci.* 14, 359–368. doi:10.1038/s41561-021-00755-8.
- Duhamel, S., Dyhrman, S. T., and Karl, D. M. (2010). Alkaline phosphatase activity and regulation in the North Pacific Subtropical Gyre. *Limnol. Oceanogr.* 55, 1414–1425. doi:10.4319/lo.2010.55.3.1414.
- Dupont, C. L., Barbeau, K., and Palenik, B. (2008). Ni uptake and limitation in marine *Synechococcus* strains. *Appl. Environ. Microbiol.* 74, 23–31. doi:10.1128/AEM.01007-07.
- Durham, B. P., Dearth, S. P., Sharma, S., Amin, S. A., Smith, C. B., Campagna, S. R., et al. (2017). Recognition cascade and metabolite transfer in a marine bacteria-phytoplankton model system. *Environ. Microbiol.* 19, 3500–3513. doi:10.1111/1462-2920.13834.
- Durham, B. P., Sharma, S., Luo, H., Smith, C. B., Amin, S. A., Bender, S. J., et al. (2015). Cryptic carbon and sulfur cycling between surface ocean plankton. *Proc. Natl. Acad. Sci. U. S. A.* 112, 453–457. doi:10.1073/pnas.1413137112.
- Dyhrman, S. T. (2016). “Nutrients and Their Acquisition: Phosphorus Physiology in Microalgae,” in *The Physiology of Microalgae* (Cham: Springer International Publishing), 155–183. doi:10.1007/978-3-319-24945-2_8.
- Dyhrman, S. T., Chappell, P. D., Haley, S. T., Moffett, J. W., Orchard, E. D., Waterbury, J. B., et al. (2006a). Phosphonate utilization by the globally important marine diazotroph

- Trichodesmium. *Nature* 439, 68–71. doi:10.1038/nature04203.
- Dyhrman, S. T., and Haley, S. T. (2006). Phosphorus scavenging in the unicellular marine diazotroph *Crocospaera watsonii*. *Appl. Environ. Microbiol.* 72, 1452–1458. doi:10.1128/AEM.72.2.1452-1458.2006.
- Dyhrman, S. T., Haley, S. T., Birkeland, S. R., Wurch, L. L., Cipriano, M. J., and McArthur, A. G. (2006b). Long serial analysis of gene expression for gene discovery and transcriptome profiling in the widespread marine coccolithophore *Emiliana huxleyi*. *Appl. Environ. Microbiol.* 72, 252–260. doi:10.1128/AEM.72.1.252-260.2006.
- Dyhrman, S. T., Jenkins, B. D., Rynearson, T. A., Saito, M. A., Mercier, M. L., Alexander, H., et al. (2012). The transcriptome and proteome of the diatom *thalassiosira pseudonana* reveal a diverse phosphorus stress response. *PLoS One* 7. doi:10.1371/journal.pone.0033768.
- Dyhrman, S. T., and Ruttenberg, K. C. (2006). Presence and regulation of alkaline phosphatase activity in eukaryotic phytoplankton from the coastal ocean: Implications for dissolved organic phosphorus remineralization. *Limnol. Oceanogr.* 51, 1381–1390. doi:10.4319/lo.2006.51.3.1381.
- Fábregas, J., Maseda, A., Domínguez, A., and Otero, A. (2004). The cell composition of *Nannochloropsis* sp. changes under different irradiances in semicontinuous culture. *World J. Microbiol. Biotechnol.* doi:10.1023/B:WIBI.0000013288.67536.ed.
- Fabry, V. J., Seibel, B. A., Feely, R. A., and Orr, J. C. (2008). Impacts of ocean acidification on marine fauna and ecosystem processes. *ICES J. Mar. Sci.* 65, 414–432. doi:10.1093/icesjms/fsn048.
- Falkner, R., Priewasser, M., and Falkner, G. (2006). Information Processing by Cyanobacteria During Adaptation to Environmental Phosphate Fluctuations. *Plant Signal. Behav.* 1, 212–220. doi:10.4161/psb.1.4.3242.
- Falkowski, P. G. (1997). Evolution of the nitrogen cycle and its influence on the biological sequestration of CO₂ in the ocean. *Nature* 387, 272–275. doi:10.1038/387272a0.
- Falkowski, P. G., and Raven, J. A. (2007). *Aquatic Photosynthesis*. Princeton: Princeton University Press doi:10.1515/9781400849727.
- Feingersch, R., Philosof, A., Mejuch, T., Glaser, F., Alalouf, O., Shoham, Y., et al. (2012). Potential for phosphite and phosphonate utilization by *Prochlorococcus*. *ISME J.* 6, 827–834. doi:10.1038/ismej.2011.149.
- Fiehn, O. (2002). “Metabolomics — the link between genotypes and phenotypes,” in *Functional Genomics* (Dordrecht: Springer Netherlands), 155–171. doi:10.1007/978-94-010-0448-0_11.
- Field, C. B., Behrenfeld, M. J., Randerson, J. T., and Falkowski, P. (1998). Primary production of the biosphere: Integrating terrestrial and oceanic components. *Science (80-.)*. 281, 237–240. doi:10.1126/science.281.5374.237.
- Fiore, C. L., Longnecker, K., Kido Soule, M. C., and Kujawinski, E. B. (2015). Release of ecologically relevant metabolites by the cyanobacterium *Synechococcus elongatus* CCMP

1631. *Environ. Microbiol.* 17, 3949–3963. doi:10.1111/1462-2920.12899.
- Fischer, R., Andersen, T., Hillebrand, H., and Ptacnik, R. (2014). The exponentially fed batch culture as a reliable alternative to conventional chemostats. *Limnol. Oceanogr. Methods* 12, 432–440. doi:10.4319/lom.2014.12.432.
- Follett, C. L., Dutkiewicz, S., Karl, D. M., Inomura, K., and Follows, M. J. (2018a). Seasonal resource conditions favor a summertime increase in North Pacific diatom-diazotroph associations. *ISME J.* 12, 1543–1557. doi:10.1038/s41396-017-0012-x.
- Follett, C. L., White, A. E., Wilson, S. T., and Follows, M. J. (2018b). Nitrogen fixation rates diagnosed from diurnal changes in elemental stoichiometry. *Limnol. Oceanogr.* 63, 1911–1923. doi:10.1002/lno.10815.
- Foster, R. A., and Zehr, J. P. (2019). Diversity, genomics, and distribution of phytoplankton-cyanobacterium single-cell symbiotic associations. *Annu. Rev. Microbiol.* 73, 435–456. doi:10.1146/annurev-micro-090817-062650.
- Frischkorn, K. R., Haley, S. T., and Dyhrman, S. T. (2018a). Coordinated gene expression between *Trichodesmium* and its microbiome over day-night cycles in the North Pacific Subtropical Gyre. *ISME J.* 12, 997–1007. doi:10.1038/s41396-017-0041-5.
- Frischkorn, K. R., Haley, S. T., and Dyhrman, S. T. (2019). Transcriptional and proteomic choreography under phosphorus deficiency and re-supply in the N₂ fixing cyanobacterium *trichodesmium erythraeum*. *Front. Microbiol.* 10, 1–13. doi:10.3389/fmicb.2019.00330.
- Frischkorn, K. R., Rouco, M., Van Mooy, B. A. S., and Dyhrman, S. T. (2018b). The *Trichodesmium* microbiome can modulate host N₂ fixation. *Limnol. Oceanogr. Lett.* 3, 401–408. doi:10.1002/lol2.10092.
- Gallon, J. R. (1981). The oxygen sensitivity of nitrogenase: a problem for biochemists and micro-organisms. *Trends Biochem. Sci.* 6, 19–23. doi:10.1016/0968-0004(81)90008-6.
- Garcia, N. S., Fu, F., Sedwick, P. N., and Hutchins, D. A. (2015). Iron deficiency increases growth and nitrogen-fixation rates of phosphorus-deficient marine cyanobacteria. *ISME J.* 9, 238–245. doi:10.1038/ismej.2014.104.
- Geider, R. J., and La Roche, J. (1994). The role of iron in phytoplankton photosynthesis, and the potential for iron-limitation of primary productivity in the sea. *Photosynth. Res.* 39, 275–301. doi:10.1007/BF00014588.
- Geider, R. J., and La Roche, J. (2002). Redfield revisited: Variability of C:N:P in marine microalgae and its biochemical basis. *Eur. J. Phycol.* 37, 1–17. doi:10.1017/S0967026201003456.
- Geider, R. J., Roche, J., Greene, R. M., and Olaizola, M. (1993). RESPONSE OF THE PHOTOSYNTHETIC APPARATUS OF PHAEODACTYLUM TRICORNUTUM (BACILLARIOPHYCEAE) TO NITRATE, PHOSPHATE, OR IRON STARVATION1. *J. Phycol.* 29, 755–766. doi:10.1111/j.0022-3646.1993.00755.x.
- Gong, N., Chen, C., Xie, L., Chen, H., Lin, X., and Zhang, R. (2005). Characterization of a thermostable alkaline phosphatase from a novel species *Thermus yunnanensis* sp. nov. and investigation of its cobalt activation at high temperature. *Biochim. Biophys. Acta - Proteins*

- Proteomics*. doi:10.1016/j.bbapap.2005.05.007.
- Gordillo, F. J. L., Goutx, M., Figueroa, F. L., and Niell, F. X. (1998). Effects of light intensity, CO₂ and nitrogen supply on lipid class composition of *Dunaliella viridis*. *J. Appl. Phycol.* doi:10.1023/A:1008067022973.
- Gradoville, M. R., Crump, B. C., Letelier, R. M., Church, M. J., and White, A. E. (2017). Microbiome of *Trichodesmium* colonies from the North Pacific Subtropical Gyre. *Front. Microbiol.* 8, 1–16. doi:10.3389/fmicb.2017.01122.
- Gray, M. J., and Jakob, U. (2015). Oxidative stress protection by polyphosphate-new roles for an old player. *Curr. Opin. Microbiol.* 24, 1–6. doi:10.1016/j.mib.2014.12.004.
- Heal, K. R., Kellogg, N. A., Carlson, L. T., Lionheart, R. M., and Ingalls, A. E. (2019). Metabolic Consequences of Cobalamin Scarcity in the Diatom *Thalassiosira pseudonana* as Revealed Through Metabolomics. *Protist* 170, 328–348. doi:10.1016/j.protis.2019.05.004.
- Heal, K. R., Qin, W., Ribalet, F., Bertagnolli, A. D., Coyote-Maestas, W., Hmelo, L. R., et al. (2017). Two distinct pools of B12 analogs reveal community interdependencies in the ocean. *Proc. Natl. Acad. Sci. U. S. A.* 114, 364–369. doi:10.1073/pnas.1608462114.
- Held, N. A., Waterbury, J. B., Webb, E. A., Kellogg, R. M., McIlvin, M. R., Jakuba, M., et al. (2022). Dynamic diel proteome and daytime nitrogenase activity supports buoyancy in the cyanobacterium *Trichodesmium*. *Nat. Microbiol.* doi:10.1038/s41564-021-01028-1.
- Held, N. A., Webb, E. A., McIlvin, M. M., Hutchins, D. A., Cohen, N. R., Moran, D. M., et al. (2020). Co-occurrence of Fe and P stress in natural populations of the marine diazotroph *Trichodesmium*. *Biogeosciences* 17, 2537–2551. doi:10.5194/bg-17-2537-2020.
- Hernandez, J. A., George, S. J., and Rubio, L. M. (2009). Molybdenum trafficking for nitrogen fixation. *Biochemistry* 48, 9711–9721. doi:10.1021/bi901217p.
- Hmelo, L. R., Van Mooy, B. A. S., and Mincer, T. J. (2012). Characterization of bacterial epibionts on the cyanobacterium *Trichodesmium*. *Aquat. Microb. Ecol.* 67, 1–14. doi:10.3354/ame01571.
- Ho, T.-Y. (2013). Nickel limitation of nitrogen fixation in *Trichodesmium*. *Limnol. Oceanogr.* 58, 112–120. doi:10.4319/lo.2013.58.1.0112.
- Ho, T.-Y., Quigg, A., Finkel, Z. V., Milligan, A. J., Wyman, K., Falkowski, P. G., et al. (2003a). THE ELEMENTAL COMPOSITION OF SOME MARINE PHYTOPLANKTON1. *J. Phycol.* 39, 1145–1159. doi:10.1111/j.0022-3646.2003.03-090.x.
- Ho, T.-Y., Quigg, A., Finkel, Z. V., Milligan, A. J., Wyman, K., Falkowski, P. G., et al. (2003b). THE ELEMENTAL COMPOSITION OF SOME MARINE PHYTOPLANKTON1. *J. Phycol.* 39, 1145–1159. doi:10.1111/j.0022-3646.2003.03-090.x.
- Ho, T. Y., Chu, T. H., and Hu, C. L. (2013). Interrelated influence of light and Ni on *Trichodesmium* growth. *Front. Microbiol.* 4, 1–6. doi:10.3389/fmicb.2013.00139.
- Hoffman, B. M., Lukoyanov, D., Yang, Z. Y., Dean, D. R., and Seefeldt, L. C. (2014). Mechanism of nitrogen fixation by nitrogenase: The next stage. *Chem. Rev.* 114, 4041–4062. doi:10.1021/cr400641x.

- Honey, D., Gledhill, M., Bibby, T., Legiret, F., Pratt, N., Hickman, A., et al. (2013). Heme b in marine phytoplankton and particulate material from the North Atlantic Ocean. *Mar. Ecol. Prog. Ser.* 483, 1–17. doi:10.3354/meps10367.
- Hudek, L., Premachandra, D., Webster, W. A. J., and Bräu, L. (2016). Role of phosphate transport system component PstB1 in phosphate internalization by *Nostoc punctiforme*. *Appl. Environ. Microbiol.* 82, 6344–6356. doi:10.1128/AEM.01336-16.
- Hynes, A. M., Chappell, P. D., Dyhrman, S. T., Doney, S. C., and Webb, E. A. (2009). Cross-basin comparison of phosphorus stress and nitrogen fixation in *Trichodesmium*. *Limnol. Oceanogr.* 54, 1438–1448. doi:10.4319/lo.2009.54.5.1438.
- IPCC (2019). 5: Changing ocean, marine ecosystems, and dependent communities. *Intergov. Panel Clim. Chang. IPCC Spec. Rep. Ocean Cryosph. a Chang. Clim.*
- Irving, H., and Williams, Rjp. (1953). 637. The stability of transition-metal complexes. *J. Chem. Soc.*, 3192–3210.
- Jakuba, R. W., Moffett, J. W., and Dyhrman, S. T. (2008). Evidence for the linked biogeochemical cycling of zinc, cobalt, and phosphorus in the western North Atlantic Ocean. *Global Biogeochem. Cycles* 22, 1–13. doi:10.1029/2007GB003119.
- Jo, J., Oh, J., and Park, C. (2020). Microbial community analysis using high-throughput sequencing technology: a beginner's guide for microbiologists. *J. Microbiol.* 58, 176–192. doi:10.1007/s12275-020-9525-5.
- Johnson, W. (2021). Insights into the controls on metabolite distributions along a latitudinal transect of the western Atlantic Ocean. doi:10.1101/2021.03.09.434501.
- Johnson, W. M., Kido Soule, M. C., and Kujawinski, E. B. (2016). Evidence for quorum sensing and differential metabolite production by a marine bacterium in response to DMSP. *ISME J.* 10, 2304–2316. doi:10.1038/ismej.2016.6.
- Kalacheva, G. S., Zhila, N. O., Volova, T. G., and Gladyshev, M. I. (2002). The effect of temperature on the lipid composition of the green alga *Botryococcus*. *Microbiology*. doi:10.1023/A:1015898426573.
- Karl, D. M. (2014). Microbially Mediated Transformations of Phosphorus in the Sea: New Views of an Old Cycle. *Ann. Rev. Mar. Sci.* 6, 279–337. doi:10.1146/annurev-marine-010213-135046.
- Karl, D. M., and Björkman, K. M. (2002). “Dynamics of DOP,” in *Biogeochemistry of Marine Dissolved Organic Matter*, eds. D. A. Hansell and C. A. Carlson (San Diego: Elsevier), 249–366. doi:10.1016/B978-012323841-2/50008-7.
- Kaushik, M. S., Srivastava, M., Verma, E., and Mishra, A. K. (2015). Role of manganese in protection against oxidative stress under iron starvation in cyanobacterium *Anabaena* 7120. *J. Basic Microbiol.* 55, 729–740. doi:10.1002/jobm.201400742.
- Kido Soule, M. C., Longnecker, K., Johnson, W. M., and Kujawinski, E. B. (2015). Environmental metabolomics: Analytical strategies. *Mar. Chem.* 177, 374–387. doi:10.1016/j.marchem.2015.06.029.
- Kim, E. E., and Wyckoff, H. W. (1991). Reaction Mechanism of Alkaline Phosphatase Based

- on Crystal Structures. *J. Mol. Biol.* 218, 449–464.
- Klug, A. (2010). The Discovery of Zinc Fingers and Their Applications in Gene Regulation and Genome Manipulation. *Annu. Rev. Biochem.* doi:10.1146/annurev-biochem-010909-095056.
- Knoll, A. H. (2003). The geological consequences of evolution. *Geobiology* 1, 3–14. doi:10.1046/j.1472-4669.2003.00002.x.
- Kobayashi, M., and Shimizu, S. (1999). Cobalt proteins. *Eur. J. Biochem.* 261, 1–9. doi:10.1046/j.1432-1327.1999.00186.x.
- Krauk, J. M., Villareal, T. A., Sohm, J. A., Montoya, J. P., and Capone, D. G. (2006). Plasticity of N:P ratios in laboratory and field populations of *Trichodesmium* spp. *Aquat. Microb. Ecol.* 42, 243–253. doi:10.3354/ame042243.
- Kruskopf, M., and Flynn, K. J. (2006). Erratum: Chlorophyll content and fluorescence responses cannot be used to gauge reliably phytoplankton biomass, nutrient status or growth rate (New Phytologist (2006) 169, (525-536)). *New Phytol.* 169, 841–842. doi:10.1111/j.1469-8137.2006.01652.x.
- Kujawinski, E. B., Longnecker, K., Alexander, H., Dyhrman, S. T., Fiore, C. L., Haley, S. T., et al. (2017). Phosphorus availability regulates intracellular nucleotides in marine eukaryotic phytoplankton. *Limnol. Oceanogr. Lett.* 2, 119–129. doi:10.1002/lol2.10043.
- Kupriyanova, E. V., and Pronina, N. A. (2011). Carbonic anhydrase: Enzyme that has transformed the biosphere. *Russ. J. Plant Physiol.* doi:10.1134/S1021443711020099.
- Kustka, A. B., Sañudo-Wilhelmy, S. A., Carpenter, E. J., Capone, D., Burns, J., and Sunda, W. G. (2004). Iron requirements for dinitrogen- and ammonium-supported growth in cultures of *Trichodesmium* (IMS 101): Comparison with nitrogen fixation rates and iron : carbon ratios of field populations. *Limnol. Oceanogr.* 49, 1224–1224. doi:10.4319/lo.2004.49.4.1224.
- Langlois, R. J., Hümmer, D., and LaRoche, J. (2008). Abundances and distributions of the dominant nifH phylotypes in the Northern Atlantic Ocean. *Appl. Environ. Microbiol.* 74, 1922–1931. doi:10.1128/AEM.01720-07.
- Lee, M. D., Walworth, N. G., McParland, E. L., Fu, F. X., Mincer, T. J., Levine, N. M., et al. (2017). The *Trichodesmium* consortium: Conserved heterotrophic co-occurrence and genomic signatures of potential interactions. *ISME J.* 11, 1813–1824. doi:10.1038/ismej.2017.49.
- Lee, M. D., Webb, E. A., Walworth, N. G., Fu, F. X., Held, N. A., Saito, M. A., et al. (2018). Transcriptional activities of the microbial consortium living with the marine nitrogenfixing cyanobacterium *Trichodesmium* reveal potential roles in community-level nitrogen cycling. *Appl. Environ. Microbiol.* 84, 1–16. doi:10.1128/AEM.02026-17.
- Letelier, R., and Karl, D. (1998). *Trichodesmium* spp. physiology and nutrient fluxes in the North Pacific subtropical gyre. *Aquat. Microb. Ecol.* 15, 265–276. doi:10.3354/ame015265.
- Liaw, S. -H, Kuo, I., and Eisenberg, D. (1995). Discovery of the ammonium substrate site on

- glutamine synthetase, A third cation binding site. *Protein Sci.* 4, 2358–2365. doi:10.1002/pro.5560041114.
- Lionetto, M. G., Caricato, R., Giordano, M. E., and Schettino, T. (2016). The complex relationship between metals and carbonic anhydrase: New insights and perspectives. *Int. J. Mol. Sci.* 17. doi:10.3390/ijms17010127.
- Liu, S., Guo, Z., Li, T., Huang, H., and Lin, S. (2011). Photosynthetic efficiency, cell volume, and elemental stoichiometric ratios in *Thalassiosira weissflogii* under phosphorus limitation. *Chinese J. Oceanol. Limnol.* 29, 1048–1056. doi:10.1007/s00343-011-0224-2.
- Los, D. A., Suzuki, I., Zinchenko, V. V., and Murata, N. (2008). Stress responses in *Synechocystis*: regulated genes and regulatory systems. *Cyanobacteria. Mol. Biol. Genomics Evol.*, 117–157.
- Luo, H., Zhang, H., Long, R. A., and Benner, R. (2011). Depth distributions of alkaline phosphatase and phosphonate utilization genes in the North Pacific Subtropical Gyre. *Aquat. Microb. Ecol.* 62, 61–69. doi:10.3354/ame01458.
- Luxem, K. E., Ellwood, M. J., and Strzepek, R. F. (2017). Intraspecific variability in *Phaeocystis antarctica*'s response to iron and light stress. *PLoS One* 12, 1–14. doi:10.1371/journal.pone.0179751.
- Lyons, T. W., Reinhard, C. T., and Planavsky, N. J. (2014). The rise of oxygen in Earth's early ocean and atmosphere. *Nature* 506, 307–315. doi:10.1038/nature13068.
- Mahaffey, C. (2005). The conundrum of marine N₂ fixation. *Am. J. Sci.* 305, 546–595. doi:10.2475/ajs.305.6-8.546.
- Mahaffey, C., Reynolds, S., Davis, C. E., and Lohan, M. C. (2014). Alkaline phosphatase activity in the subtropical ocean: insights from nutrient, dust and trace metal addition experiments. *Front. Mar. Sci.* 1, 1–13. doi:10.3389/fmars.2014.00073.
- Makino, K., Shinagawa, H., Amemura, M., Kimura, S., Nakata, A., and Ishihama, A. (1988). Regulation of the phosphate regulon of *Escherichia coli*. Activation of *pstS* transcription by PhoB protein in vitro. *J. Mol. Biol.* 203, 85–95. doi:10.1016/0022-2836(88)90093-9.
- Marchetti, A., and Harrison, P. J. (2007). Coupled changes in the cell morphology and elemental (C, N, and Si) composition of the pennate diatom *Pseudo-nitzschia* due to iron deficiency. *Limnol. Oceanogr.* 52, 2270–2284. doi:10.4319/lo.2007.52.5.2270.
- Mark Moore, C., Mills, M. M., Achterberg, E. P., Geider, R. J., Laroche, J., Lucas, M. I., et al. (2009). Large-scale distribution of Atlantic nitrogen fixation controlled by iron availability. *Nat. Geosci.* 2, 867–871. doi:10.1038/ngeo667.
- Marki, A., Fischer, R., Browning, T. J., Louropoulou, E., Ptacnik, R., and Gledhill, M. (2020). Stoichiometry of Fe, Mn and Co in the marine diazotroph *Crocospaera subtropica* ATCC51142 in Fe- And P-limited continuous cultures. *Mar. Ecol. Prog. Ser.* 656, 19–33. doi:10.3354/meps13523.
- Martínez, A., Osburne, M. S., Sharma, A. K., Delong, E. F., and Chisholm, S. W. (2012). Phosphite utilization by the marine picocyanobacterium *Prochlorococcus* MIT9301. *Environ. Microbiol.* 14, 1363–1377. doi:10.1111/j.1462-2920.2011.02612.x.

- Martinez, A., Tyson, G. W., and Delong, E. F. (2010). Widespread known and novel phosphonate utilization pathways in marine bacteria revealed by functional screening and metagenomic analyses. *Environ. Microbiol.* 12, 222–238. doi:10.1111/j.1462-2920.2009.02062.x.
- Martiny, A. C., Coleman, M. L., and Chisholm, S. W. (2006). Phosphate acquisition genes in *Prochlorococcus* ecotypes: Evidence for genome-wide adaptation. *Proc. Natl. Acad. Sci. U. S. A.* 103, 12552–12557. doi:10.1073/pnas.0601301103.
- Martiny, A. C., Lomas, M. W., Fu, W., Boyd, P. W., Chen, Y. ling L., Cutter, G. A., et al. (2019). Biogeochemical controls of surface ocean phosphate. *Sci. Adv.* 5, 1–10. doi:10.1126/sciadv.aax0341.
- Mausz, M. A., and Pohnert, G. (2015). Phenotypic diversity of diploid and haploid *Emiliania huxleyi* cells and of cells in different growth phases revealed by comparative metabolomics. *J. Plant Physiol.* 172, 137–148. doi:10.1016/j.jplph.2014.05.014.
- McGrath, J. W., Chin, J. P., and Quinn, J. P. (2013). Organophosphonates revealed: New insights into the microbial metabolism of ancient molecules. *Nat. Rev. Microbiol.* 11, 412–419. doi:10.1038/nrmicro3011.
- McKew, B. A., Metodieva, G., Raines, C. A., Metodiev, M. V., and Geider, R. J. (2015). Acclimation of *Emiliania huxleyi* (1516) to nutrient limitation involves precise modification of the proteome to scavenge alternative sources of N and P. *Environ. Microbiol.* 17, 4050–4062. doi:10.1111/1462-2920.12957.
- Merchant, S. S., and Helmann, J. D. (2012). “Elemental Economy: Microbial Strategies for Optimizing Growth in the Face of Nutrient Limitation,” in *Advances in Microbial Physiology* (Elsevier Ltd.), 91–210. doi:10.1016/B978-0-12-398264-3.00002-4.
- Metcalf, W. W., Griffin, B. M., Cicchillo, R. M., Gao, J., Janga, S. C., Cooke, H. A., et al. (2012). Synthesis of Methylphosphonic Acid by Marine Microbes: A Source for Methane in the Aerobic Ocean. *Science (80-.).* 337, 1104–1107. doi:10.1126/science.1219875.
- Miller, A. F. (2012). Superoxide dismutases: Ancient enzymes and new insights. *FEBS Lett.* 586, 585–595. doi:10.1016/j.febslet.2011.10.048.
- Mock, T., and Kroon, B. M. A. (2002). Photosynthetic energy conversion under extreme conditions - II: The significance of lipids under light limited growth in Antarctic sea ice diatoms. *Phytochemistry*. doi:10.1016/S0031-9422(02)00215-7.
- Montsant, A., Allen, A. E., Coesel, S., Martino, A. De, Falciatore, A., Mangogna, M., et al. (2007). Identification and comparative genomic analysis of signaling and regulatory components in the diatom *Thalassiosira pseudonana*. *J. Phycol.* 43, 585–604. doi:10.1111/j.1529-8817.2007.00342.x.
- Moore, C. M., Mills, M. M., Arrigo, K. R., Berman-Frank, I., Bopp, L., Boyd, P. W., et al. (2013). Processes and patterns of oceanic nutrient limitation. *Nat. Geosci.* 6, 701–710. doi:10.1038/ngeo1765.
- Moore, J. K., Doney, S. C., Glover, D. M., and Fung, I. Y. (2001). Iron cycling and nutrient-limitation patterns in surface waters of the World Ocean. *Deep Sea Res. Part II Top. Stud. Oceanogr.* 49, 463–507. doi:10.1016/S0967-0645(01)00109-6.

- Morel, F. M. M., Lam, P. J., and Saito, M. A. (2020). Trace Metal Substitution in Marine Phytoplankton. *Annu. Rev. Earth Planet. Sci.* 48, 491–517. doi:10.1146/annurev-earth-053018-060108.
- Morel, F. M. M., Milligan, A. J., and Saito, M. A. (2003). Marine Bioinorganic Chemistry: The Role of Trace Metals in the Oceanic Cycles of Major Nutrients. *Treatise on Geochemistry* 6–9, 113–143. doi:10.1016/B0-08-043751-6/06108-9.
- Morris, I., Glover, H. E., and Yentsch, C. S. (1974). Products of photosynthesis by marine phytoplankton: the effect of environmental factors on the relative rates of protein synthesis. *Mar. Biol.* doi:10.1007/BF00394754.
- Morrissey, J., and Bowler, C. (2012). Iron utilization in marine cyanobacteria and eukaryotic algae. *Front. Microbiol.* 3, 1–13. doi:10.3389/fmicb.2012.00043.
- Mulholland, M. R., and Bernhardt, P. W. (2005). The effect of growth rate, phosphorus concentration, and temperature on N₂ fixation, carbon fixation, and nitrogen release in continuous cultures of *Trichodesmium* IMS101. *Limnol. Oceanogr.* 50, 839–849. doi:10.4319/lo.2005.50.3.0839.
- Murata, N., and Los, D. A. (2006). Histidine kinase Hik33 is an important participant in cold-signal transduction in cyanobacteria. *Physiol. Plant.* 126, 17–27. doi:10.1111/j.1399-3054.2006.00608.x.
- Muratore, D., Boysen, A. K., Harke, M. J., Becker, K. W., Casey, J. R., Coesel, S. N., et al. (2022). Complex marine microbial communities partition metabolism of scarce resources over the diel cycle. *Nat. Ecol. Evol.* doi:10.1038/s41559-021-01606-w.
- Nakamura, Y., and Miyachi, S. (1982). Effect of Temperature on Starch Degradation in *Chlorella vulgaris* 11 h Cells. *Changes*.
- Naselli-Flores, L., Zohary, T., and Padisák, J. (2020). Life in suspension and its impact on phytoplankton morphology: an homage to Colin S. Reynolds. *Hydrobiologia*. doi:10.1007/s10750-020-04217-x.
- Nuester, J., Vogt, S., Newville, M., Kustka, A. B., and Twining, B. S. (2012). The Unique Biogeochemical Signature of the Marine Diazotroph *Trichodesmium*. *Front. Microbiol.* 3, 1–15. doi:10.3389/fmicb.2012.00150.
- O’Neil, J. M., and Roman, M. R. (1992). “Grazers and associated organisms of *Trichodesmium*,” in *Marine pelagic cyanobacteria: Trichodesmium and other diazotrophs* (Springer), 61–73.
- Orchard, E. D., Ammerman, J. W., Lomas, M. W., and Dyhrman, S. T. (2010a). Dissolved inorganic and organic phosphorus uptake in *Trichodesmium* and the microbial community: The importance of phosphorus ester in the Sargasso Sea. *Limnol. Oceanogr.* 55, 1390–1399. doi:10.4319/lo.2010.55.3.1390.
- Orchard, E. D., Benitez-Nelson, C. R., Pellechia, P. J., Lomas, M. W., and Dyhrman, S. T. (2010b). Polyphosphate in *Trichodesmium* from the low-phosphorus Sargasso Sea. *Limnol. Oceanogr.* 55, 2161–2169. doi:10.4319/lo.2010.55.5.2161.
- Paerl, H. W., Prufert-Bebout, L. E., and Guo, C. (1994). Iron-stimulated N₂ fixation and growth

- in natural and cultured populations of the planktonic marine cyanobacteria *Trichodesmium* spp. *Appl. Environ. Microbiol.* 60, 1044–1047. doi:10.1128/aem.60.3.1044-1047.1994.
- Paerly, H. W., Bebout, B. M., and Prufert, L. E. (1989). BACTERIAL ASSOCIATIONS WITH MARINE OSCILLATORIA SP. (TRICHODESMIUM SP.) POPULATIONS: ECOPHYSIOLOGICAL IMPLICATIONS1. *J. Phycol.* 25, 773–784. doi:10.1111/j.0022-3646.1989.00773.x.
- Palenik, B., Brahamsha, B., Larimer, F. W., Land, M., Hauser, L., Chain, P., et al. (2003). The genome of a motile marine *Synechococcus*. *Nature* 424, 1037–1042. doi:10.1038/nature01943.
- Palenik, B., and Morel, F. M. M. (1991). Amine oxidases of marine phytoplankton. *Appl. Environ. Microbiol.* 57, 2440–2443. doi:10.1128/aem.57.8.2440-2443.1991.
- Panzeca, C., Tovar-Sanchez, A., Agustí, S., Reche, I., Duarte, C. M., Taylor, G. T., et al. (2006). B vitamins as regulators of phytoplankton dynamics. *Eos (Washington, DC)*. doi:10.1029/2006EO520001.
- Parkhill, J. P., Maillet, G., and Cullen, J. J. (2001). Fluorescence-based maximal quantum yield for PSII as a diagnostic of nutrient stress. *J. Phycol.* 37, 517–529. doi:10.1046/j.1529-8817.2001.037004517.x.
- Pau, R. N. (2004). “Molybdenum uptake and homeostasis,” in *Genetics and regulation of nitrogen fixation in free-living bacteria* (Springer), 225–256.
- Paytan, A., and McLaughlin, K. (2007). The Oceanic Phosphorus Cycle. *Chem. Rev.* 107, 563–576. doi:10.1021/cr0503613.
- Peers, G., and Price, N. M. (2004). A role for manganese in superoxide dismutases and growth of iron-deficient diatoms. *Limnol. Oceanogr.* 49, 1774–1783. doi:10.4319/lo.2004.49.5.1774.
- Peers, G., and Price, N. M. (2006). Copper-containing plastocyanin used for electron transport by an oceanic diatom. *Nature* 441, 341–344. doi:10.1038/nature04630.
- Peers, G., Quesnel, S. A., and Price, N. M. (2005). Copper requirements for iron acquisition and growth of coastal and oceanic diatoms. *Limnol. Oceanogr.* 50, 1149–1158. doi:10.4319/lo.2005.50.4.1149.
- Peng, Z., Feng, L., Wang, X., and Miao, X. (2019). Adaptation of *Synechococcus* sp. PCC 7942 to phosphate starvation by glycolipid accumulation and membrane lipid remodeling. *Biochim. Biophys. Acta - Mol. Cell Biol. Lipids* 1864, 158522. doi:10.1016/j.bbalip.2019.158522.
- Pickell, L. D., Wells, M. L., Trick, C. G., and Cochlan, W. P. (2009). A sea-going continuous culture system for investigating phytoplankton community response to macro-and micro-nutrient manipulations. *Limnol. Oceanogr. Methods* 7, 21–32.
- Pierella Karlusich, J. J., Pelletier, E., Lombard, F., Carsique, M., Dvorak, E., Colin, S., et al. (2021). Global distribution patterns of marine nitrogen-fixers by imaging and molecular methods. *Nat. Commun.* 12, 4160. doi:10.1038/s41467-021-24299-y.
- Pitt, F. D., Mazard, S., Humphreys, L., and Scanlan, D. J. (2010). Functional Characterization

- of *Synechocystis* sp. Strain PCC 6803 *pst1* and *pst2* Gene Clusters Reveals a Novel Strategy for Phosphate Uptake in a Freshwater Cyanobacterium. *J. Bacteriol.* 192, 3512–3523. doi:10.1128/JB.00258-10.
- Polovina, J. J., Howell, E. A., and Abecassis, M. (2008). Ocean's least productive waters are expanding. *Geophys. Res. Lett.* 35, 2–6. doi:10.1029/2007GL031745.
- Polyviou, D., Hitchcock, A., Baylay, A. J., Moore, C. M., and Bibby, T. S. (2015). Phosphite utilization by the globally important marine diazotroph *Trichodesmium*. *Environ. Microbiol. Rep.* 7, 824–830. doi:10.1111/1758-2229.12308.
- Post, A. F., Rihtman, B., and Wang, Q. (2012). Decoupling of ammonium regulation and *ntcA* transcription in the diazotrophic marine cyanobacterium *Trichodesmium* sp. IMS101. *ISME J.* 6, 629–637. doi:10.1038/ismej.2011.121.
- Raven, J. A. (2009). Contributions of anoxygenic and oxygenic phototrophy and chemolithotrophy to carbon and oxygen fluxes in aquatic environments. in *Aquatic Microbial Ecology* doi:10.3354/ame01315.
- Raven, J. A., Evans, M. C. W., and Korb, R. E. (1999). The role of trace metals in photosynthetic electron transport in O₂-evolving organisms. *Photosynth. Res.* 60, 111–150. doi:10.1023/a:1006282714942.
- Ray, J. M., Bhaya, D., Block, M. A., and Grossman, A. R. (1991). Isolation, transcription, and inactivation of the gene for an atypical alkaline phosphatase of *Synechococcus* sp. strain PCC 7942. *J. Bacteriol.* 173, 4297–4309. doi:10.1128/jb.173.14.4297-4309.1991.
- Redfield, A. C. (1934). James Johnstone memorial volume. *proportions Org. Deriv. sea water their Relat. to Compos. Plankt.*, 176–192.
- Redfield, A. C. (1958). The biological control of chemical factors in the environment. 46, 205–221. Available at: www.jstor.org/stable/27827150.
- Reistetter, E. N., Krumhardt, K., Callnan, K., Roache-Johnson, K., Saunders, J. K., Moore, L. R., et al. (2013). Effects of phosphorus starvation versus limitation on the marine cyanobacterium *Prochlorococcus* MED4 II: Gene expression. *Environ. Microbiol.* 15, 2129–2143. doi:10.1111/1462-2920.12129.
- Reynolds, C. S. (1984). *The ecology of freshwater phytoplankton*. Cambridge university press.
- Richier, S., Macey, A. I., Pratt, N. J., Honey, D. J., Moore, C. M., and Bibby, T. S. (2012). Abundances of iron-binding photosynthetic and nitrogen-fixing proteins of *Trichodesmium* both in culture and in situ from the North Atlantic. *PLoS One* 7. doi:10.1371/journal.pone.0035571.
- Roche, J., Geider, R. J., Graziano, L. M., Murray, H., and Lewis, K. (1993). INDUCTION OF SPECIFIC PROTEINS IN EUKARYOTIC ALGAE GROWN UNDER IRON-, PHOSPHORUS-, OR NITROGEN-DEFICIENT CONDITIONS1. *J. Phycol.* 29, 767–777. doi:10.1111/j.0022-3646.1993.00767.x.
- Rodriguez, F., Lillington, J., Johnson, S., Timmel, C. R., Lea, S. M., and Berks, B. C. (2014). Crystal Structure of the *Bacillus subtilis* Phosphodiesterase PhoD Reveals an Iron and Calcium-containing Active Site. *J. Biol. Chem.* 289, 30889–30899.

- doi:10.1074/jbc.M114.604892.
- Rodriguez, I. B., and Ho, T. Y. (2015). Influence of Co and B12 on the growth and nitrogen fixation of *Trichodesmium*. *Front. Microbiol.* 6, 1–9. doi:10.3389/fmicb.2015.00623.
- Romans, K. M., Carpenter, E. J., and Bergman, B. (1994). BUOYANCY REGULATION IN THE COLONIAL DIAZOTROPHIC CYANOBACTERIUM *TRICHODESMIUM TENUE*: ULTRASTRUCTURE AND STORAGE OF CARBOHYDRATE, POLYPHOSPHATE, AND NITROGEN¹. *J. Phycol.* 30, 935–942. doi:10.1111/j.0022-3646.1994.00935.x.
- Roshan, S., DeVries, T., Wu, J., and Chen, G. (2018). The Internal Cycling of Zinc in the Ocean. *Global Biogeochem. Cycles* 32, 1833–1849. doi:10.1029/2018GB006045.
- Saino, T., and Hattori, A. (1978). Diel variation in nitrogen fixation by a marine blue-green alga, *Trichodesmium thiebautii*. *Deep Sea Res.* 25, 1259–1263.
- Saito, M. A., and Goepfert, T. J. (2008). Zinc-cobalt colimitation of *Phaeocystis antarctica*. *Limnol. Oceanogr.* 53, 266–275. doi:10.4319/lo.2008.53.1.0266.
- Saito, M. A., Goepfert, T. J., and Ritt, J. T. (2008). Some thoughts on the concept of colimitation: Three definitions and the importance of bioavailability. *Limnol. Oceanogr.* 53, 276–290. doi:10.4319/lo.2008.53.1.0276.
- Saito, M. A., McIlvin, M. R., Moran, D. M., Goepfert, T. J., DiTullio, G. R., Post, A. F., et al. (2014). Multiple nutrient stresses at intersecting Pacific Ocean biomes detected by protein biomarkers. *Science* (80-.). 345, 1173–1177. doi:10.1126/science.1256450.
- Salomon, E., and Keren, N. (2011). Manganese Limitation Induces Changes in the Activity and in the Organization of Photosynthetic Complexes in the Cyanobacterium *Synechocystis* sp. Strain PCC 6803. *Plant Physiol.* 155, 571–579. doi:10.1104/pp.110.164269.
- Salomon, E., and Keren, N. (2015). Acclimation to environmentally relevant Mn concentrations rescues a cyanobacterium from the detrimental effects of iron limitation. *Environ. Microbiol.* 17, 2090–2098. doi:10.1111/1462-2920.12826.
- Sarmiento, J. L., and Gruber, N. (2006). *Ocean Biogeochemical Dynamics*. doi:10.2307/j.ctt3fgxqx.
- Scanlan, D. J., Ostrowski, M., Mazard, S., Dufresne, A., Garczarek, L., Hess, W. R., et al. (2009). Ecological Genomics of Marine Picocyanobacteria. *Microbiol. Mol. Biol. Rev.* 73, 249–299. doi:10.1128/mmbr.00035-08.
- Schlosser, C., Klar, J. K., Wake, B. D., Snow, J. T., Honey, D. J., Woodward, E. M. S., et al. (2014). Seasonal ITCZ migration dynamically controls the location of the (sub)tropical Atlantic biogeochemical divide. *Proc. Natl. Acad. Sci. U. S. A.* 111, 1438–1442. doi:10.1073/pnas.1318670111.
- Schmidt, and Husted (2019). The Biochemical Properties of Manganese in Plants. *Plants* 8, 381. doi:10.3390/plants8100381.
- Schoffman, H., Lis, H., Shaked, Y., and Keren, N. (2016). Iron–Nutrient Interactions within Phytoplankton. *Front. Plant Sci.* 7, 1–12. doi:10.3389/fpls.2016.01223.

- Schrader, P. S., Milligan, A. J., and Behrenfeld, M. J. (2011). Surplus photosynthetic antennae complexes underlie diagnostics of iron limitation in a cyanobacterium. *PLoS One* 6. doi:10.1371/journal.pone.0018753.
- Sebastian, M., and Ammerman, J. W. (2009). The alkaline phosphatase PhoX is more widely distributed in marine bacteria than the classical PhoA. *ISME J.* 3, 563–572. doi:10.1038/ismej.2009.10.
- Sebastián, M., Smith, A. F., González, J. M., Fredricks, H. F., Van Mooy, B., Koblížek, M., et al. (2016). Lipid remodelling is a widespread strategy in marine heterotrophic bacteria upon phosphorus deficiency. *ISME J.* 10, 968–978. doi:10.1038/ismej.2015.172.
- Sharon, S., Salomon, E., Kranzler, C., Lis, H., Lehmann, R., Georg, J., et al. (2014). The hierarchy of transition metal homeostasis: Iron controls manganese accumulation in a unicellular cyanobacterium. *Biochim. Biophys. Acta - Bioenerg.* 1837, 1990–1997. doi:10.1016/j.bbabo.2014.09.007.
- Sheridan, C. C., Steinberg, D. K., and Kling, G. W. (2002). The microbial and metazoan community associated with colonies of *Trichodesmium* spp.: A quantitative survey. *J. Plankton Res.* 24, 913–922. doi:10.1093/plankt/24.9.913.
- Shi, D., Kranz, S. A., Kim, J. M., and Morel, F. M. M. (2012). Ocean acidification slows nitrogen fixation and growth in the dominant diazotroph *Trichodesmium* under low-iron conditions. *Proc. Natl. Acad. Sci. U. S. A.* 109. doi:10.1073/pnas.1216012109.
- Shi, D., Xu, Y., Hopkinson, B. M., and Morel, F. M. M. (2010). Effect of ocean acidification on iron availability to marine phytoplankton. *Science* (80-.). 327, 676–679. doi:10.1126/science.1183517.
- Shi, T., Sun, Y., and Falkowski, P. G. (2007). Effects of iron limitation on the expression of metabolic genes in the marine cyanobacterium *Trichodesmium erythraeum* IMS101. *Environ. Microbiol.* 9, 2945–2956. doi:10.1111/j.1462-2920.2007.01406.x.
- Shire, D. M., and Kustka, A. B. (2021). Proteomic responses of the coccolithophore *Emiliania huxleyi* to zinc limitation and trace metal substitution. *Environ. Microbiol.* 00, 1462–2920.15644. doi:10.1111/1462-2920.15644.
- Sinoir, M., Ellwood, M. J., Butler, E. C. V., Bowie, A. R., Mongin, M., and Hassler, C. S. (2016). Zinc cycling in the Tasman Sea: Distribution, speciation and relation to phytoplankton community. *Mar. Chem.* 182, 25–37. doi:10.1016/j.marchem.2016.03.006.
- Snow, J. T., Polyviou, D., Skipp, P., Christmas, N. A. M., Hitchcock, A., Geider, R., et al. (2015). Quantifying integrated proteomic responses to iron stress in the globally important marine diazotroph *Trichodesmium*. *PLoS One* 10, 1–24. doi:10.1371/journal.pone.0142626.
- Sohm, J. A., Webb, E. A., and Capone, D. G. (2011). Emerging patterns of marine nitrogen fixation. *Nat. Rev. Microbiol.* 9, 499–508. doi:10.1038/nrmicro2594.
- Sommer, U. (1986). Nitrate-and silicate-competition among Antarctic phytoplankton. *Mar. Biol.* 91, 345–351.
- Sorokin, C., and Krauss, R. W. (1958). The Effects of Light Intensity on the Growth Rates of Green Algae. *Plant Physiol.* doi:10.1104/pp.33.2.109.

- Sosa, O. A., Repeta, D. J., DeLong, E. F., Ashkezari, M. D., and Karl, D. M. (2019). Phosphate-limited ocean regions select for bacterial populations enriched in the carbon-phosphorus lyase pathway for phosphonate degradation. *Environ. Microbiol.* 21, 2402–2414. doi:10.1111/1462-2920.14628.
- Sowell, S. M., Wilhelm, L. J., Norbeck, A. D., Lipton, M. S., Nicora, C. D., Barofsky, D. F., et al. (2009). Transport functions dominate the SAR11 metaproteome at low-nutrient extremes in the Sargasso Sea. *ISME J.* 3, 93–105. doi:10.1038/ismej.2008.83.
- Spackeen, J. L., Sipler, R. E., Bertrand, E. M., Xu, K., McQuaid, J. B., Walworth, N. G., et al. (2018). Impact of temperature, CO₂, and iron on nutrient uptake by a late-season microbial community from the Ross Sea, Antarctica. *Aquat. Microb. Ecol.* 82, 145–159.
- Sperfeld, E., Raubenheimer, D., and Wacker, A. (2016). Bridging factorial and gradient concepts of resource co-limitation: Towards a general framework applied to consumers. *Ecol. Lett.* 19, 201–215. doi:10.1111/ele.12554.
- Sterner, R. ., and Elser, J. . (2002). *Ecological Stoichiometry: The Biology of Elements from Molecules to the Biosphere: Robert W. Sterner, James J. Elser, Peter Vitousek: 9780691074917: Amazon.com: Books.*
- Stosiek, N., Talma, M., and Klimek-Ochab, M. (2020). Carbon-Phosphorus Lyase—the State of the Art. *Appl. Biochem. Biotechnol.* 190, 1525–1552. doi:10.1007/s12010-019-03161-4.
- Strzepek, R. F., and Harrison, P. J. (2004). Photosynthetic architecture differs in coastal and oceanic diatoms. *Nature* 431, 689–692. doi:10.1038/nature02954.
- Sunda, W. G. (1988). Trace metal interactions with marine phytoplankton. *Biol. Oceanogr.* 6, 411–442. doi:10.1080/01965581.1988.10749543.
- Sunda, W. G. (2012). Feedback interactions between trace metal nutrients and phytoplankton in the ocean. *Front. Microbiol.* 3, 1–22. doi:10.3389/fmicb.2012.00204.
- Sunda, W. G., and Huntsman, S. A. (1992). Feedback interactions between zinc and phytoplankton in seawater. *Limnol. Oceanogr.* 37, 25–40. doi:10.4319/lo.1992.37.1.0025.
- Sunda, W. G., and Huntsman, S. A. (1995). Iron uptake and growth limitation in oceanic and coastal phytoplankton. *Mar. Chem.* 50, 189–206. doi:10.1016/0304-4203(95)00035-P.
- Sunda, W. G., and Huntsman, S. A. (1998). Processes regulating cellular metal accumulation and physiological effects: Phytoplankton as model systems. *Sci. Total Environ.* 219, 165–181. doi:10.1016/S0048-9697(98)00226-5.
- Sunda, W. G., and Huntsman, S. A. (2005). Effect of CO₂ supply and demand on zinc uptake and growth limitation in a coastal diatom. *Limnol. Oceanogr.* doi:10.4319/lo.2005.50.4.1181.
- Sunda, W. G., Price, N. M., and Morel, F. M. M. (2005). Trace metal ion buffers and their use in culture studies. *Algal Cult. Tech.* 4, 35–63.
- Swalwell, J. E., Ribalet, F., and Armbrust, E. V. (2011). Seaflow: A novel underway flow-cytometer for continuous observations of phytoplankton in the ocean. *Limnol. Oceanogr. Methods* 9, 466–477. doi:10.4319/lom.2011.9.466.

- Tagliabue, A., Bowie, A. R., Boyd, P. W., Buck, K. N., Johnson, K. S., and Saito, M. A. (2017). The integral role of iron in ocean biogeochemistry. *Nature* 543, 51–59. doi:10.1038/nature21058.
- Tilman, D. (1981). Tests of resource competition theory using four species of Lake Michigan algae. *Ecology* 62, 802–815.
- Toulza, E., Tagliabue, A., Blain, S., and Piganeau, G. (2012). Analysis of the global ocean sampling (GOS) project for trends in iron uptake by surface ocean microbes. *PLoS One* 7. doi:10.1371/journal.pone.0030931.
- Tovar-Sanchez, A., Sañudo-Wilhelmy, S. A., Kustka, A. B., Agustí, S., Dachs, J., Hutchins, D. A., et al. (2006). Effects of dust deposition and river discharges on trace metal composition of *Trichodesmium* spp. in the tropical and subtropical North Atlantic Ocean. *Limnol. Oceanogr.* 51, 1755–1761. doi:10.4319/lo.2006.51.4.1755.
- Trick, C. G., Bill, B. D., Cochlan, W. P., Wells, M. L., Trainer, V. L., and Pickell, L. D. (2010). Iron enrichment stimulates toxic diatom production in high-nitrate, low-chlorophyll areas. *Proc. Natl. Acad. Sci. U. S. A.* 107, 5887–5892. doi:10.1073/pnas.0910579107.
- Tuit, C., Waterbury, J., and Ravizza, G. (2004). Diel variation of molybdenum and iron in marine diazotrophic cyanobacteria. *Limnol. Oceanogr.* 49, 978–990. doi:10.4319/lo.2004.49.4.0978.
- Tuo, S. how, Rodriguez, I. B., and Ho, T. Y. (2020). H₂ accumulation and N₂ fixation variation by Ni limitation in *Cyanothece*. *Limnol. Oceanogr.* 65, 377–386. doi:10.1002/lno.11305.
- Twining, B. S., and Baines, S. B. (2013). The trace metal composition of marine phytoplankton. *Ann. Rev. Mar. Sci.* 5, 191–215. doi:10.1146/annurev-marine-121211-172322.
- Twining, B. S., Nuñez-Milland, D., Vogt, S., Johnson, R. S., and Sedwick, P. N. (2010). Variations in *Synechococcus* cell quotas of phosphorus, sulfur, manganese, iron, nickel, and zinc within mesoscale eddies in the Sargasso Sea. *Limnol. Oceanogr.* 55, 492–506. doi:10.4319/lo.2009.55.2.0492.
- Tzubari, Y., Magnezi, L., Be’Er, A., and Berman-Frank, I. (2018). Iron and phosphorus deprivation induce sociality in the marine bloom-forming cyanobacterium *Trichodesmium*. *ISME J.* 12, 1682–1693. doi:10.1038/s41396-018-0073-5.
- Vallee, B. L., and Auld, D. S. (1990). Zinc coordination, function, and structure of zinc enzymes and other proteins. *Biochemistry* 29, 5647–5659.
- Van Mooy, B. A. S., Fredricks, H. F., Pedler, B. E., Dyhrman, S. T., Karl, D. M., Koblížek, M., et al. (2009). Phytoplankton in the ocean use non-phosphorus lipids in response to phosphorus scarcity. *Nature* 458, 69–72. doi:10.1038/nature07659.
- Van Mooy, B. A. S., Hmelo, L. R., Sofen, L. E., Campagna, S. R., May, A. L., Dyhrman, S. T., et al. (2012). Quorum sensing control of phosphorus acquisition in *Trichodesmium* consortia. *ISME J.* 6, 422–429. doi:10.1038/ismej.2011.115.
- Verslues, P. E., and Sharma, S. (2010). Proline Metabolism and Its Implications for Plant-Environment Interaction. *Arab. B.* 8, e0140. doi:10.1199/tab.0140.
- Vidoudez, C., and Pohnert, G. (2012). Comparative metabolomics of the diatom *Skeletonema*

- marinoi in different growth phases. *Metabolomics* 8, 654–669. doi:10.1007/s11306-011-0356-6.
- Villareal, T. A., and Carpenter, E. J. (2003). Buoyancy regulation and the potential for vertical migration in the oceanic cyanobacterium *Trichodesmium*. *Microb. Ecol.* 45, 1–10. doi:10.1007/s00248-002-1012-5.
- Villarreal-Chiu, J. F., Quinn, J. P., and McGrath, J. W. (2012). The genes and enzymes of phosphonate metabolism by bacteria, and their distribution in the marine environment. *Front. Microbiol.* 3, 1–13. doi:10.3389/fmicb.2012.00019.
- von Liebig, J. (1841). *Die organische Chemie in ihrer Anwendung auf Agricultur und Physiologie*. Vieweg.
- Waldron, K. J., Rutherford, J. C., Ford, D., and Robinson, N. J. (2009). Metalloproteins and metal sensing. *Nature* 460, 823–830. doi:10.1038/nature08300.
- Walsby, A. E., Hayes, P. K., and Boje, R. (1995). The gas vesicles, buoyancy and vertical distribution of cyanobacteria in the Baltic Sea. *Eur. J. Phycol.* 30, 87–94. doi:10.1080/09670269500650851.
- Walworth, N. G., Fu, F. X., Lee, M. D., Cai, X., Saito, M. A., Webb, E. A., et al. (2018). Nutrient-colimited *Trichodesmium* as a nitrogen source or sink in a future ocean. *Appl. Environ. Microbiol.* 84, 1–14. doi:10.1128/AEM.02137-17.
- Walworth, N. G., Fu, F. X., Webb, E. A., Saito, M. A., Moran, D., McIlvin, M. R., et al. (2016). Mechanisms of increased *Trichodesmium* fitness under iron and phosphorus co-limitation in the present and future ocean. *Nat. Commun.* 7, 1–11. doi:10.1038/ncomms12081.
- Walworth, N. G., Saito, M. A., Lee, M. D., McIlvin, M. R., Moran, D. M., Kellogg, R. M., et al. (2022). Why Environmental Biomarkers Work: Transcriptome–Proteome Correlations and Modeling of Multistressor Experiments in the Marine Bacterium *Trichodesmium*. *J. Proteome Res.* 21, 77–89. doi:10.1021/acs.jproteome.1c00517.
- Wang, X., Browning, T. J., Achterberg, E. P., and Gledhill, M. (2022). Phosphorus Limitation Enhances Diazotroph Zinc Quotas. *Front. Microbiol.* 13, 1–9. doi:10.3389/fmicb.2022.853519.
- Wang, Z., Tsementzi, D., Williams, T. C., Juarez, D. L., Blinbry, S. K., Garcia, N. S., et al. (2021). Environmental stability impacts the differential sensitivity of marine microbiomes to increases in temperature and acidity. *ISME J.* 15, 19–28. doi:10.1038/s41396-020-00748-2.
- Wanner, B. L. (1996). Phosphorus Assimilation and Control of the Phosphate Regulon. *Escherichia coli Salmonella Cell. Mol. Biol.* 1, 1357–1381.
- Waterbury, J. B. (2006). The cyanobacteria—isolation, purification and identification. *The prokaryotes* 4, 1053–1073.
- Weber, T., John, S., Tagliabue, A., and DeVries, T. (2018). Biological uptake and reversible scavenging of zinc in the global ocean. *Science* (80-.). 361, 72–76. doi:10.1126/science.aap8532.
- Wei, T., Quareshy, M., Zhang, Y., Scanlan, D. J., and Chen, Y. (2018). Manganese Is Essential

- for PlcP Metallophosphoesterase Activity Involved in Lipid Remodeling in Abundant Marine Heterotrophic Bacteria. *Appl. Environ. Microbiol.* 84. doi:10.1128/AEM.01109-18.
- Welkie, D., Zhang, X., Markillie, L. L., Taylor, R., Orr, G., Jacobs, J., et al. (2014). Transcriptomic and proteomic dynamics in the metabolism of a diazotrophic cyanobacterium, *Cyanothece* sp. PCC 7822 during a diurnal light-dark cycle. *BMC Genomics* 15, 1–16. doi:10.1186/1471-2164-15-1185.
- Welschmeyer, N. A. (1994). Fluorometric analysis of chlorophyll a in the presence of chlorophyll b and pheopigments. *Limnol. Oceanogr.* doi:10.4319/lo.1994.39.8.1985.
- White, A. E., Spitz, Y. H., Karl, D. M., and Letelier, R. M. (2006a). Flexible elemental stoichiometry in *Trichodesmium* spp. and its ecological implications. *Limnol. Oceanogr.* 51, 1777–1790. doi:10.4319/lo.2006.51.4.1777.
- White, A. E., Spitz, Y. H., and Letelier, R. M. (2006b). Modeling carbohydrate ballasting by *Trichodesmium* spp. *Mar. Ecol. Prog. Ser.* 323, 35–45. doi:10.3354/meps323035.
- White, A. K., and Metcalf, W. W. (2004). Two C-P lyase operons in *Pseudomonas stutzeri* and their roles in the oxidation of phosphonates, phosphite, and hypophosphite. *J. Bacteriol.* 186, 4730–4739. doi:10.1128/JB.186.14.4730-4739.2004.
- White, A. K., and Metcalf, W. W. (2007). Microbial metabolism of reduced phosphorus compounds. *Annu. Rev. Microbiol.* 61, 379–400. doi:10.1146/annurev.micro.61.080706.093357.
- Whittaker, S., Bidle, K. D., Kustka, A. B., and Falkowski, P. G. (2011). Quantification of nitrogenase in *Trichodesmium* IMS 101: Implications for iron limitation of nitrogen fixation in the ocean. *Environ. Microbiol. Rep.* 3, 54–58. doi:10.1111/j.1758-2229.2010.00187.x.
- Wilhelm, S. W., and Trick, C. G. (1995). PHYSIOLOGICAL PROFILES OF SYNECHOCOCCUS (CYANOPHYCEAE) IN IRON-LIMITING CONTINUOUS CULTURES 1. *J. Phycol.* 31, 79–85.
- Wilson, S. T., Aylward, F. O., Ribalet, F., Barone, B., Casey, J. R., Connell, P. E., et al. (2017). Coordinated regulation of growth, activity and transcription in natural populations of the unicellular nitrogen-fixing cyanobacterium *Crocospaera*. *Nat. Microbiol.* 2, 1–9. doi:10.1038/nmicrobiol.2017.118.
- Wu, J., Sunda, W., Boyle, E. A., and Karl, D. M. (2000). Phosphate depletion in the Western North Atlantic Ocean. *Science* (80-.). 289, 759–762. doi:10.1126/science.289.5480.759.
- Yamaguchi, T., Furuya, K., Sato, M., and Takahashi, K. (2016). Phosphate release due to excess alkaline phosphatase activity in *Trichodesmium erythraeum*. *Plankt. Benthos Res.* 11, 29–36. doi:10.3800/pbr.11.29.
- Yamaguchi, T., Sato, M., Gonda, N., Takahashi, K., and Furuya, K. (2020). Phosphate diester utilization by marine diazotrophs *trichodesmium erythraeum* and *crocospaera watsonii*. *Aquat. Microb. Ecol.* 85, 211–218. doi:10.3354/AME01951.
- Yong, S. C., Roversi, P., Lillington, J., Rodriguez, F., Krehenbrink, M., Zeldin, O. B., et al.

References

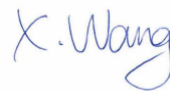
- (2014). A complex iron-calcium cofactor catalyzing phosphotransfer chemistry. *Science* (80-.). 345, 1170–1173. doi:10.1126/science.1254237.
- Zehr, J. P. (2011). Nitrogen fixation by marine cyanobacteria. *Trends Microbiol.* 19, 162–173. doi:10.1016/j.tim.2010.12.004.
- Zehr, J. P., and Capone, D. G. (2020). Changing perspectives in marine nitrogen fixation. *Science* (80-.). 368, eaay9514. doi:10.1126/science.aay9514.
- Zhang, F., Hong, H., Kranz, S. A., Shen, R., Lin, W., and Shi, D. (2019). Proteomic responses to ocean acidification of the marine diazotroph *Trichodesmium* under iron-replete and iron-limited conditions. *Photosynth. Res.* 142, 17–34. doi:10.1007/s11120-019-00643-8.

References

Declaration

I, Xuechao Wang, hereby declare that I have written this Ph.D. thesis independently, under compliance of the rules for good scientific practice of the German Research Foundation. I declare that I have used only the sources, the data and the support that I have clearly mentioned. Moreover, I assure that this Ph.D. thesis has not been submitted for the conferral of a degree elsewhere, and that none of my academic degrees has ever been withdrawn. Published or submitted for publication manuscripts are identified at the relevant places.

Kiel, April 2022



(Xuechao Wang)